UTILIZATION OF ERTS-1 DATA TO MONITOR AND CLASSIFY EUTROPHICATION OF INLAND LAKES

Dr. Robert H. Rogers
Bendix Aerospace Systems Division
3300 Plymouth Road
Ann Arbor, Michigan 48107

Dr. V. Elliot Smith
Cranbrook Institute of Science
500 Lone Pine Road
Bloomfield Hills, Michigan 48103

August 1973
Interim Report for Period February 1973 - July 1973

Prepared for

GODDARD SPACE FLIGHT CENTER

Greenbelt, Maryland 20771

Original photography may be purchased from:
EROS Data Center
10th and Dakota Avenue
Sioux Falls, SD 57198

TECHNICAL REPORT STANDARD TITLE PAGE

1. Report No.	2. Government Accession No.	3. Recipient's Catalog No.
4. Title and Subtitle Utilization of ERTS-1 Data to Monitor and Classify Eutrophication of Inland Lakes		5. Report Date August 1973 6. Performing Organization Code
7. Author(s) Robert H. Rogers (Bendix) & V. Elliott Smith (Cranbrook Institute of Science)		8. Performing Organization Report No. BSR 4089
9. Performing Organization Name and Address Bendix Aerospace Systems Division 3300 Plymouth Road Ann Arbor, Michigan 48107		10. Work Unit No. 11. Contract or Grant No. NAS 521810 13. Type of Report and Period Covered Interim - February through July 1973
12. Sponsoring Agency Name and Address Goddard Space Flight Center Greenbelt, Maryland 20771		14. Sponsoring Agency Code
15. Supplementary Notes The Co-investigator, Elliott Smith, is a staff member at the Cranbrook Institute of Science in Bloomfield Hills, Michigan.		

16. Abstract

The report summarizes the technical activity over the reporting period. Significant findings are (a) one-acre lakes and one-acre islands are detectable, (b) removal of atmospheric parameters derived from RPMI measurements show test lakes to have reflectances of 3.1 to 5.5% in band 4 and 0.3 to 2.3% in band 5, (c) failure to remove reflectance caused by atmosphere results in errors up to 500% in computing lake reflectance from ERTS data, (d) in band 4, up to seven reflectance levels were observed in test lakes, (e) these reflectance patterns have been displayed on a color-coded TV monitor and on computer-generated gray scales, (f) deep and shallow water can be separated by a trained photo-interpreter and automatic machine processing; estimates of water depth may be possible in some cases, (g) the RPMI provides direct spectral signature measurements of lakes and lake features, i.e., algal scums, floating plants, etc., (h) a method is reported for obtaining lake color, as estimated by the Forel-Ule standards, from ERTS data; (i) a strong correlation between browner water color, diminishing water transparency, and increasing particulate carbon and algal diversity is observed, (j) classifying lake eutrophication by observation of surface scums or macrophytes in shallow water seems straightforward.

17. Key Words (Selected by Author(s))	18. Distribution Statement		
19. Security Classif. (of this report)	20. Security Classif. (of this page)	21. No. of Pages	22. Price*

PREFACE

OBJECTIVE OF THE PROGRAM

The objective of this experiment is to demonstrate the feasibility of ERTS in measuring the state of eutrophication of inland lakes as a broad survey monitor. Specific objectives are:

a. Determine the minimum size of inland lakes detected by ERTS when considering factors of color, size, shape, and shore definition.

b. Determine correlation of surface color to various indices of eutrophication for preparing charts of eutrophication versus surface color. Such indices are algal count, Secchi Disk transparency, leptopel (detrital) content, macrophyte extent, nutrients, etc.

c. Determine if algal blooms are detectable by ERTS when they occur and color the surfaces of small inland lakes. Algal blooms are an indicator of enrichment.

d. Determine if changes in leptopel level are detectable by ERTS. This is another measure of eutrophication that can be related to ERTS.

e. Determine the feasibility of establishing classification of levels of inland lake eutrophication by either lake, pond, and swamp taxonomies or by individual indicators such as surface color, transparency, leptopel level, and appearance of algal blooms.

SCOPE OF WORK

The scope is to compare the ERTS-1 to ground truth and to aircraft imagery. The ERTS-1 imagery will be that as received from NASA and that as produced by the Bendix data processing facility from the Computer Compatible Tapes (CCT's). Comparison of the eutrophication monitoring capability will be made for several seasons.

CONCLUSIONS

Progress to date is based on analysis of ERTS-1 bulk imagery and CCT's for the dates September 28, 1972 and March 27, 1972. Field sampling of the study lakes has been conducted generally at 18-day intervals since March 27, 1973. Lake reflectance measurements with a Radiant Power Measuring Instrument (RPMI) have been made periodically.

It is concluded that lakes and islands of one acre or more are detectable in ERTS imagery under clear atmospheric conditions. Lake boundaries are resolved best in MSS bands 6 and 7; variations in water reflectance, i.e., effects of water color, are observed best in bands 4 and 5.

The ERTS CCT's of 27 March were corrected for atmospheric parameters and transformed into reflectance gray level printouts. Banding effects were a problem (horizontal lines), particularly in band 5. However, in band 4, up to seven reflectance levels were viewed within the test lakes. The distribution of these reflectance patterns in Orchard Lake is illustrated in a gray-scale printout. On comparison of this with a bathymetry map and aerial photograph taken on the same day, it is concluded that (a) deep-shallow water separation based on reflectance level is good, (b) two or more deep-water types may be classified from ERTS data and (c) ability to determine water depth in clear shallow areas is fair to good.

It is concluded that ERTS band reflectance ratios (band 4 to 5 and band 4 to 6) are useful as a means of expressing "signatures" of water color/turbidity types. The ratio of band 4 to band 5, as determined from ERTS and from ground base reflectance measurements with RPMI, was found to decrease significantly as lake color/turbidity values increased. Ratios for "clear-green" and "turbid-brown" lakes were compared.

It is concluded that the RPMI is a valuable aid in obtaining measurements of solar and atmospheric parameters needed to transform ERTS data from lakes into absolute reflectance units. The RPMI is also useful in directly measuring spectral reflectance signatures of lake features, such as algal scums and floating plants. The "transfer calibration" method, which utilizes panels of known reflectance, has proved to be a quick way of finding water reflectance and reflectance ratios with the RPMI.

A method has been partly worked out for obtaining absolute comparisons of lake color, as estimated by the Forel-Ule standards, with that derived from ERTS and RPMI measurements. To accomplish this, both the standard (Forel-Ule) and reflectance (ERTS and RPMI) values are being converted to the CIE system of color specification.

It is concluded that there appears to be a strong correlation between browner water color, diminishing water transparency, and increasing particulate carbon and algal diversity in the study lakes. Dominance of green algae (Chlorophyta) was often accompanied or followed by clearer and greener water. The average conditions, rather than the extremes, are most important in classifying trophic levels and comparing lakes.

Further efforts must be concentrated on completing the development of techniques to transform ERTS data from deep-water areas, into water color and on developing decision imagery which automatically sorts out similar water colors in different lakes. The band-ratio method may be helpful.

CONTENTS

ILLUSTRATIONS

ILLUSTRATIONS (CONT.)

ILLUSTRATIONS (CONT.)

TABLES

1. INTRODUCTION

Previous reports have described progress in several phases of this study, briefly summarized as follows:

a. Software and procedures were established for analysis of ERTS computer compatible tapes acquired on inland lakes.

b. A program was set up for collecting ground truth and analyzing lake water quality coincident with ERTS passes.

c. Study of initial ERTS images by visual and densitometric means revealed that the resolution and sensitivity of ERTS sensors was adequate, even under fair atmospheric conditions (70% cloud cover). Consistent differences in image density were detectable between lakes and within each lake in a given MSS channel. The minimum size of lakes detectable by ERTS was found to be less than one acre. MSS bands 4 and 5 (0.5 to 0.7μ) proved to be more informative as to lake color reflectance and differences than did bands 6 and 7 (0.7 to 1.1μ).

d. Six study lakes were arranged in order of trophic state (enrichment level), based on the study of water quality data collected since 1969.

e. Digital processing of ERTS computer compatible tapes (CCT's) has resulted in separation (autographic theme extraction) of deep and shallow waters, as well as in discrimination of "color" patterns over deep-water areas. In band 4, four to seven levels of water reflectance were evident over the six study lakes. No such discrimination level was possible in aerial color photographs of the lakes taken at the same time.

At midpoint in this program, it is clear that ERTS is capable of sensing variations in water reflectance that are not visible to the eye or discernable in aerial photographs. As discussed below, the variations seem to be related to differences of water color and quality. These are very encouraging signs. However, a number of steps must be successfully taken before ERTS can be used to monitor trophic levels in lakes. These tasks are very broad but they help to describe the general approach being taken to achieve the specific objectives of this investigation, as defined in the preface to this report. The steps are described, in their proper chronology, as follows:

a. Determine the effectiveness of ERTS in resolving small lakes and lake features, as a function of their size, shape, depth, color, and shore definitions. (This includes specific objective a of the preface and has been largely accomplished.)

b. Detect differences in the color and reflectivity of lakes by analysis of multispectral data from ERTS, aircraft, and ground monitors.

c. Correct ERTS data for solar and atmospheric effects so that resulting measurements are directly comparable with those obtained from ground measurements. Transform corrected ERTS measurements and surface measurements into a common color specification, i.e., CIE number.

d. Account for color differences in terms of physical, chemical, and biological variables, which influence water color within lakes.

e. Correlate these color-related variables with the general trophic condition of each lake by considering additional water quality indicators.

f. Evaluate ERTS-1 as a broad survey monitor of eutrophication (its extent and rate) in inland lakes.

Progress in the first two areas has been reported previously. The emphasis in this report is on our efforts to establish and correlate ERTS and ground measurements of lake color. As explained below, this is important to the whole concept of using ERTS to monitor eutrophication in lakes or other waters. This report will indicate how data from ERTS can be treated so as to yield an objective, numerical expression for water color. It is also important, however, that this expression be relatable to human (visual) values of color, since these have been the traditional means of describing water color in the field. They are still widely used today. Both the visual and remote estimates of water color need to be related to a common system of color specification, the CIE or trichromatic system. These basic relationships are especially important in the early stages of ERTS monitoring when ground truth should be used often to confirm results.

This report also includes some discussion of lake trophic levels and their relationship to water color. More detailed analysis should wait for completion of the summer's data collection program. Such a complexity of factors influence water color that any evaluation of its causes and sources should be based on as many examples as possible. Suffice to say that this study will not resolve the problem for lakes everywhere. The complex relationship between water color and quality will be studied for years to come, although much general information for marine and fresh waters is now at hand.

Finally, this report deals, in a provisional way, with recent progress in ERTS data processing techniques. The unique problems of water color sensing call for innovations in data handling which are being developed at Bendix Aerospace Systems Division.

Our subsequent work will follow the general guidelines given in Section 5.

2. RESULTS AND DISCUSSION

2.1 VISUAL ESTIMATION OF WATER COLOR

Estimation or measurement of water color is an important part of any water quality monitoring concerned with trophic levels or organic production. Much of the biology and chemistry of natural water is manifested in water color. Plant and animal cells, their particulate remains (seston or leptopel), and their soluble residues (the "yellow stuff" or humic acids of fresh and salt waters) all contribute to water color indirectly by their effects on plant growth. Consequently, water color is highly variable and responsive to trophic changes, especially in small, urban lakes.

Ideally, the determination of water color should be objective, sensitive, and repeatable. It should also be sufficiently convenient for use in the field (preferably in a small boat) if large numbers of routine observations are to be made. An important consideration in developing ground-truth techniques for ERTS studies is that the methods and tools should be widely available. Thus, the results presented here may be tested easily by other investigators on lakes throughout the world.

2.1.1 DIRECT OBSERVATION OF WATER COLOR

Most non-scientists know intuitively that decreasing water quality is associated with increasing water color and turbidity but few can express this relationship in quantitative terms. Simple observations of color without reference to any standard, even if done by an experienced individual, are likely to be unreliable since they depend on elements of color recognition and memory. Human beings vary widely with respect to both of these properties of vision and judgement. It is, undoubtedly, true that distinctions of water quality based on color will require far more dependable means of water color estimation or measurement. Visual comparisons of water with color standards have become acceptable as the simplest means of estimating lake and ocean colors.

2.1.2 USE OF PLATINUM-COBALT STANDARDS

Hazen (1892) first developed a series of water color standards composed of varying concentrations of potassium chloroplatinate and cobalt chloride in dilute hydrochloric acid. On a scale of 1,000, each unit is comparable to 1 ppm of chloroplatinate ion. This forms a stable solution of pale yellow to brown color. In common use, the standards and sample water are compared in long glass tubes by transmitted light. Alternatively, color class discs are substituted for the

liquid standards. Although accepted widely in water analysis practice (Standard Methods, 1969), the platinum standard has serious drawbacks. Even small amounts of turbidity increase the "apparent" color of water samples (removal of particles by lengthy centrifugation is recommended for estimation of "true color."). Second, lake color may vary greatly with depth, especially below the epilimnion. Thus, a small sample is scarcely representative of the entire photic zone. Third, the yellow-brown component of color in lakes is pH dependent and somewhat unstable to sunlight. Therefore, transport of samples or even dilution in the field, for color matching purposes, may introduce errors. Finally, from the standpoint of correlating water color with ERTS, it is inadvisable to gauge lake color based on samples removed from the natural environment of transmitted, scattered, and reflected light. These variables and others contribute to the apparent color of lakes as recorded by remote sensors. For the reasons above, the platinum-cobalt standards are not used in the present study.

2.1.3 USE OF FOREL-ULE STANDARDS

Forel (1889) devised a series of blue to green water color standards, which was extended by Ule (1892) to include yellow to reddish-brown colors. The combined scale, still widely used, consists of 22 different proportions of cuprammonium sulfate (blue), potassium chromate (yellow), and cobalt ammonium sulfate (red-brown), combined as in Figure 1(a).

The color ratios are also shown graphically in Figure 1(b). Units of the Forel-Ule scale do not correspond to any quantitative measure of ions, however. The solutions, normally contained in sealed glass vials (13mm O. D.), are stable and form a series of roughly equal gradations in color. Though arbitrary, the scale was designed to furnish an empirical standard of actual water colors as viewed downward from the surface, whether with or without a submerged, white disc as background.

LaMotte Chemical Company of Chestertown, Maryland manufactured the Forel-Ule standards used in this work. Their instructions for field use are as follows:

a. Immerse the Secchi disk with the white side up. Lower the disk to a total depth of one meter below the water's surface. Avoid direct light reflection.

b. Insert the distilled water ampoules in the blank holes in the comparator.

B

Figure 1. (a) Composition of Forel-Ule standards (according to Hutchinson, 1957).

Solution*	I	II	III	IV	V	VI	VII	VIII	IX	X
1	100	98	95	91	86	80	73	65	56	46
2	0	2	5	9	14	20	27	35	44	54
3	0	0	0	0	0	0	0	0	0	0
Color	Blue		Greenish blue		Bluish green			Green		

Solution*	XI	XII	XIII	XIV	XV	XVI	XVII	XVIII	XIX	XX	XXI	XXII
1	35	35	35	35	35	35	35	35	35	35	35	35
2	65	60	55	50	45	40	35	30	25	20	15	10
3	0	5	10	15	20	25	30	35	40	45	50	55
Color	Greenish yellow					Yellow				Brown		

* Solution 1 = 0.5 g. $CuSO_4 \cdot 5H_2O$ + 5 ml. strong NH_4OH + to 100 ml. H_2O
2 = 0.5 g. $K_2CrO_4 \cdot 5H_2O$ + 5 ml. strong NH_4OH + to 100 ml. H_2O
3 = 0.5 g. $CoSO_4 \cdot 7H_2O$ + 5 ml. strong NH_4OH + to 100 ml. H_2O

(b) Proportions of color components in Forel-Ule standards.

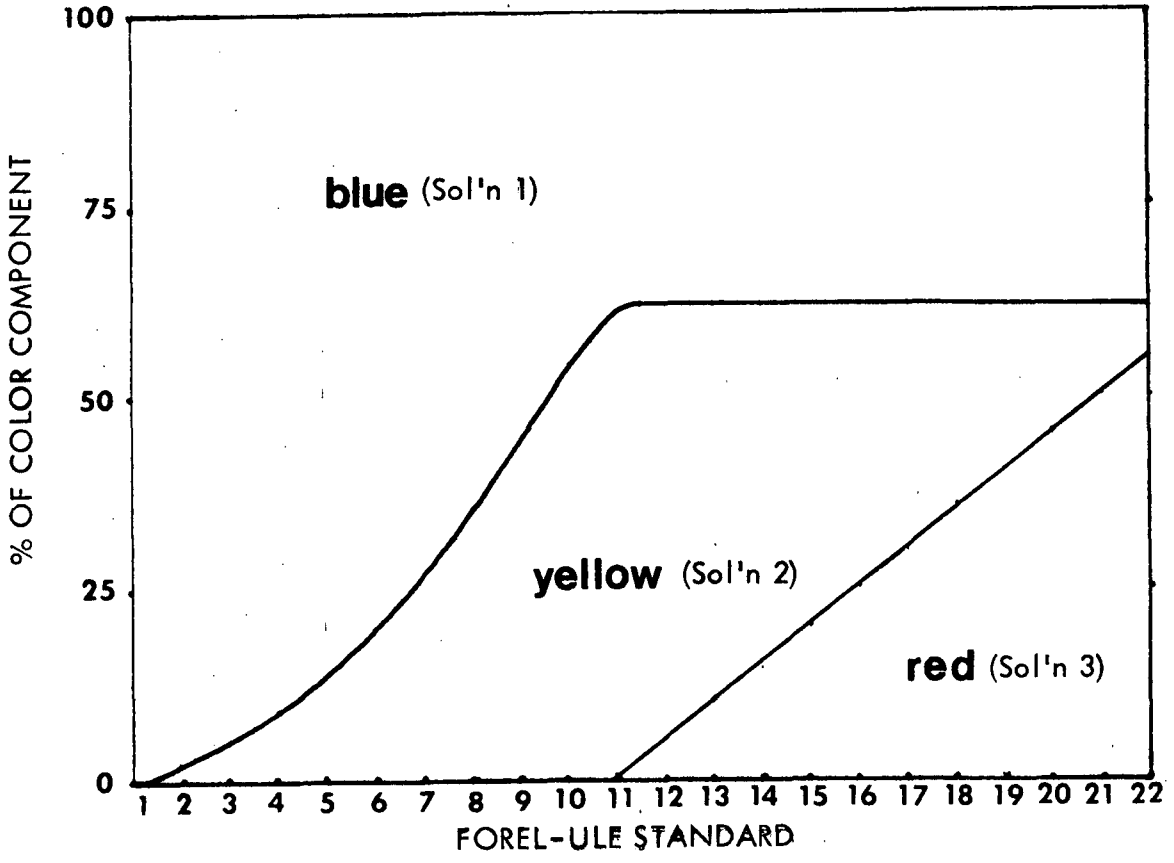

c. Hold the comparator at arm's length so as to view both the Secchi disk and the Forel-Ule scale.

d. Compare the color as seen through the blank hole in the comparator with the color of the water as viewed over the Secchi disk.

e. The value in the comparator that most nearly matched the color of the water is taken as the value for that sampling location. Record this value.

As prescribed, this method is unworkable and leads to faulty estimates of water color. After considerable experimentation, we found that a far more effective method requires the use of a special viewing tube which allows a side-by-side comparison of the standards. The standards are viewed in a mirror by transmitted sky light and the upwelling light ("light of the water") is viewed through the glass bottom of the tube. No Secchi disk is used. Seen in this manner, the standard colors compare favorably in saturation and brightness to those of the deep water illuminated by the same daylight. The observer has little difficulty making the best choice of a matching standard. This procedure and the viewing device used will be described more fully in the final report.

2.1.4 SPECTRAL ANALYSIS OF FOREL-ULE STANDARDS

The inorganic contents of the Forel-Ule standard bear no relations to the largely organic substances that produce color in natural waters. Even so, the obvious similarity between the standard and water colors suggests that their reflectance or transmittance spectra are similar. Any such relationship becomes important when one considers that the ratios of reflectance between ERTS spectral bands might be useful in characterizing the colors of lakes. As the dominant color of water shifts by even steps toward longer wavelengths (i.e., green-to-brown-to-red), the transmittance or reflectance ratios of band 4 to band 5 should decrease in some corresponding regular fashion. Similarly, if the Forel-Ule scale is composed of even hue increments, the same correlation should apply. Since Forel-Ule standards are used here to characterize lake colors in situ, we decided to define each of their spectral curves with respect to the ratios of total transmittance within three of the ERTS MSS bands; band 4, band 5, and band 6. At the time, no means were available to obtain reflectance curves of these solutions in the 400 to 800 nm range. The standards were prepared according to Hutchinson, 1957.

Transmittance (% T) curves of the three component solutions, read on a Zeiss recording spectrophotometer, are shown in Figure 2. Transmittance curves of the 22 standards composed of the three solutions as defined by Hutchinson are shown in Figures 3 through 7. The areas under each curve within the first

Figure 2. Transmittance (%) of Forel-Ule component solutions.

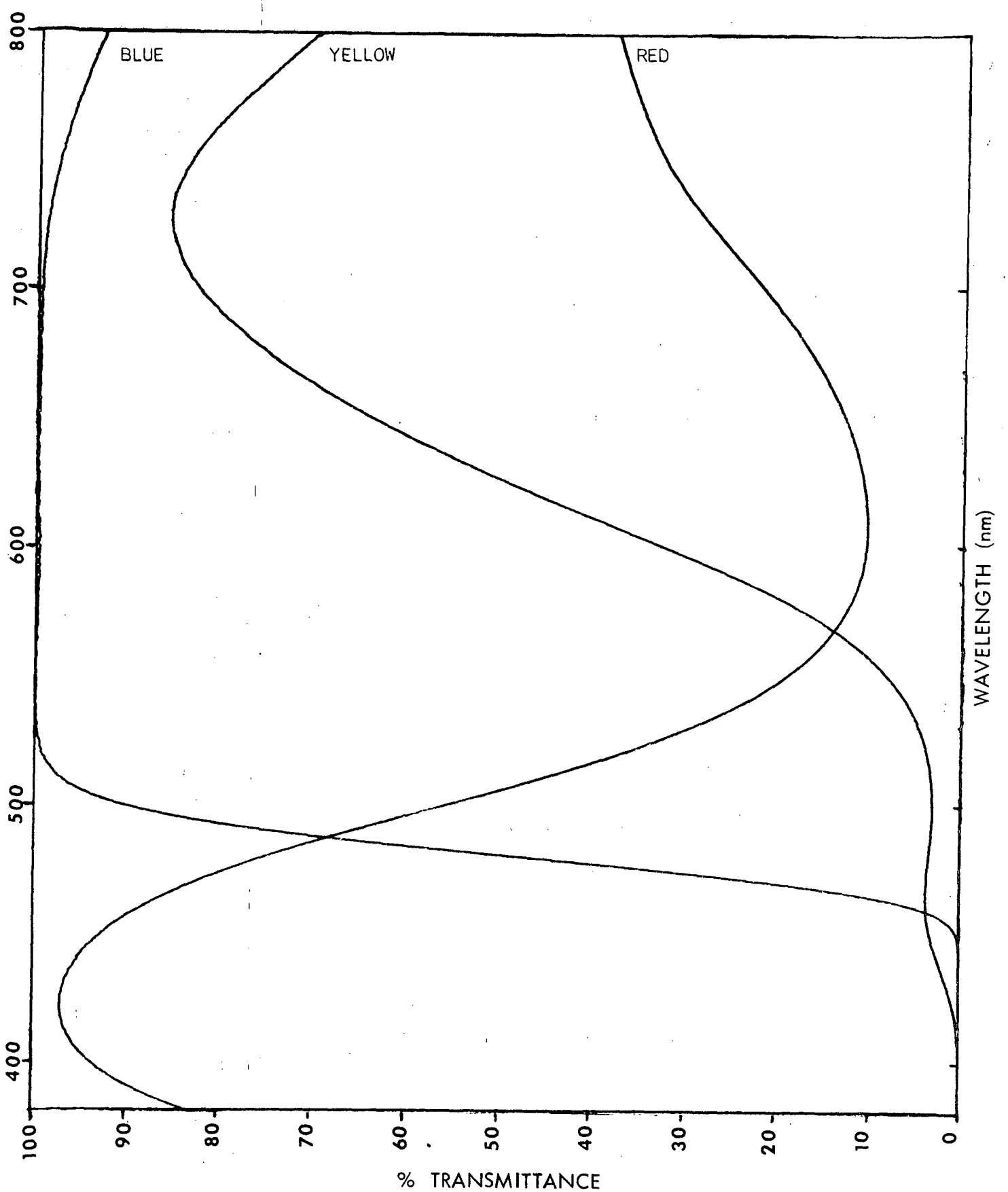

Figure 3. Transmittance (%) of Forel-Ule standards.

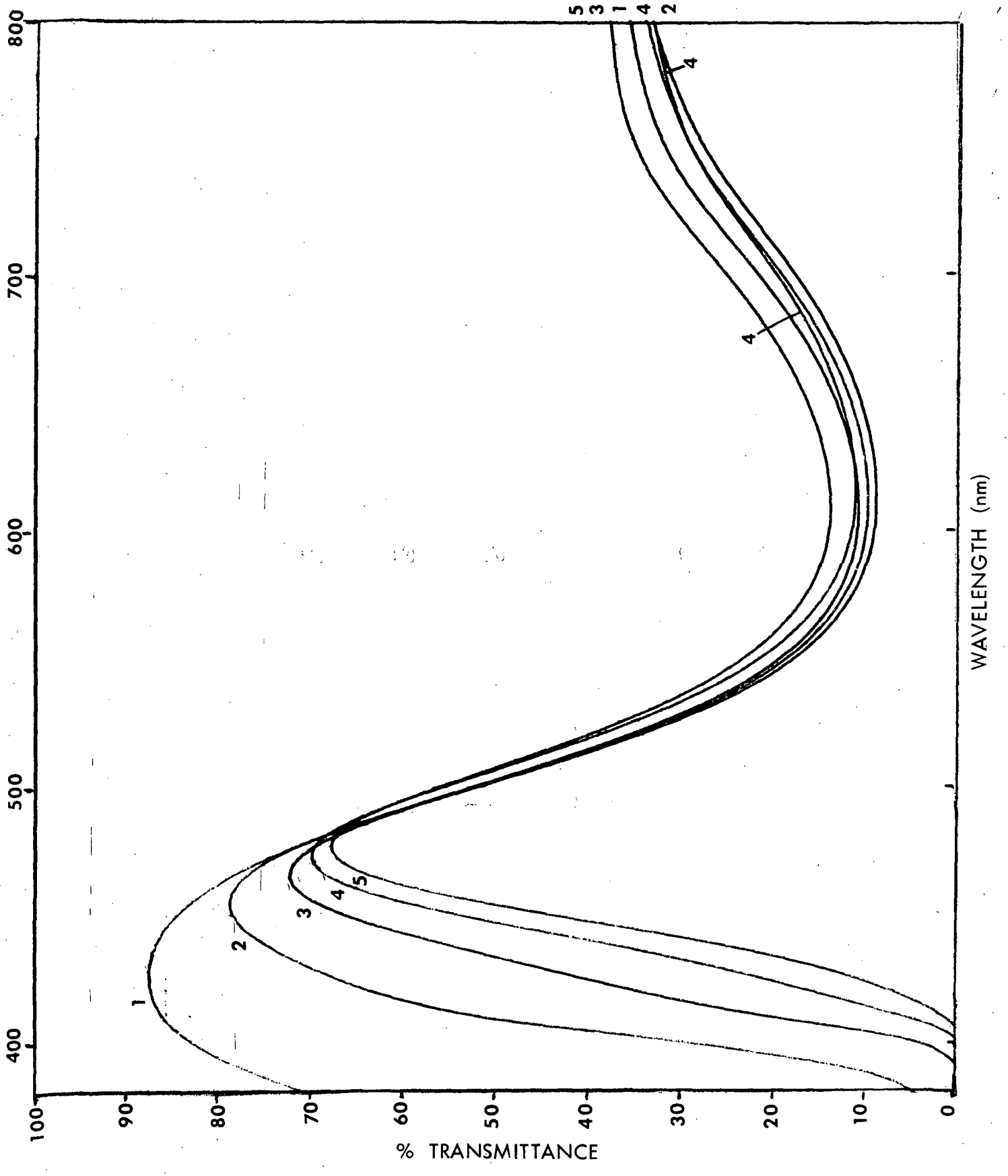

Figure 4. Transmittance (%) of Forel-Ule standards.

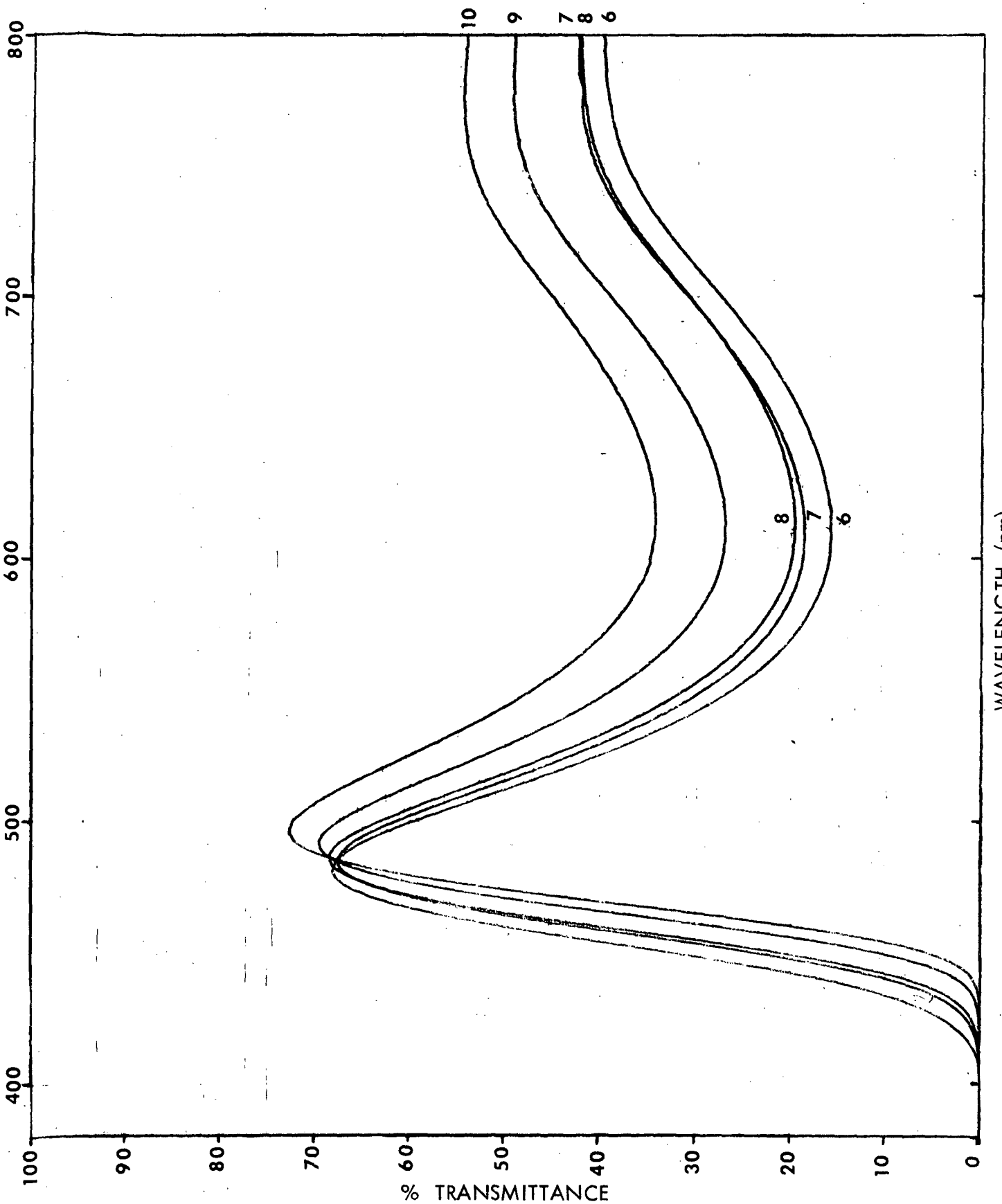

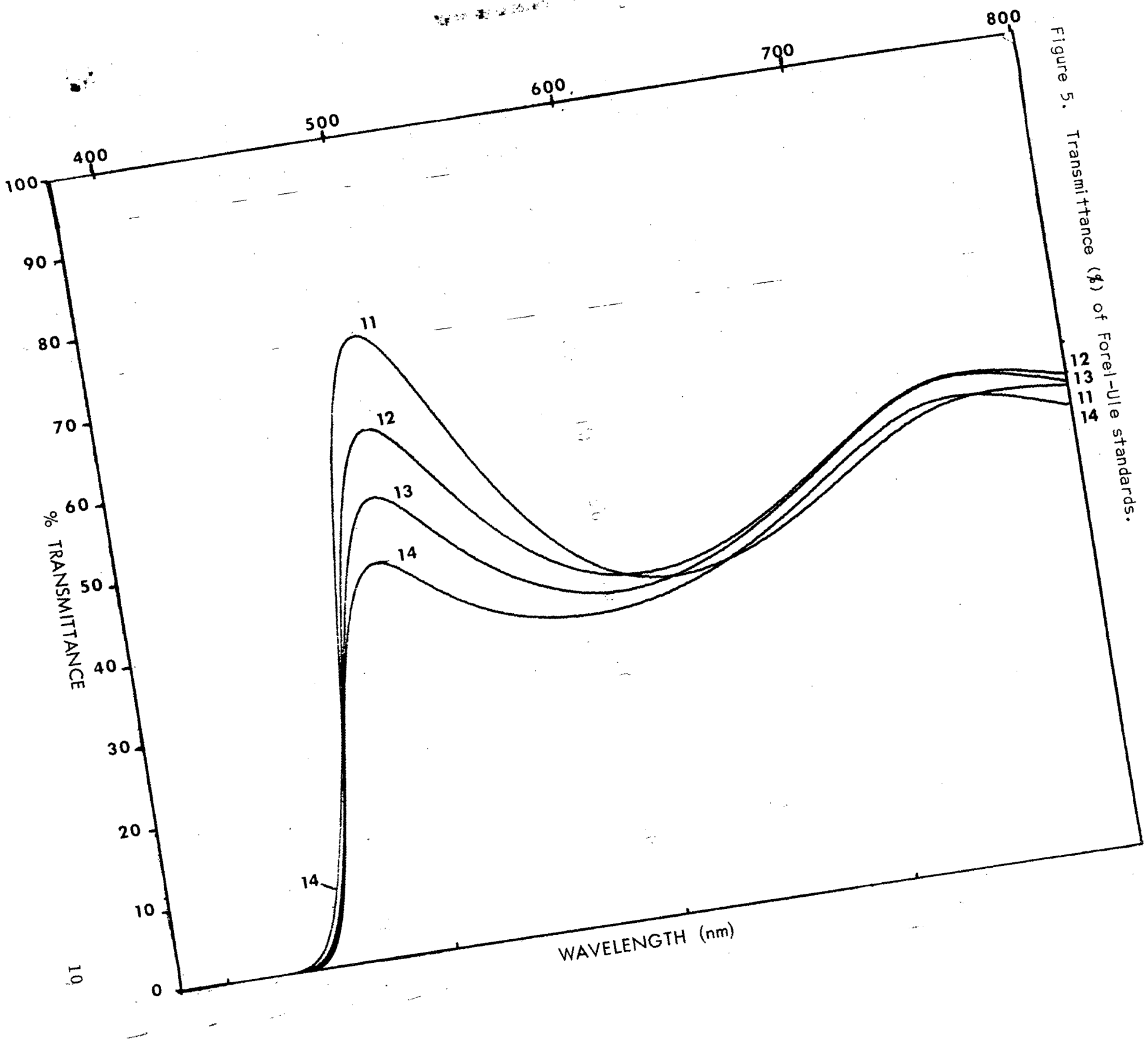

Figure 5. Transmittance (%) of Forel-Ule standards.

Figure 6. Transmittance (%) of Forel-Ule standards.

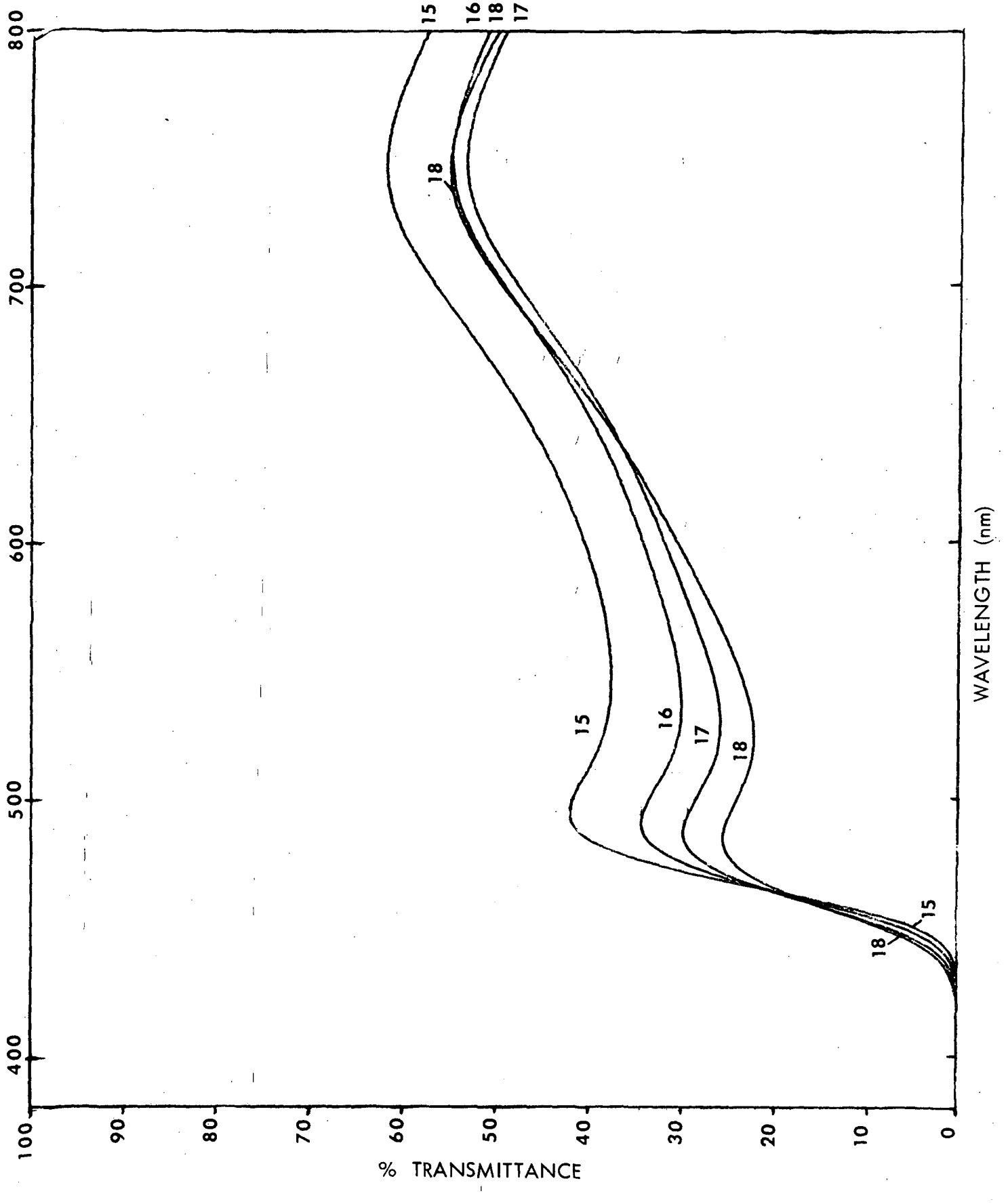

Figure 7. Transmittance (%) of Forel-Ule standards.

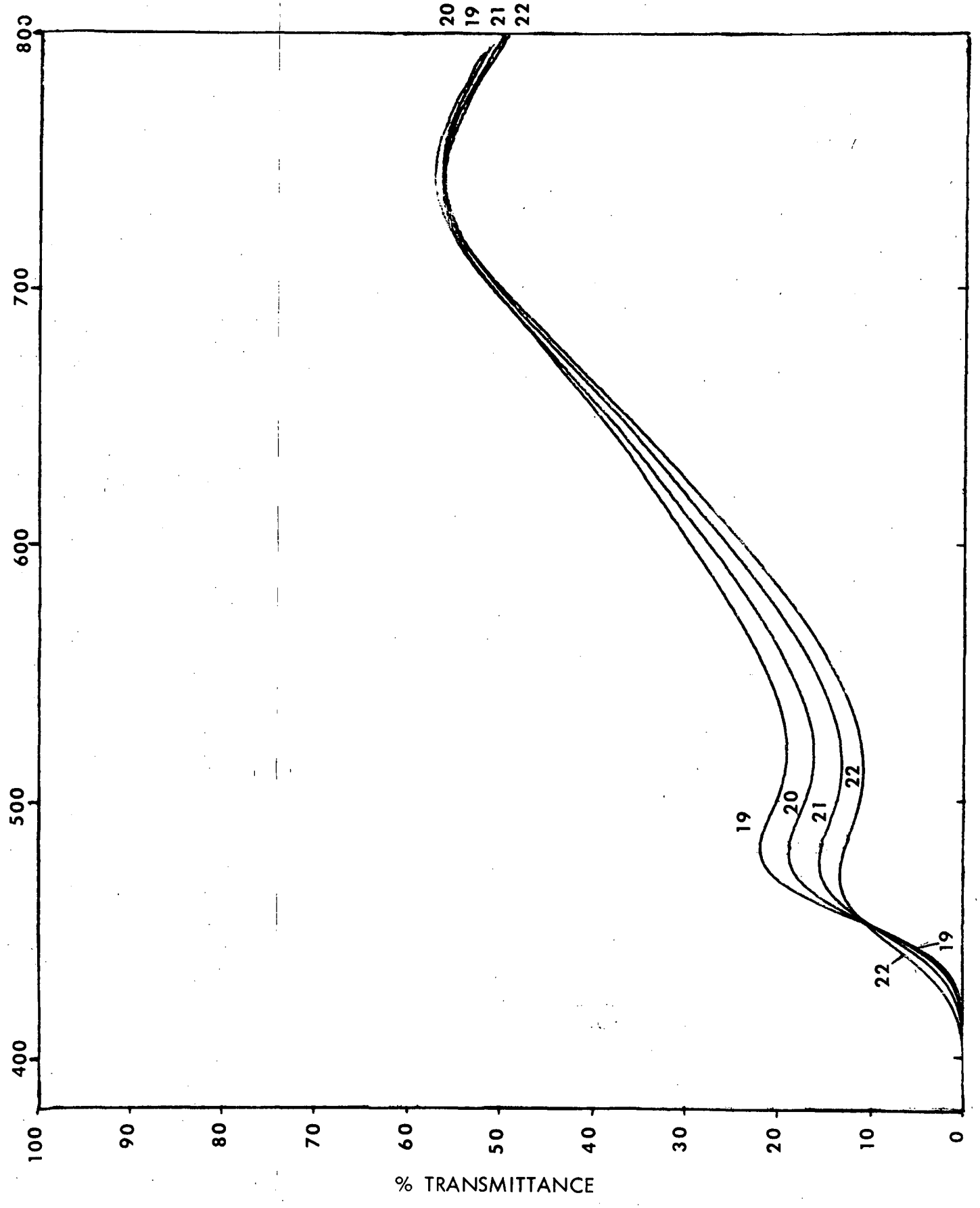

three ERTS bands, assuming rectangular bandpass characteristics, were measured with a planimeter. Using these values, we determined certain transmittance ratios of the ERTS band-equivalents for each curve; band 4 (0.5 to 0.6μ), band 5 (0.6 to 0.7μ). The results are given in Table 1. The point of this exercise was to see whether these ERTS band ratios for Forel-Ule standards resembled the corresponding reflectance ratios for lake waters. This comparison is discussed later in connection with the data in Table 5.

The band ratios as determined above by measuring the area under Forel-Ule transmittance curves were also determined experimentally in the field, using a clear sky background and reading the transmittance through each of the 22 standards with the RPMI. The RPMI, which has the same bands as ERTS, is described in detail in Appendix A. This was done to examine the "ratio technique" further as a means of characterizing the spectral shift of standards from blue to red-brown. The results of both methods are compared in Figure 8.

2.1.5 CONVERSION OF FOREL-ULE COLOR TO THE CIE SYSTEM

At present, a second method is being developed to compare the Forel-Ule expression for water color with reflectance measurements made by ERTS or similar multispectral sensors. Transmittance curves of the standards have been converted to tristimulus values in the CIE system of color specification. The 22 standards were then plotted in the CIE chromaticity diagram, as shown in Figure 9. Lines drawn from the illuminant or neutral point through these loci intersect the boundary line, indicating the "dominant wavelength" value for each standard. The percentage-distance that each standard point is displaced from the neutral point toward the boundary line is the "excitation purity." These values, summarized in Table 2, indicate that the color differences between standards are fairly constant, although standards 7 and 15 are somewhat anomalous with respect to the others.

At present, we are converting the RPMI and ERTS reflectance data to CIE coordinates by analysis of the transmission spectra of RPMI and ERTS bandpass filters. ERTS bandpass characteristics are plotted in Hugh's report (1972). This will permit a simple comparison of the lake colors recorded by ERTS with those estimated by Forel-Ule and RPMI measurements on the ground. It is important that ERTS data be evaluated in terms not only of % reflectance in each band but of the spectral colors that these values represent.

2.2 RPMI (REFLECTANCE) MEASUREMENTS OF WATER COLOR

The RPMI, developed for ERTS Experiment PR303, is being used in this investigation to measure lake reflectance (i.e., ratio of upwelling to downwelling light) in the four ERTS spectral bands. Percent reflectance, ρ, in each band is determined from the meter readings by calculation and by transfer calibration.

Table 1. Percent transmittance (integrated by planimeter) within ERTS bands 4, 5, and 6. Ratios of band transmittance.

Forel-Ule #	ERTS SPECTRAL BANDS 4	5	6	BAND RATIOS 4/5	4/6
1	.228	.127	.279	1.795	.817
2	.221	.113	.270	1.956	.819
3	.235	.144	.309	1.632	.761
4	.258	.135	.282	1.911	.915
5	.277	1.70	.343	1.629	.808
6	.296	.200	.358	1.480	.827
7	.318	.233	.396	1.365	.803
8	.357	.240	.391	1.488	.913
9	.408	.312	.454	1.308	.899
10	.496	.383	.511	1.295	.971
11	.565	.435	.539	1.299	1.048
12	.514	.447	.592	1.150	.868
13	.433	.443	.591	.977	.733
14	.406	.440	.550	.923	.738
15	.387	.482	.596	.803	.649
16	.312	.408	.532	.765	.586
17	.280	.383	.501	.731	.559
18	.250	.392	.538	.638	.465
19	.226	.402	.534	.562	.423
20	.199	.396	.552	.503	.361
21	.174	.381	.542	.457	.321
22	.152	.371	.532	.410	.286

Figure 8. Comparison of % transmittance of color standards within ERTS bands 4 and 5. Planimeter measurement of area under T-curves (——) ; direct RPMI measurement of standards (- - - -).

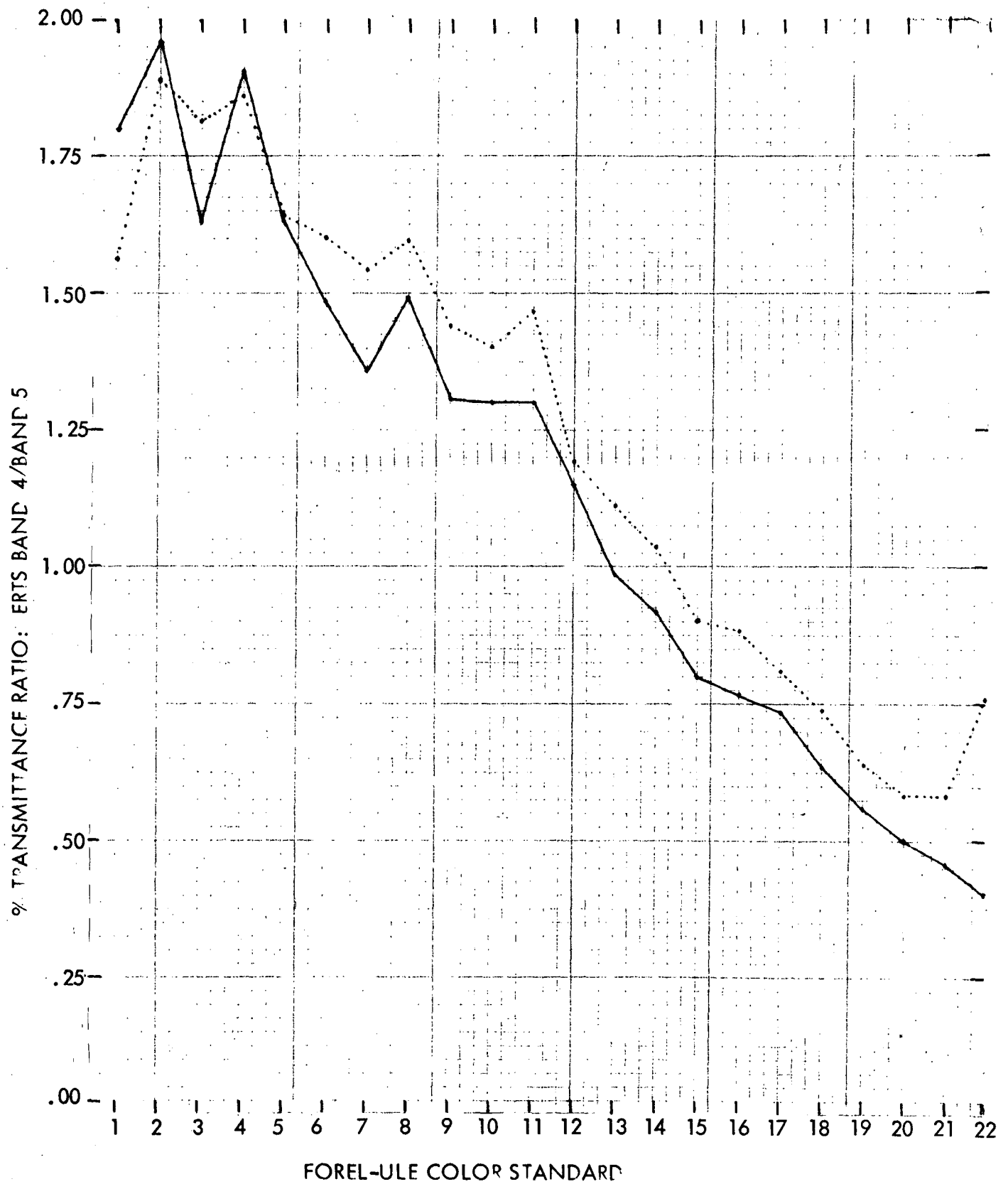

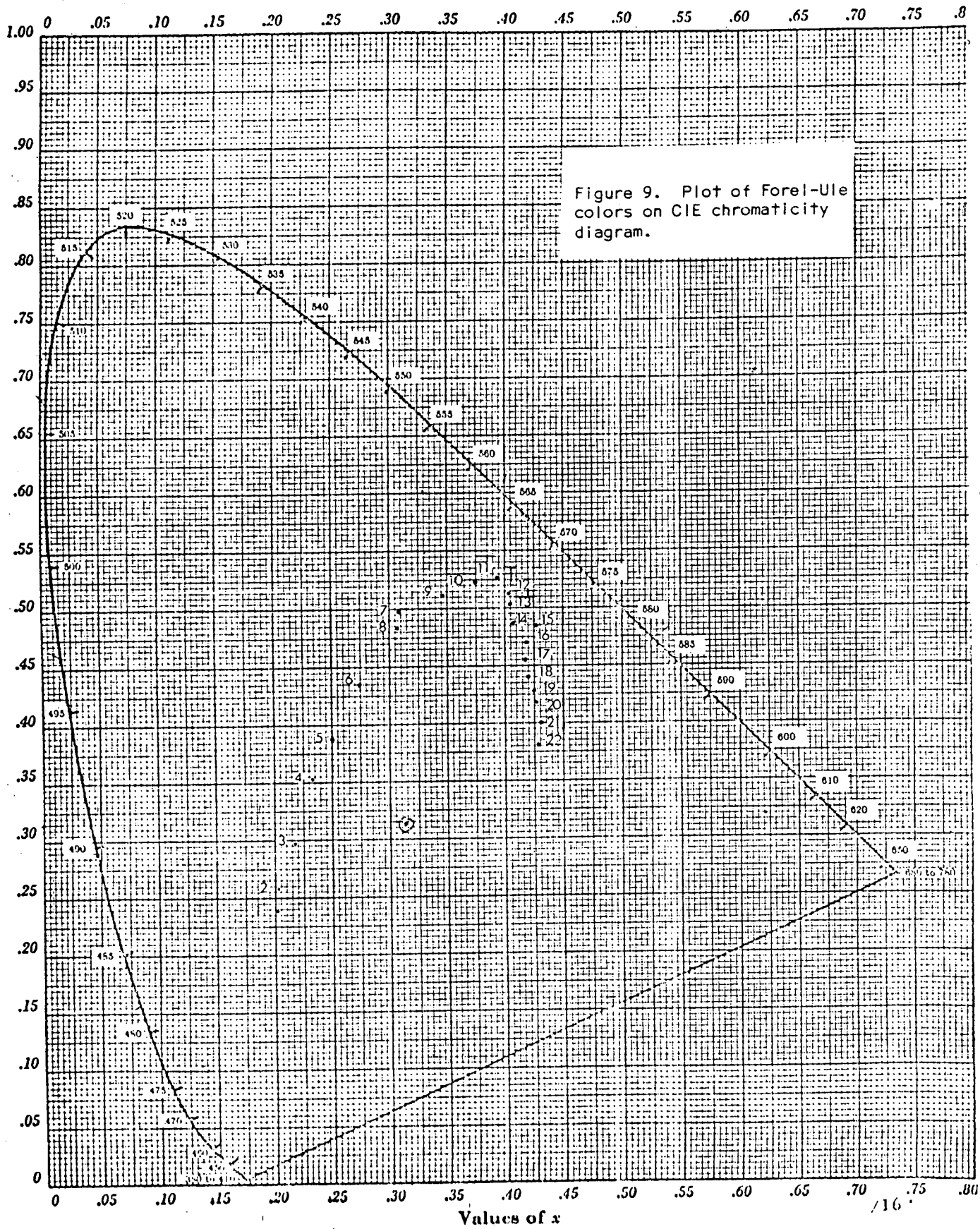

Figure 9. Plot of Forel-Ule colors on CIE chromaticity diagram.

Table 2. CIE color specification of Forel-Ule standards.

Forel-Ule Standard	CIE Coordinates X	Y	Dominant Wavelength (Hue)	Excitation Purity (Saturation)	Luminous Reflectance (Brightness)
1	.202	.238	482	.49	
2	.203	.259	484	.46	
3	.218	.298	488	.36	
4	.233	.353	497	.27	
5	.250	.386	506.5	.20	
6	.274	.435	530	.25	
7	.309	.499	550	.49	
8	.306	.483	550.5	.45	
9	.346	.512	558	.63	
10	.374	.524	563	.73	
11	.394	.526	566	.79	
12	.403	.514	568	.78	
13	.405	.503	568.5	.76	
14	.407	.488	570	.72	
15	.426	.485	572.5	.77	
16	.419	.470	572.5	.71	
17	.418	.455	573.5	.67	
18	.420	.440	575.5	.62	
19	.425	.428	578	.61	
20	.427	.419	579	.59	
21	.429	.400	582.5	.55	
22	.427	.380	585.5	.50	

(Not yet determined)

2.2.1 CALCULATION OF ABSOLUTE REFLECTANCE

If solar and atmospheric variables are known, the target reflectance, ρ, is computed from the expression:

$$\rho = \frac{\pi L K_1}{K_2 (H_{SUN} \cos Z + 1.11 H_{SKY})} ,$$

where:

L = RPMI radiance measurement (W/m^2 - Sr) made by aiming the RPMI telescope at the target.

H_{SUN} = direct sun irradiance (W/m^2) made by aiming the RPMI telescope directly at the sun.

Z = sun angle in degrees, measured from the zenith.

H_{SKY} = sky irradiance (W/m^2) made with the telescope off and the RPMI viewing the total sky with the direct sun blocked out.

K_1 = the calibration factor to correct radiance measurements (refer to Table 3a)

K_2 = the calibration factor to correct irradiance measurements (refer to Table 3b).

Table 3(a) RPMI Radiance Correction Factors, K1 (5,500°K)

MSS Band	Instrument			
	100	101	102	103
4	1.01×10^3	9.02×10^2	9.08×10^2	8.95×10^2
5	7.98×10^2	7.88×10^2	7.85×10^2	7.59×10^2
6	7.96×10^2	7.94×10^2	7.86×10^2	7.78×10^2
7	7.85×10^2	7.77×10^2	7.77×10^2	7.49×10^2

Table 3(b) Irradiance Correction Factors, K2

MSS band	Instrument			
	100	101	102	103
4	12.43	11.81	12.30	11.58
5	10.72	10.43	10.64	9.85
6	10.71	10.46	10.67	10.10
7	32.3	31.05	32.3	29.65

2.2.2 REFLECTANCE MEASUREMENT BY TRANSFER CALIBRATION

If the procedure described in Section 2.2.1 is used to establish the reflectance of color panels in each ERTS band, the calibrated panels can, in turn, be used as points of reference to determine, by "transfer calibration", the reflectance of unknown surfaces. Since the RPMI provides an output that is linear with target reflectance, the procedure is, simply, to aim the RPMI at the calibration panel(s), note the meter indication, aim the RPMI at the target of unknown reflectance, and again note the meter indication. A straight-line extrapolation transforms the meter indication obtained from the unknown target to a reflectance value.

For example, Figure 10 is a plot of the RPMI meter indication versus the reflectance of four cardboard panels, denoted A, B, C, and D. The absolute reflectance of the panels was determined for each of the ERTS bands as described in Section 2.2.1. The panels are approximately these colors (in matte finish):

- Panel A - medium brown
- Panel B - white
- Panel C - black
- Panel D - medium green.

The relationship of RPMI indications to percent reflectance in each band is noted to be a linear function. The reflectance calibrations of these panels are checked periodically by the procedure described in Section 2.2.1 to test for any change in reflectance that might be caused by fading or other pigment changes.

Figure 10. Plot of reflectance (%) vs. RPMI readings for reference panels A-D.

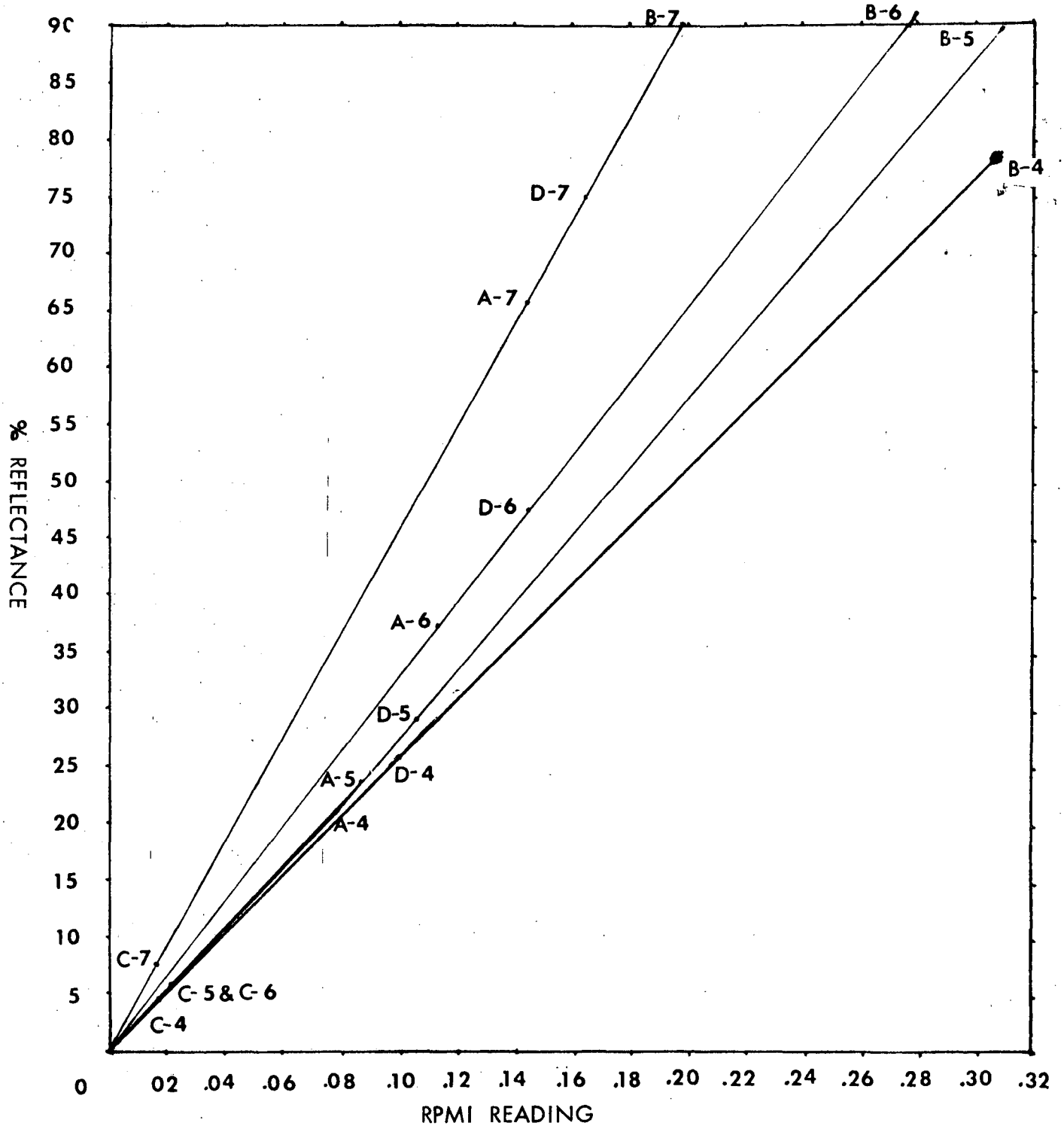

2.2.3 RPMI FIELD MEASUREMENTS

On July 13, 1973, the reflectance of Forest Lake water was estimated from a boat using this method, as illustrated in Figure 11. RPMI readings were made with the instrument held 1 meter above each panel. Immediately afterward, readings were taken with the instrument held 1 meter above the lake surface and just below the surface. The resulting reflectance values are shown in Table 4.

Table 4 Reflectance, in Percent, of Forest Lake Water on July 13, 1972

RPMI Position	ERTS Spectral Band				Band Ratios	
	4	5	6	7	4 to 5	4 to 6
Above Water	1.225	0.850	0.575	0.425	1.44	2.13
Below Water	0.730	0.485	0.210	0.075	1.51	3.48

Notably, readings taken above water are greater than those taken below water because of some specular reflectance from surface wavelets. However, as expected, the band ratio (band 4 to band 5) of upwelling light is smaller above water because of a selective loss of shorter wavelengths reflected back downward from the undersurface (Hutchinson, 1957; pg. 410). Of these, the above-water measurements should be more comparable to those recorded by ERTS.

2.3 ERTS (REFLECTANCE) MEASUREMENTS OF LAKE COLOR

The absolute (percent) reflectance of lake waters can only be derived from ERTS data if corrections are made for solar and atmospheric variables. The procedure explored, to date, is to deploy the RPMI in concert with ERTS overflights. The RPMI is then used to obtain direct measurements, within the four ERTS MSS bands, of (1) sky irradiance H_{SKY} (i.e., by shadowing sun and reading global minus direct beam-solar), (2) radiance from a narrow solid angle of sky $L_{MEAS}(\phi)$, and (3) direct beam-solar irradiance $H_{SUN}(m)$. From these measurements, additional solar and atmospheric parameters, such as beam transmittance, τ; path radiance, L_A; and direct beam-solar irradiance above the atmosphere, H_o, are determined. With these parameters, the equation

$$\rho = \frac{(L - L_A) \cdot \pi}{(H_o \tau^m \cos Z + H_{SKY})}$$

Figure 11. Transfer calibration method of determining unknown reflectance (of water) based on that of reference panels.

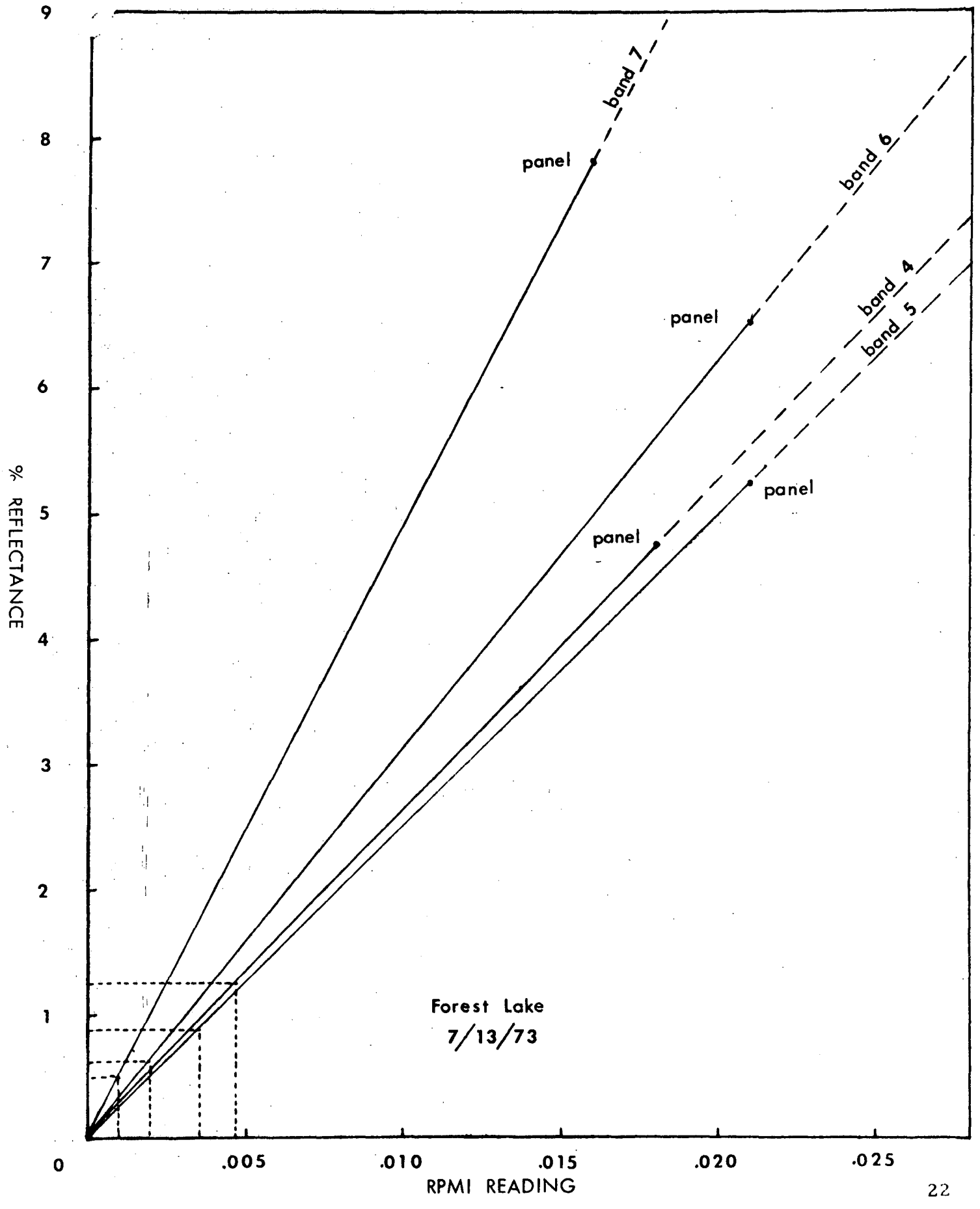

is applied, in the machine processing of ERTS CCT's, to transform the ERTS radiance measurements, L, into absolute target reflectance units. The RPMI, the procedure for obtaining the atmospheric parameters, and the use of these parameters in the machine processing of ERTS data are discussed by Rogers and Peacock in Appendix A.

2.3.1 DEPTH CONSIDERATIONS

In ERTS measurements of lake reflectance and color whether the values apply for shallow or deep water must be specified. By definition, the bottom or submerged vegetation is visible in ERTS imagery of shallow waters but not in imagery of deep waters. Reflectance values for both shallow and deep areas can be important in gauging lake trophic levels, but for different reasons. Strictly for assessments of water color caused by suspended and dissolved matter, only deep water, uncomplicated by bottom reflections, is useful. Therefore, appropriate deep areas in each study lake were chosen by these criteria:

- The area must be sufficiently deep so that the bottom is never visible, even in periods of high water transparency (For lakes in this area, this depth is 8 or more meters.)

- The area must be large enough for adequate resolution in ERTS imagery. Lake areas of 16 or more acres are desired.

The selected deep-water test areas are shown in Figures 12 through 14.

2.3.2 COMPARISON OF ERTS AND RPMI REFLECTANCE DATA

Table 5 shows reflectance measurements of the deep water areas derived from the ERTS data of March 27, 1973 using solar and atmospheric parameters derived from RPMI measurements. The table also includes lake reflectance measured directly with the RPMI and water transparency and color estimates which were made concurrently on the lakes. Finally, the ERTS and RPMI MSS band ratios (band 4 to band 5) are compared.

The test lakes are listed in the table in order of increasing trophic level, as indicated by their transparency and color values. On comparing the ERTS and RPMI data by MSS band, we note the following trends with increasing turbidity and color:

a. Bands 4 and 5 - ERTS values are consistently larger than RPMI values (except for Orchard Lake, band 5).

Figure 12. Map of study lakes showing sampling stations and areas selected for reflectance measurements (ERTS data).

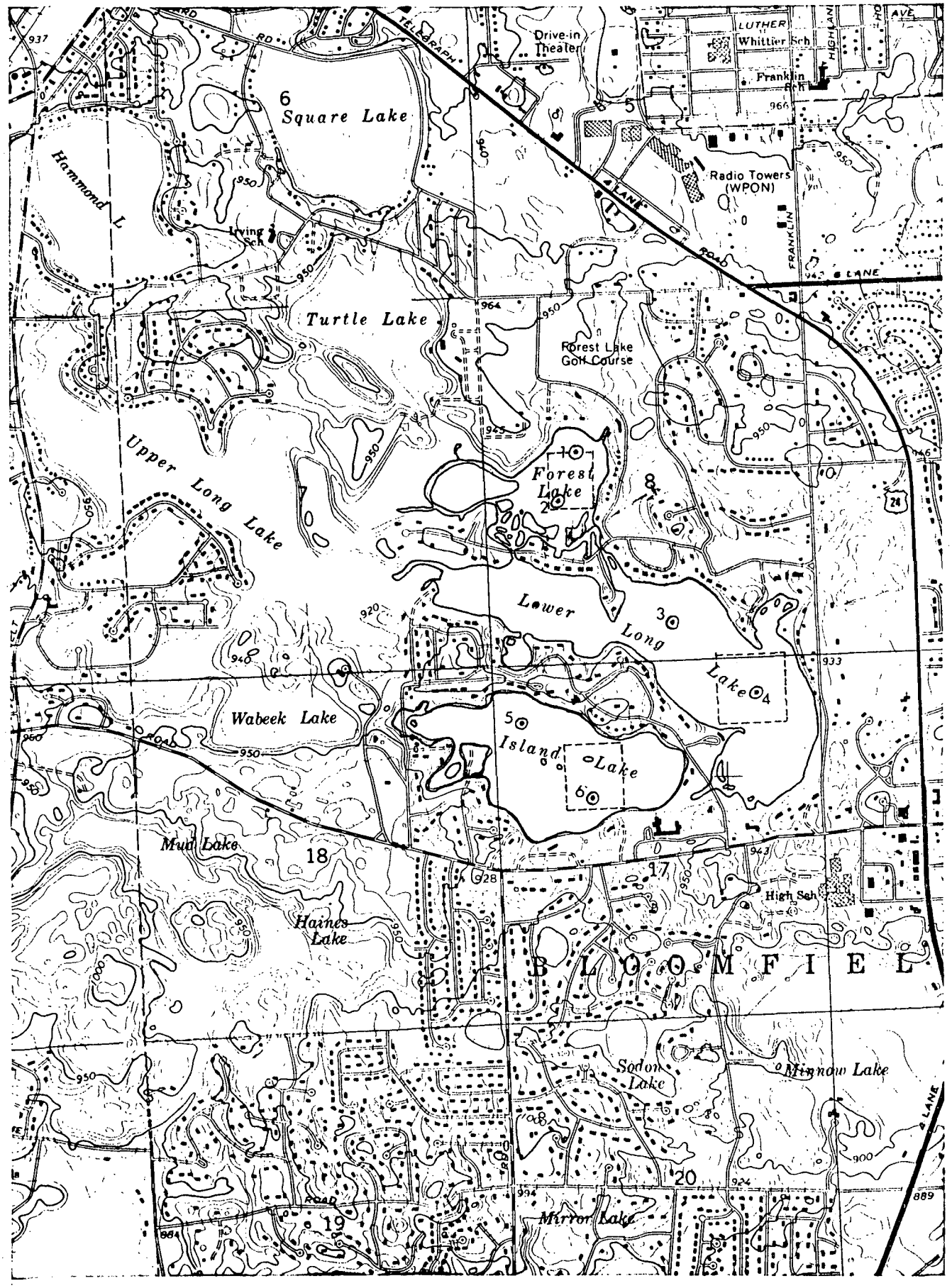

Figure 13. Map of study lakes showing sampling stations and areas selected for reflectance measurements (ERTS data).

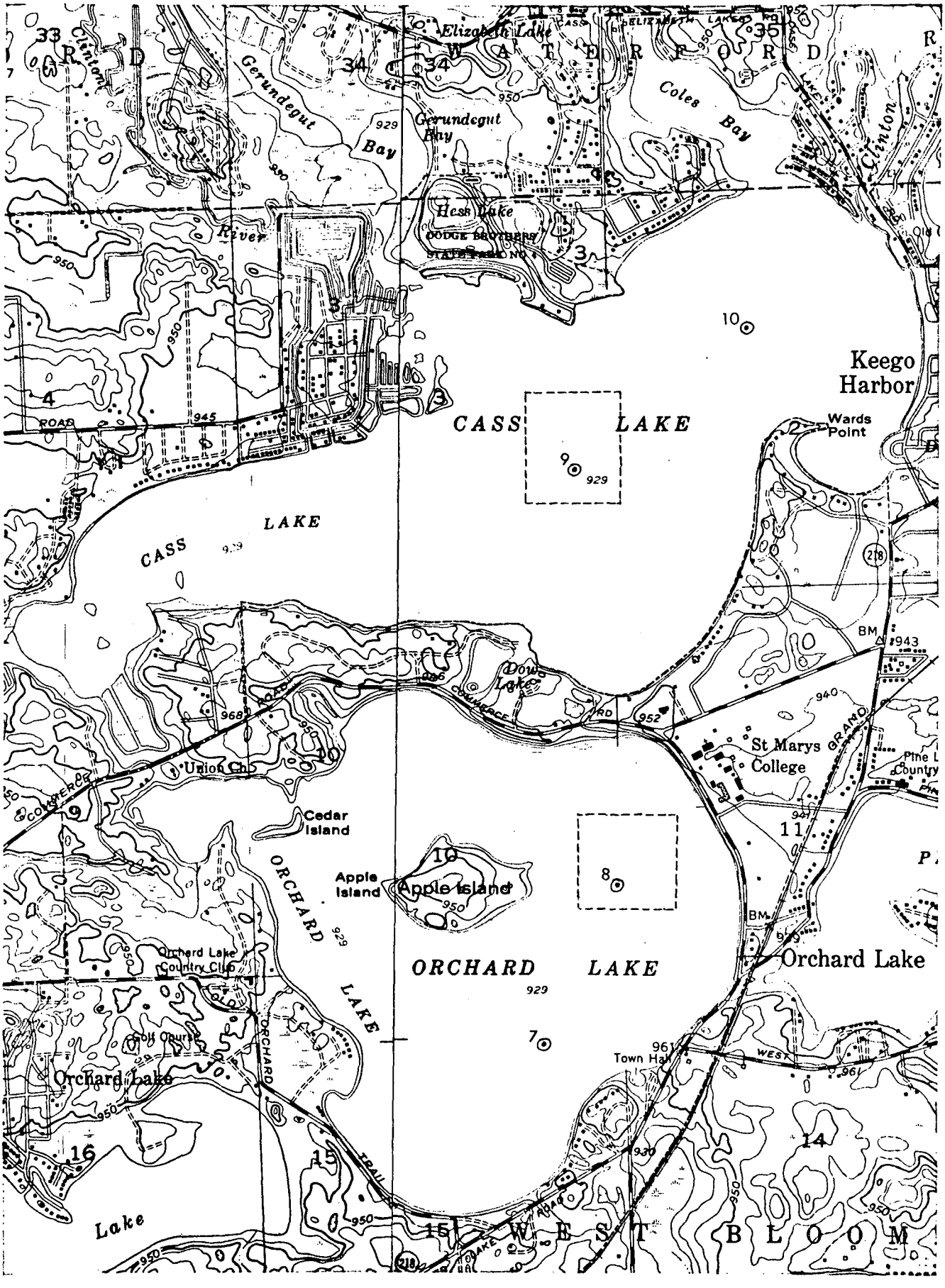

Figure 14. Map of study lakes showing sampling stations and areas selected for reflectance measurements (ERTS data).

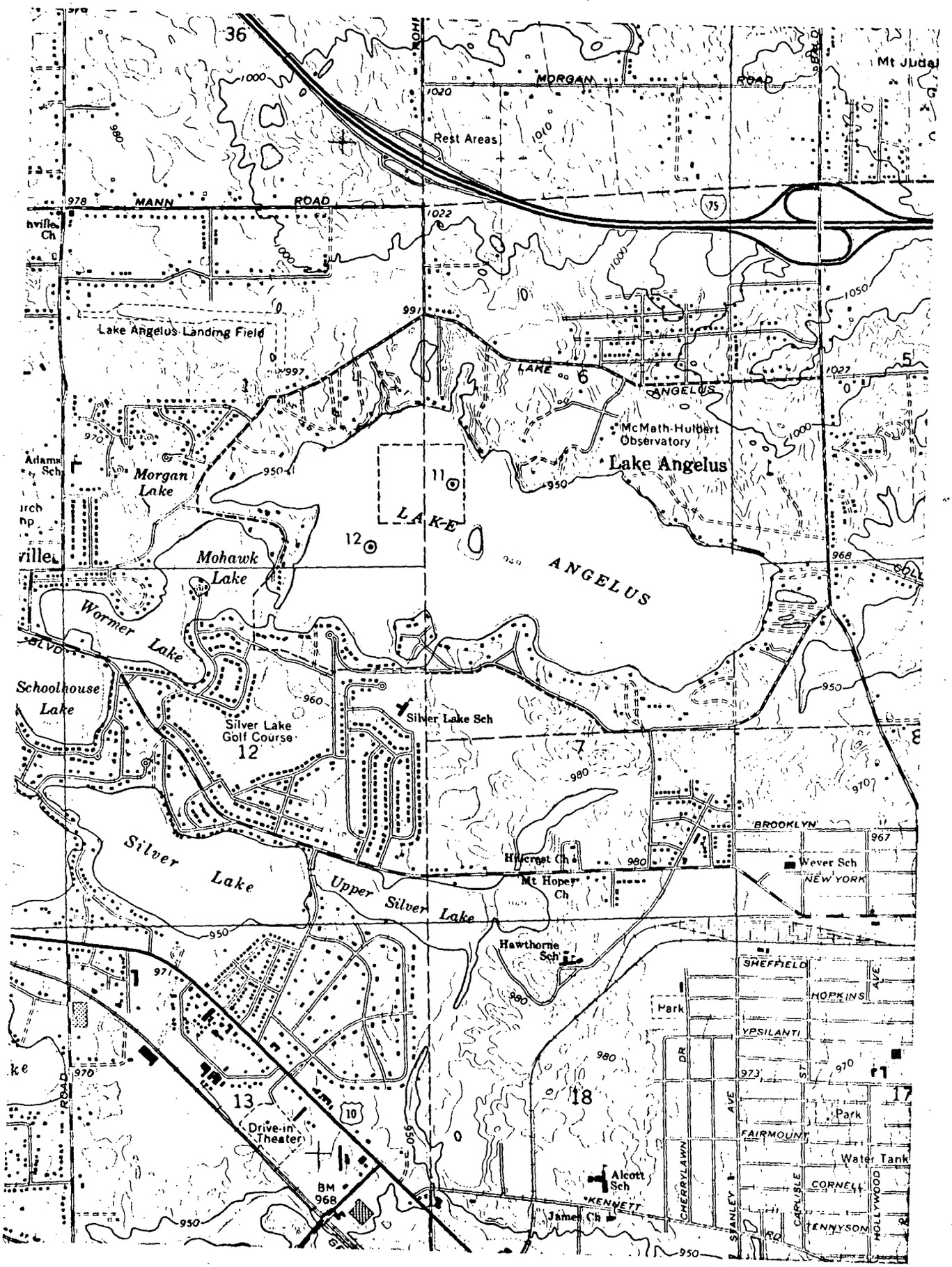

Table 5 Surface Reflectance, in Percent, of Lakes Recorded by ERTS and RPMI Sensors on March 27, 1973, Compared to Water Transparency and Color on the Same Date

Lake	Sensor	MSS Band 4	MSS Band 5	MSS Band 6	MSS Band 7	MSS Band Ratio (4 to 5)	Transparency (Secchi Depth)	Forel-Ule Color
Huron	ERTS	4.40	0.060	0	0	73.33	No readings taken	
	RPMI	No readings taken						
Orchard (Sta. 8)	ERTS	4.00	0.520	0	0	7.69	4 m	10
	RPMI	2.38	0.717	0.218	0	3.32		
Lower Long (Sta. 4)	ERTS	3.60	1.20	0.270	0.150	3.00	4.0 m	14
	RPMI	1.84	0.997	0.490	-	1.85		
Forest (Sta. 1 and 2)	ERTS	3.30	1.20	0	0	2.75	2.8 m	16-17
	RPMI	1.34	0.997	0.474	-	1.34		
Island (Sta. 5 and 6)	ERTS	3.97	1.60	0.350	0.370	2.48	1.5 m	16
	RPMI	1.610	1.010	0.460	0.0767	1.59		

b. Bands 4 and 5 - The proportional differences between ERTS and RPMI data increase.

c. Bands 6 and 7 - ERTS values are consistently smaller than RPMI values.

d. Band 4 to band 5 ratio - ERTS ratios are consistently larger (although both ERTS and RPMI ratios decrease).

The significance of the differences between ERTS and RPMI is hard to assess with so few data. However, it appears that either ERTS MSS is not fully calibrated, as expected, or atmospheric corrections for the ERTS data are not yet fully adequate. The margin of error seems to vary with wavelength. Yet it is important to note that the band ratios (band 4 to band 5) in both ERTS and RPMI data follow the expected pattern; that is, the proportion of green to red upwelling light decreases as the lakes become more turbid and brown-colored. Jerlov (1968) has described the same kind of relationship for ocean waters, as shown in Figure 15(a). Clarke et al. (1970) also presented radiometric curves of Atlantic Ocean water, showing that a spectral shift toward longer wavelengths was correlated with increasing chlorophyll content, as shown in Figure 15(b).

2.3.3 SURFACE EFFECTS

Pertinent to the spectral signatures given above for deep lake waters are those for lakes which have surface films or mats of plant material. Algal scums, for example, are typical of highly eutrophic lakes and may well occur over deep water. Some macrophytes, like Lemna (duckweed) and Wolffia (water meal) are floating species which may cover large areas.

On July 5, 1973, using the RPMI, we measured the radiance reflected from plant materials on the surface of two ponds adjacent to Upper and Lower Long Lakes. The appearance and nature of these scums is shown in Figures 16 and 17. The results are given in Table 6.

The following conclusions can be drawn from the data in Table 6.

- Floating films of plant material (25 to 100% coverage) greatly increase the reflectance of water (Refer to Table 4).

- Increased reflectance caused by floating plants is much more strongly increased in the reflective infrared (band 6) than in the visible range (bands 4 and 5).

Figure 15. Correlations of organic content and spectra of upwelling light for ocean waters.

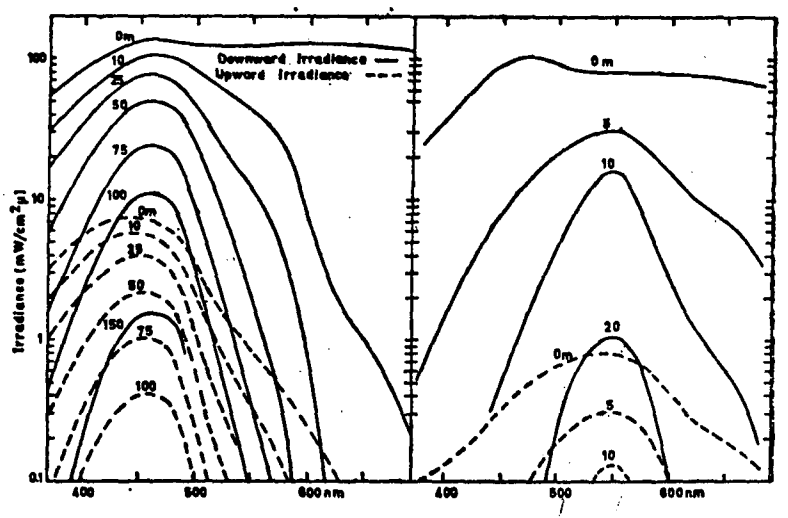

(a) (from Jerlov, 1968)

Fig.53. Comparison between spectral distribution of downward and upward irradiance for solar elevation of 55—60°. Left: Sargasso Sea ("Dana" expedition, 1966). Right: Baltic Sea (after AHLQUIST, 1965).

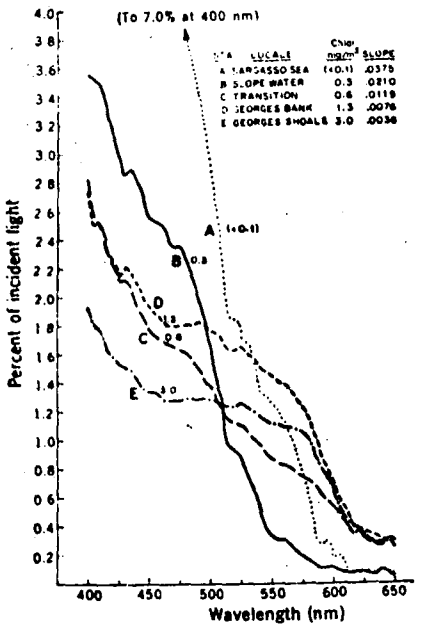

Fig. 4. Spectra of backscattered light measured from the aircraft at 305 m on 27 August 1968 at the following stations (Fig. 2) and times (all E.D.T.): Station A, 1238 hours; Station B, 1421 hours; Station C, 1428.5 hours; Station D, 1445 hours; Station E, 1315 hours. The spectrometer with polarizing filter was mounted at 53° tilt and directed away from the sun. Concentrations of chlorophyll a were measured from shipboard as follows: on 27 August, Station A, 1238 hours; on 28 August, Station B, 0600 hours; Station C, 0730 hours; Station D, 1230 hours.

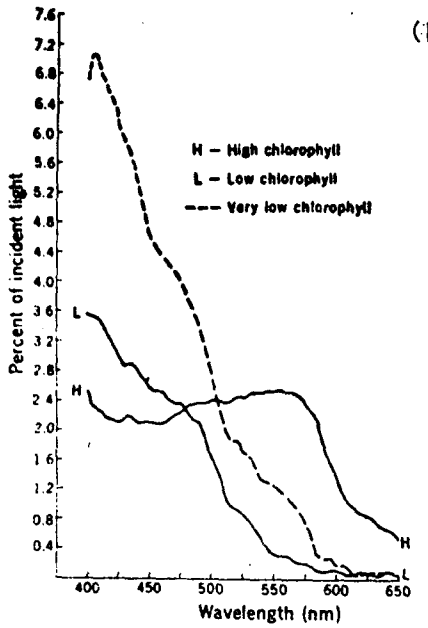

(b) (from Clarke, et al., 1970)

Fig. 3. Data from the high and low chlorophyll curves plotted as percentage of the incident light and compared with data taken on the same day from an area with very low chlorophyll concentration south of the Gulf Stream.

A. Algal scum (spirogyra) on Upper Long Lake channel, July 5, 1973. Reflectance measured by RPMI.

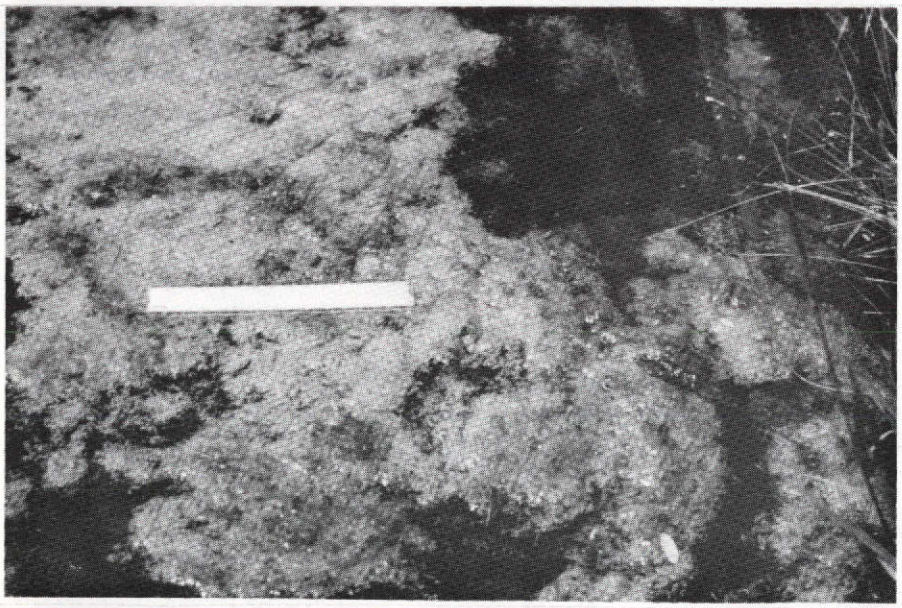

B. Spirogyra mat with trapped oxygen bubbles near shore. Scale is 6 inches.

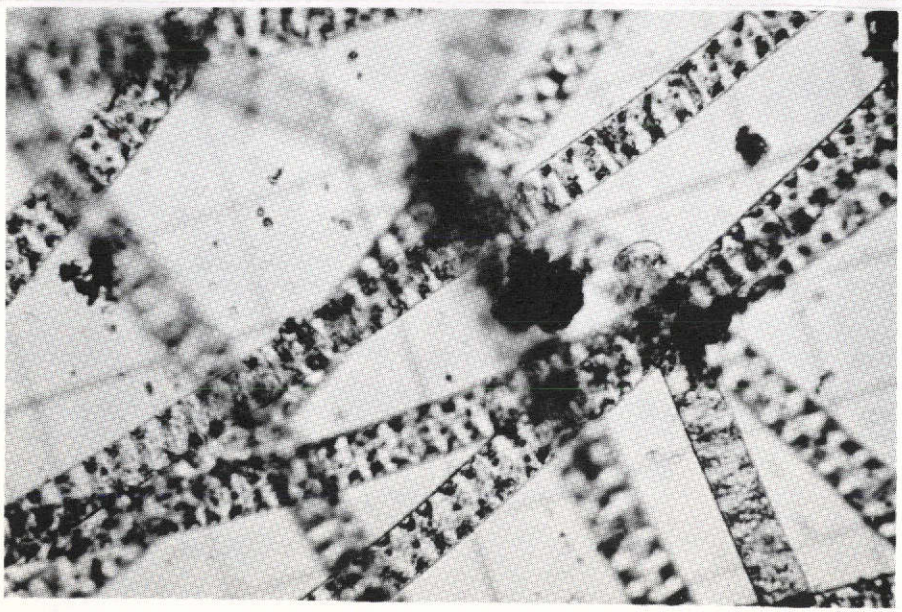

C. Microscopic view of spirogyra as above. (100x)

Figure 16

A. Floating Macrophytes (Wolffia) on Dollar Pond near Lower Long Lake, July 5, 1973. Reflectance measured by RPMI.

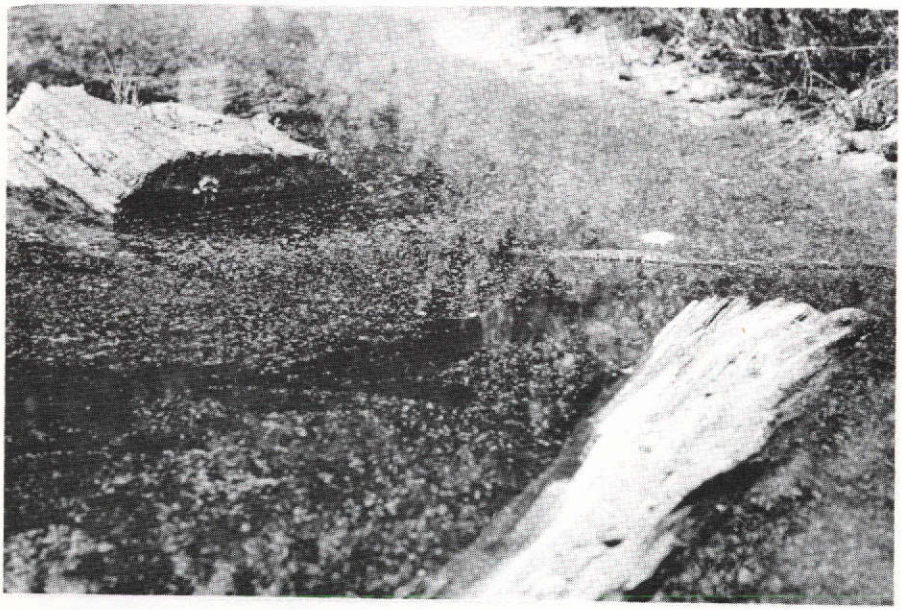

B. Wolffia covering about 30 percent of water surface.

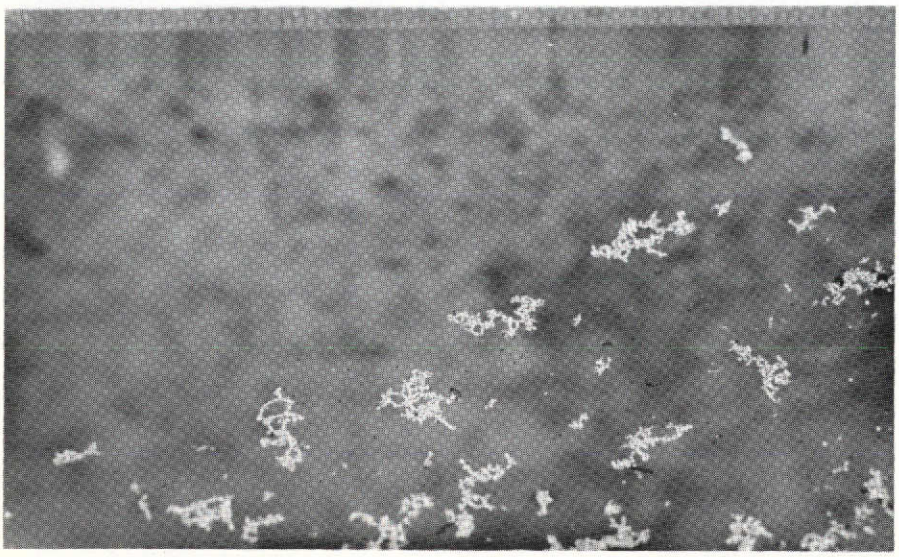

C. Close-up view of Wolffia plants. Approximately 1/2 natural size.

Figure 17

Table 6 Radiance, in W/m^2-Sr, of Floating Plants on July 5, 1973

RPMI Indication	Surface Cover (%)	Spectral Band				Band Ratios	
		4	5	6	7	4 to 5	4 to 6
Wolffia sp.* (healthy)	25	21.79	20.41	1.41	1.40	1.07	15.45
Spirogyra sp. (green) (healthy)	100	50.84	40.82	55.02	54.39	1.25	0.92
Spirogyra sp. (brown-green) (unhealthy)	100	51.96	48.67	53.45	52.84	1.06	0.97

*Underlying water brown and turbid.

- Healthy green Spirogyra as compared to unhealthy brown-green Spirogyra is less reflective in the visible spectrum (bands 4 and 5) and more reflective in the infrared.

- In band 4 relative to band 5, healthy Spirogyra is more reflective than the unhealthy alga, but less reflective relative to band 6.

- Surface films of plant material should be readily distinguished in ERTS data from their absolute reflectance in relation to open water, particularly in the infrared. The band ratio band 4 to band 6 or band 4 to band 7 seems to be proportional to the amount of surface coverage.

2.4 MULTISPECTRAL IMAGERY AND LAKE COLOR

As noted previously, March 27 was the only occasion so far in this study for which ERTS data, aircraft MSS data, aerial color photography, RPMI readings, and water color/quality data are available. The CCT's from the NASA C-130 overflight have just been received and are not yet processed. The ERTS CCT's over the lake area for the March data were processed, using the RPMI-derived atmospheric parameters to transform ERTS data to reflectance units. The reflectance units were displayed as color on a color-coded TV monitor and by computer symbols on a gray-scaled printout. The procedures used are discussed in Appendix A.

D

Figure 18 shows the color-coded TV display of reflectance patterns in Orchard and Cass Lakes in ERTS channels 4, 5, and 7. Interferences caused by a "banding effect" are apparent as horizontal lines, particularly in bands 5 and 7. A gray-scaled reflectance printout of band 4 of Orchard Lake is shown in Figure 19 for comparison with an aerial photograph on the same date. Although the upper portion of the reflectance gray-scale is missing, some vertical elongation of the lake is evident in comparison to its shape in the photograph. This is partially caused by the non-symmetry of the printout technique. However, it is still possible to make some observations about the significance of the reflectance level patterns.

Within the gray-scale printout of Orchard Lake, six discrete levels of reflectance are observed in band 4. Over the six test lakes, up to seven levels were observed in this same band.

The distribution of computer symbols indicating a reflectance ranging from 3.1 to 5.5 percent corresponds generally with the known deep-water areas. Shallow waters in this same band (bottom visible in the aerial photograph) correspond to a reflectance distribution in the order of 5.5 to 8.7 percent. The progressively more reflective areas within that range compare fairly well with shallower and shallower water. The reflective character of the bottom itself is important, as well as the water depth. This image will be more interesting when compared to a mid-summer view in which the "optical depth" will be reduced in places by growths of aquatic plants. Finally, the reflectance levels from 8.7 percent upward correspond to land. As noted earlier, surface films of plants on lakes will produce higher ranges of lake reflectance.

2.5 CORRELATION OF REFLECTANCE DATA AND WATER QUALITY

Field and laboratory analyses of lake water have been conducted at the time of each ERTS pass. Inclement weather has caused some gaps in sampling and some of the ground truth has not been accompanied by ERTS imagery because of cloud cover. To date, a total of eight days should have been clear enough to provide acceptable imagery.

The correlation of water reflectance values and water quality is difficult, owing to the many factors that influence water color, directly or secondarily. Nonetheless, certain factors considered good indicators of lake trophic levels also have a definite effect on lake color and reflectivity. Among these are transparency (Secchi depth), apparent color (Forel-Ule number), particulate carbon, turbidity, chlorophyll, and planktonic algae (Refer to Table 7). Additional guideposts of trophic level are particulate nitrogen and soluble nitrite-nitrate. The data on most of these variables are summarized in Figures 20 through 56 in Appendix B. It is too early to offer a general review of these variables for each lake or to attempt

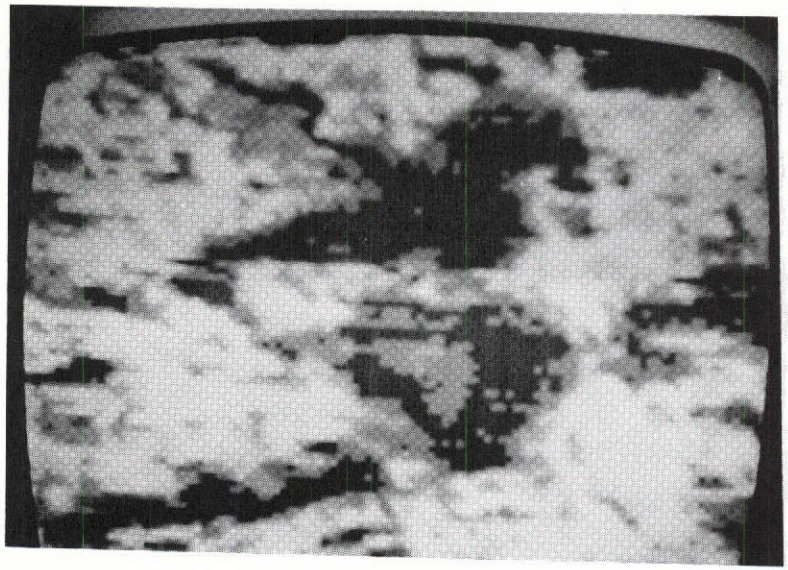

ERTS Band 4

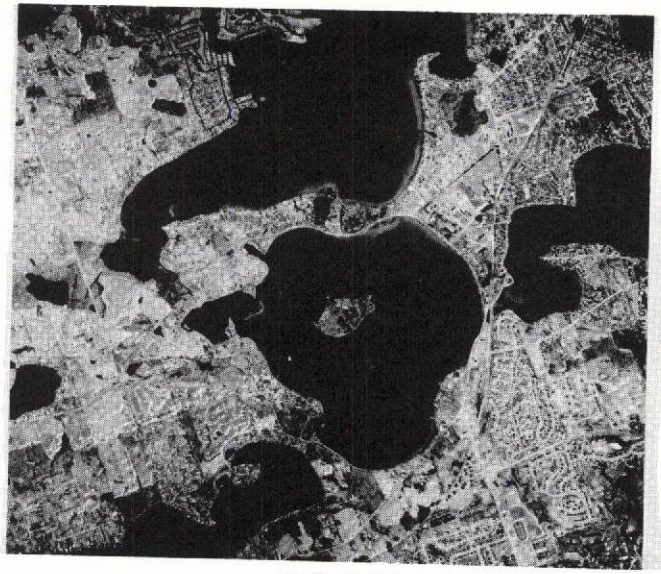

Aerial Photograph

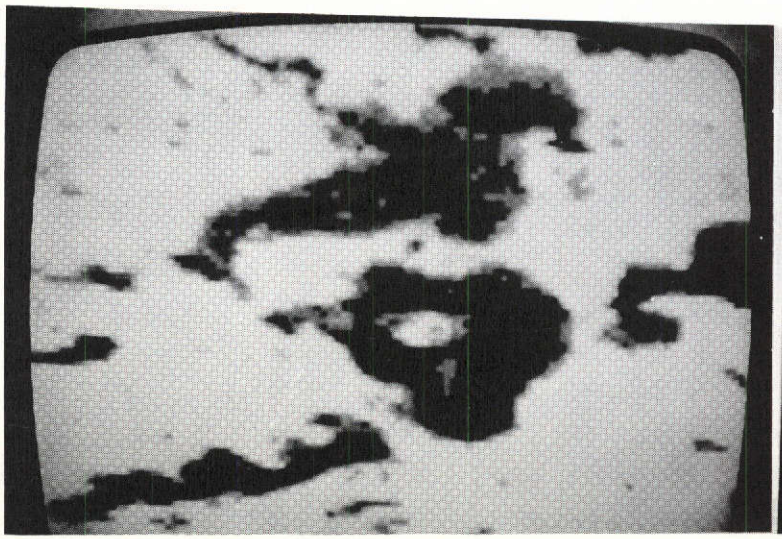

ERTS Band 5

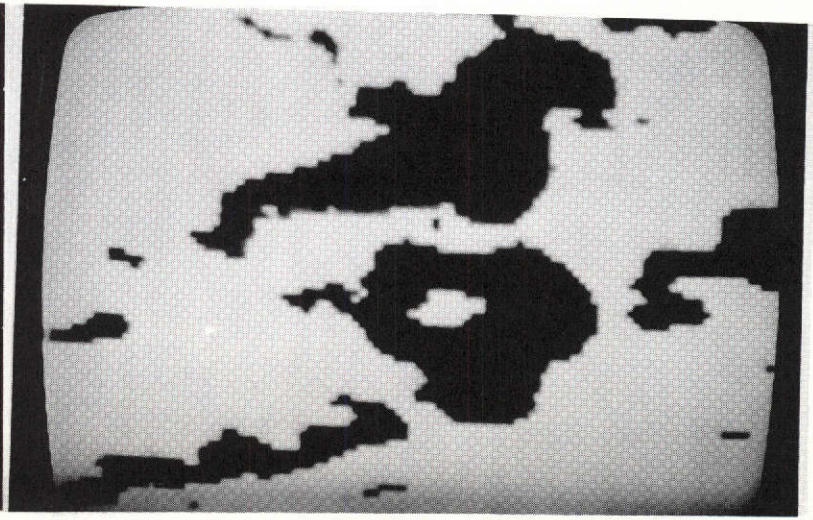

ERTS Band 7

Figure 18 Comparison of Orchard and Cass Lakes Using Color Reflectance Displays and Aerial Photograph. ERTS Imagery of March 27, 1973

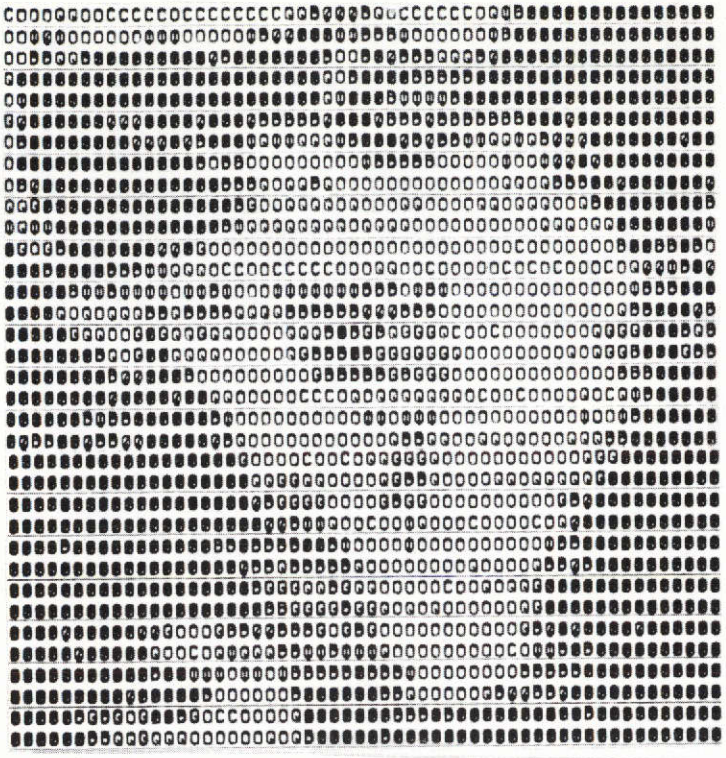

CHARACTER	REFLECTANCE RANGE
	0.000 - 0.006
.	0.010 - 0.014
/	0.018 - 0.027
C	0.031 - 0.035
0	0.039 - 0.047
Q	0.051 - 0.055
@	0.059 - 0.067
G	0.071 - 0.075
B	0.079 - 0.087
8	0.091 - 0.095
8	0.099 - 0.100

Figure 19 Comparision of ERTS reflectance printout (band 4) and aerial photograph. Orchard Lake, March 27, 1973

Table 7 Classification of Algae Identified in Water Samples
(See Figures 32 to 43 of Appendix B)

Taxonomy	Identification No.
Div. Cyanophyta	
Cl. Myxophyceae	
Ord. Oscillatoriales	
Fam. Oscillatoriaceae	
Gen. Oscillatoria	1
Ord. Chroococcales	
Fam. Chroococcaceae	
Gen. Anacystis	2
Gen. Merismopedia	4
Fam. Nostocaceae	
Gen. Anabena	3
Div. Chrysophyta	
Cl. Bacillariophyceae	
Ord. Pennales	
Fam. Fragillariaceae	
Gen. Fragillaria	11
Gen. Asterionella	12
Cl. N/A	
Ord. Chrysomonadales	
Fam. Ochromonadaceae	
Gen. Dinobryon	13
Gen. Ankistrodesmus	14
Div. Chlorophyta	
Cl. N/A	
Ord. Zygnematales	
Fam. Desmidiaceae	
Gen. Closterium	21
Gen. Cosmarium	22
Gen. Schenedesmus	23
Div. Pyrrophyta	
Cl. Dinophyceae	
Ord. Peridiniales	
Fam. Ceratiaceae	
Gen. Ceratium	31

to correlate them with ERTS data. At this point, however, the following comments about the dominant factors of water color in each lake are in order:

- Water color and quality do not appear to vary greatly at the two sampling stations on each lake. At least, the differences between lakes are far more significant. This means that only one central, deep-water station in each lake is needed to provide a good representation of surface water conditions in all deep areas within the lake.

- Apparent trends for each lake follow:

  Forest Lake. A good correlation has usually existed between water color, transparency, and particulate carbon. On June 7, lowest carbon and highest transparency values coincided with a population of mainly green algae. The brownest water color occurred on May 21 between periods of blue-green and green algal dominance. Highest color/turbidity values coincided with high diversity in algal flora. Forest Lake was consistently browner than the other lakes.

  Lower Long Lake. Very good correlation was noted between color, transparency, and carbon. The highest transparency on May 21 was accompanied by the dominance of green algae over blue-green algae. On June 7 and July 13, the highest color/turbidity coincided with high algal diversity.

  Island Lake. The best transparency values on May 21 corresponded to the dominance of green algae over blue-green and golden-brown algae (Chrysophyta). The extreme low transparency on March 27 was caused by green nannoplankton bloom. The water color was variable and often correlated with carbon and transparency.

  Orchard Lake. Algal species differ between stations. A pronounced sequence of algal dominance; golden-browns to blue-greens to greens to blue-greens; occurred. Water color became steadily bluer since March 27, then became brown, coincident with sudden high turbidity and carbon and low transparency on July 13. Orchard Lake as been the clearest and bluest of the six lakes.

  Cass Lake. Very good correlation was found between the carbon transparency and color. The lowest carbon was noted on June 6 and 25, following a green algal dominance. Again, high turbidity/color combinations during June 25-July 13 were accompanied by great algal diversity. Cass Lake has been the second brownest lake (after Forest Lake).

Lake Angelus. The data collection has been spotty at Lake Angelus, but there is apparently good correlations between color, transparency, and carbon. The color has been variable. Lake Angelus was the bluest on June 25-July 13, although turbidity was the highest on July 13. Next to Lower Long Lake and Orchard Lake, Angelus Lake has been the clearest lake.

3. NEW TECHNOLOGY

There has been no new technology developed to date.

4. FUTURE WORK PLANNED

4.1 REVIEW OF THE PROBLEM

Our experiences so far with the processing and analysis of ERTS data have resulted in a clearer picture of how ERTS can be developed as a broad survey monitor of lake eutrophication. Before discussing the course of future work, a short review is in order. The following is the general sequence of seasonal events related to eutrophication in a typical, moderately-eutrophic lake; e.g., Lake Michigan.

- Early Spring (March-April): plankton blooms, low to high turbidity; no bottom macrophyte growth; no emergent plants; water color green (i.e., algal blooms) or brown (runoff and deep water turnover).

- Early Summer (May-June): mostly low turbidity, few blooms; some bottom macrophytes; few emergents; water color blue-green to brown.

- Late Summer (July-August): moderate turbidity, blooms; macrophyte/emergent growth at peak; water color green to brown.

- Fall (September-October): blooms, high turbidity; dying macrophytes and emergents; water color green or brown.

In this scenario, there are four categories of information that relate to trophic level and may be measurable by ERTS. These are:

- Surface scums/mats (plant material)

- Turbidity/color of deep water

- Bottom vegetation (macrophytes) in shallow water

- Emergent vegetation (shallow water and lake margins).

Another important factor is how all of the above phenomena change - seasonally and from year to year. By these indicators, the rate of lake eutrophication is best measured by a remote sensor, since nutrients themselves are not

visible. It is clearly necessary that each of these indicators be monitored with respect to its seasonal distribution and gross quantitative changes within a lake. The following plan has been designed to carry out that kind of analysis.

4.2 ANALYSIS PLAN INDICATED

In subsequent work, this investigation will attempt to develop the following program for the routine analysis of lakes using ERTS data.

a. Determine lake outlines and islands by manual interpretation of band 7 printouts of ERTS data from early spring or use decision-processing to locate and plot map overlays showing water-land interface boundaries. Map out adjacent swamps, either automatically or through manual interpretation of bands 4 and 5.

b. Look for correlation between ERTS measurements and surface films (scums or mats of plant materials). RPMI measurements have shown that these are highly visible in the reflective infrared (bands 6 and 7) and contrast strongly with open water of any depth.

c. Separate, by automatic machine processing, deep and shallow water areas within lakes. In early spring imagery, identify deep waters using a gray-scale printout of a test lake with known bathymetry. Apply canonical analysis and automatic machine processing to identify deep/shallow waters in other lakes.

NOTE

The method must distinguish between deep/highly turbid water and shallow/very clear water.

d. Characterize deep water areas (Spring to Fall) as to:

1. Range of reflectance levels (data select program).

2. Absolute reflectance (average) of sample deep area. Correct for solar and atmospheric conditions by RPMI or weather data.

3. CIE color specification (average) of sample deep area and Forel-Ule equivalent.

4. Band ratios (band 4 to bands 5, 6, and 7) from percent reflectance values in sample area.

e. Characterize shallow waters (Spring to Fall) as to:

1. Range of reflectance levels (as above).

2. Vegetated versus non-vegetated bottoms. Compare early spring and late summer reflectance gray level printouts. RPMI field data will give clues as to bottom reflectance with/without macrophyte vegetation.

3. Emergent and floating vegetation in shallows and around lake margins. Compare early spring and late summer printouts.

4. Absolute reflectance and band ratios, where shallows are extensive enough. These values best relate to lake bathymetry in early spring.

5. CONCLUSIONS AND RECOMMENDATIONS

The significant conclusions which can be made by this program at this date are the following:

a. Lakes and islands of one acre or more are detectable in ERTS imagery. Lake boundaries are resolved best in band 7.

b. ERTS data can be transformed into absolute target reflectance signatures by removing solar and atmospheric parameters from ERTS radiance measurements. Reflectance within the five test lakes was determined, from the ERTS data, to range from 3.1 to 5.5 percent in band 4 and 0.3 to 2.3 percent in band 5.

c. Reflectance caused by the atmosphere (path radiance or path reflectance), L_A, if not properly determined and removed from ERTS data, causes an error of up to 500 percent in the computation of lake reflectance.

d. In ERTS band 4, up to seven reflectance levels were derived within the test lakes. The distribution of these reflectance patterns has been produced on a color-coded TV display and on computer-generated gray-scales.

e. Deep and shallow water can be separated by a trained photo-interpreter, using reflectance printout gray-scales or a TV monitor. Two or more deep-water categories may be classified from ERTS data within the test lakes. Estimates of water depth may be possible in some areas.

f. The RPMI is a valuable aid in measuring the atmospheric parameters needed to transform ERTS data to reflectance units. It also permits direct spectral signature measurements of lakes and lake features, such as algal scums and floating plants. Reflectance can be derived from the ratio of reflected radiance to global irradiance measurements or by "transfer calibration" using panels of known reflectance. These measurements permits rapid measurements of a large number of lake features in the field, thereby establishing the categories and their characteristics that will be measurable in ERTS data.

g. A method for obtaining lake color from ERTS and RPMI measurements, as estimated by the Forel-Ule standards, has been presented and partly worked out. As a step in accomplishing this, both the Forel-Ule and reflectance (ERTS and RPMI) values are being converted to the CIE tristimulus values. However, continued, detailed study of these relationships is necessary and planned.

h. There appears to be a strong correlation between browner water color, diminishing water transparency, and increasing particulate carbon and algal diversity in the study lakes. Dominance of green algae (Chlorophyta) was often accompanied or followed by clearer and greener water.

i. At this point, classifying lake eutrophication by the occurrence of surface scums or macrophytes in shallow water with ERTS data seems to be a straightforward matter. However, the most important problem remaining is how to establish and discriminate between the subtle colors of deep water, since the colors are related to plankton trophic levels. Processing software which will sort out and classify (by reflectance, band ratios, etc.) similar water colors in different lakes has the highest priority. Capability of detecting a one-to-two Forel-Ule unit separation in water color will represent significant differences in water quality and trophic level.

6. REFERENCES CITED

Clarke, G. L., G. C. Ewing, and C. J. Lorenzen; 1970. Spectra of Backscattered Light from the Sea Obtained from Aircraft as a Measure of Chlorophyll Concentration; Science, 167: 1119-1121.

Forel, F. A.; 1889. Ficerche fisiche sui laghi d'Insubria; Rend. R. 1st Lombardo, ser. 2.22: 739, 742.

Hazen. A.; 1892. A New Color Standard for Natural Waters; Amer. Chem. J. 14: 300-310.

Hughs; Report No. HS324-5214, Multispectral Scanner System for ERTS - Four-Band System", August 1972.

Hutchinson, G. E.; 1957. A Treatise on Limnology. Vol. 1.; John Wiley and Sons, Inc., New York. 1015 p.

Jerlov, H. G.; 1968. Optical Oceanography; Elsevier Publishing Company, New York. 194 p.

Ule, W.; 1892. Die Bestimmung der Wasserfarbe in den Seen. Petermanns Mitt. 38: 70-71.

APPENDICES

APPENDIX A

MACHINE PROCESSING OF ERTS AND GROUND TRUTH DATA

Dr. Robert H. Rogers and Dr. Keith Peacock

The Aerospace Systems Division
of the
Bendix Corporation, Ann Arbor, Michigan

I. ABSTRACT

Results achieved by ERTS-Atmospheric Experiment PR303, whose objective is to establish a radiometric calibration technique, are reported. This technique, which determines and removes solar and atmospheric parameters that degrade the radiometric fidelity of ERTS data, transforms the ERTS sensor radiance measurements to absolute target reflectance signatures. A Radiant Power Measuring Instrument (RPMI) and its use in determining atmospheric parameters needed for ground truth are discussed. The procedures used and results achieved in machine processing ERTS computer-compatible tapes and atmospheric parameters to obtain target reflectance are reviewed.

II. INTRODUCTION

The need for target reflectance signatures evolves from the needs of individual Principal Investigators, NASA's requirements to correlate results of a large number of investigators, and the pre-conditions of wide-area extrapolations of ground truth data for automatic data processing techniques. Target reflectance data are needed by all-man and machine systems to obtain the unambiguous interpretation of ERTS data. In response to the need for absolute target reflectance signatures, the ERTS-1 Experiment PR303 is evaluating the capabilities of a wide range of techniques for determining and removing solar and atmospheric parameters and effects from ERTS data. Techniques being evaluated include (1) transferring known ground reflectance to spacecraft measurements, (2) using the ground-based Radiant Power Measuring Instrument (RPMI) to measure, directly, the needed solar and atmospheric parameters, (3) using spacecraft data alone (no auxiliary inputs), and (4) using radiation transfer models employing inputs such as surface pressure, ground visibility, temperature, relative humidity, etc.

This paper describes the results achieved to date in the development of the ERTS radiometric calibration technique employing the RPMI. Section III describes the atmospheric problem and defines the solar and atmospheric parameters needed to transform ERTS radiance measurements into reflectance. Section IV describes the RPMI and, in Section V, methods for deploying RPMI to obtain required atmospheric parameters are described. The procedures used and the results achieved in machine-processing ERTS computer-compatible tapes and atmospheric parameters to obtain the reflectance of a number of lakes is reported in Section VI.

E

III. ATMOSPHERIC PROBLEM

The reflectivity, ρ, of a diffusely reflecting target, is given by

$$\rho = \frac{L_T \pi}{H} \quad , \tag{1}$$

in which L_T is the radiance and H is the total (global) irradiance at the target surface. When radiance is measured at a remote distance, the detected value, L, has two components; a target value $L_T \tau$, where τ is the atmospheric transmission from target to sensor, and a component due to atmospheric radiance, L_A. The desired target reflectance in terms of the remote radiance measurement, L, is then

$$\rho = \frac{L - L_A}{\tau} \cdot \frac{\pi}{H} \quad . \tag{2}$$

The target irradiance, H, also has two components; one due to the direct sun, denoted $H_{sun} \cos Z$ (in which H_{sun} is the irradiance on a surface normal to the sun's rays and Z is the solar zenith angle) and a component due to the sky, denoted H_{sky}. Expanding H of Equation 2 in terms of the direct sun and sky components results in

$$\rho = \frac{(L - L_A) \cdot \pi}{\tau (H_{sun} \cos Z + H_{sky})} \quad . \tag{3}$$

For a remote sensing system looking vertically downward, τ is the atmospheric transmission of one air mass. If m is the number of air masses referenced to the zenith air mass (for which m = 1), the atmospheric transmission through some other value of m is given by τ^m. The direct sun component of target irradiance, H_{sun}, in Equation 3 can be subdivided as

$$H_{sun} = H_o \tau^m \quad , \tag{4}$$

in terms of the solar irradiance normal to the sun's rays outside the atmosphere, H_o. Combining Equations 3 and 4, the desired target reflectance, ρ, in terms of ERTS radiance, L, measurements is

$$\rho = \frac{(L - L_A) \cdot \pi}{\tau (H_o \tau^m \cos Z + H_{sky})} \quad , \tag{5}$$

where L_A, τ, H_o, m, cos Z, and H_{sky} are the solar and atmospheric parameters that must be known to accurately compute target reflectance.

In the machine processing of ERTS computer compatible tapes (CCT's), the parameters L, H_o, m, and Z of Equation 5 are easily and quickly determined. Target counts, c_i, are recorded on ERTS CCT's and easily transformed to the desired target radiance, L of Equation 5, by

$$L_i = c_i K_i \quad mw/cm^2 - Sr \quad , \tag{6}$$

where i indicates MSS band number and constants K_i are determined as described on Page 6-14 of the ERTS Data User Handbook (K_4 = 0.0195, K_5 = 0.0157, K_6 = 0.0138, K_7 = 0.0730). The sun zenith angle, Z, is computed from $Z = 90 - \theta_E$, in which the sun elevation angle, θ_E, is also extracted from the ERTS CCT. For sun zenith angles less than 60 degrees, the air mass, m of Equation 5, is given to an accuracy better than 0.25 percent by m = sec Z. For larger sun angles, a more accurate value is given by Bemporad's formula

$$m = \sec Z - 0.001867 (\sec Z - 1) - 0.002875 (\sec Z - 1)^2 - 0.0008083 (\sec Z - 1)^3 . \tag{7}$$

The solar irradiance, H_o, outside the earth's atmosphere is well known and changes less than 6 percent over a 12-month period. Its value(s) can be determined from the published data (Thekaekara, 1971) or measured by procedures described in Section V. The remaining solar and atmospheric parameters needed for Equation 5, namely L_A, τ, and H_{sky}, depend on the specific atmosphere within the scene and must be determined by the Principal Investigator at the time of ERTS overflight, if accurate spectral reflectance of his targets are to be derived.

IV. RADIANT POWER MEASURING INSTRUMENT (RPMI)

The RPMI shown in Figure 1 was developed specifically to provide an ERTS investigator with the capability of obtaining the complete set of solar and atmospheric measurements he needs to determine target reflectance from the ERTS radiance data.

The RPMI is a rugged, hand-carried, portable instrument calibrated to measure both down welling and reflected radiation within each ERTS MSS band. A foldover handle permits a quick change from wide-angle global or sky irradiance measurements to narrow angle (7.0° circular) radiance measurements from sky and ground targets.

The RPMI's wide dynamic range (1 to 10^6) is tailored to permit measurements to be made over the full range of solar and atmospheric parameters encountered by ERTS investigators. These extremes have been found to include direct beam solar irradiance up to 25 mw/cm^2 in Band 7, sky radiance as low as 0.077 mw/cm^2 - Sr in Band 6, and radiance reflected from water surfaces in Bands 6 and 7 as low as 0.02 mw/cm^2 - Sr. The RPMI measurements are traceable to an NBS source to an accuracy of 5 percent absolute and 2 percent relative from band-to-band. The RPMI calibration is also checked, from time to time, against the NASA Goddard calibration source to ensure uniformity between RPMI and ERTS MSS measurements.

V. DETERMINATION OF ATMOSPHERIC PARAMETERS

The RPMI is deployed in concert with ERTS overflights as shown in Figure 1 to obtain the direct measurements, within the four ERTS MSS bands, of (1) global irradiance, H, (2) sky irradiance H_{sky} (i.e., by shadowing sun and reading global minus direct beam-solar), (3) radiance from a narrow solid angle of sky $L_{MEAS}(\phi)$, and (4) direct beam-solar irradiance $H_{sun}(m)$. From these measurements, additional solar and atmospheric parameters, such as beam transmittance, τ; path radiance, L_A; and direct beam-solar irradiance above the atmosphere, H_o, are determined. With these parameters, Equation 5 is then applied to transform the ERTS radiance measurements, L, into absolute target reflectance units.

GLOBAL IRRADIANCE

Global irradiance, H, is measured directly in each band as shown in Figure 1. Additional accuracy in H can be obtained by measuring the direct-beam solar irradiation, H_{sun} (m), and sky irradiance, H_{sky} (direct sun shadowed out), and then computing the total target irradiance, using

$$H = H_{sun}(m) \cos Z + H_{sky} \quad . \tag{8}$$

The sun angle, Z, may be read from the sun dial on the side of the RPMI after leveling the instrument with its bubble level.

DIRECT BEAM SOLAR IRRADIANCE

Direct beam solar irradiance, H_{sun}, is measured by pointing the instrument directly at the sun with the telescope in place and recording the irradiance at each wavelength.

BEAM TRANSMITTANCE

Beam transmittance, τ, per unit air mass is determined directly from

$$\tau = \left(\frac{H_{sun}}{H_o} \right)^{\frac{1}{m}} \tag{9}$$

when the solar irradiance outside the atmosphere, H_o, is known. The air mass is calculated from the solar zenith angle, using Equation 7.

BEAM TRANSMITTANCE AND SOLAR IRRADIANCE OUTSIDE THE ATMOSPHERE

Beam transmittance, τ, and solar irradiance outside the atmosphere, H_o, can be determined by making a series of H_{sun} measurements and then plotting an "extinction" curve as shown in Figure 2. For this case, H_{sun} is plotted on a logarithmic scale as a function of air mass. The intercepts of the lines with the vertical axis (i. e., at m = o) gives H_o in each ERTS MSS band. The beam transmittance per unit air mass, τ, is then computed from either Equation 9 or from

$$\tau = \left(\frac{H_{sun}(m_1)}{H_{sun}(m_2)} \right)^{\frac{1}{m_1 - m_2}}, \tag{10}$$

where

$H_{sun}(m_1)$ = direct beam solar irradiance at air mass m_1.

$H_{sun}(m_2)$ = direct beam solar irradiance at another air mass, m_2.

It can be shown that the slope of the extinction curve is log τ, and Equation 10 follows directly.

The value of H_o (i. e., H_{sun} at m = o), once determined for each RPMI band, may be used to test and/or recalibrate the RPMI, using the sun as a source, at any location in the world.

SKY IRRADIANCE

Sky irradiance, H_{sky}, is measured by leveling the RPMI with the built-in bubble level so that the diffuser is horizontal with the target surface and can receive irradiation from 2 π steradians. H_{sky} is the irradiance recorded when the direct beam sun is shadowed out using an opaque object.

PATH RADIANCE

Path radiance, L_A, is the energy reaching the spacecraft from Rayleigh and aerosol scattering by the atmosphere. As it cannot be measured directly, it must be derived from ground-based sky radiance measurements of the backscatter. The simplest technique is to use the RPMI to measure the sky radiance $L_{MEAS}(\phi)$ scattered at angle ϕ, as shown in Figure 3, such that ϕ is identical to ϕ', the angle through which radiation is scattered to the spacecraft, and then to correct this measurement for the difference in air masses between the direction of observation and the direction of the spacecraft. This technique provides a straightforward measurement procedure when Z > 45 degrees. If Z < 45 degrees, atmospheric modeling is necessary to extrapolate from the available measurement angles to the desired scattering angle. When L_{MEAS} is recorded at an angle equal to the scattering angle to the ERTS, the path radiance, L_A, seen by ERTS is

$$L_A = L_{MEAS} \left(\frac{1 - \tau}{1 - \tau^{m_o}} \right), \tag{11}$$

in which m_o is the air mass in the direction of observation (in this case $m_o = \frac{1}{\cos \beta}$) and τ, as previously defined, is the atmospheric transmission per unit air mass. The validity of this formula has been demonstrated by Rogers and Peacock (1973) and discussed by Gorden, Harris, and Duntley (1973). Equation 11 is adequate when the atmospheric measurements are made concurrent with the ERTS overflight (i. e., at a sun angle close to the one at the time of the ERTS flyover).

A correction factor, T_{ERTS}/T_Z, must be applied to Equation 11 to derive the path radiance, L_A, viewed by the spacecraft if the time between ERTS overpass of test site and sky radiance observations is significantly different. An approach for determining this correction factor is shown in Figure 3.

Sunlight entering the atmosphere at an angle, Z, as shown in Figure 3, is scattered at altitude h into the direction of the observer at point 0. The energy available for scattering depends on the atmospheric extinction coefficient, $\tau_{\infty h}$, measured from outside the atmosphere to altitude h. The attenuation is given by $\exp(-\tau_{\infty h} \cdot m)$. The energy scattered is a function of the scattering coefficient, α_h, at altitude h. Thus, the energy scattered in the direction of the observer from altitude h is proportional to

$$\exp(-\tau_{h\infty} \cdot m) \cdot \alpha_h . \tag{12}$$

The average attenuation, for all altitudes, suffered by the energy in passing from the sun to point x is given by

$$T = \frac{\sum_N \exp(-\tau_{h\infty} \cdot m) \cdot \alpha_h}{N \sum_N \alpha_h} , \tag{13}$$

in which N defines each atmospheric altitude used in the summation. Use of the value α_h in the equation expresses the importance of h in contributing energy at the observer location point, 0. A normalizing factor is included in the denominator. Values of $\tau_{h\infty}$ and α_h have been tabulated (Valley, 1965). To adjust $\tau_{\infty h}$ from a standard atmosphere to the actual atmospheric conditions at the observer's location, $\tau_{\infty h}$ is multiplied by $\exp(-\tau_{\infty 0})/\tau$, in which τ is the measured atmospheric transmission and $\tau_{\infty 0}$ is the extinction coefficient for a beam traversing one atmospheric air mass of a standard atmosphere. This is also given by Valley (1965). Variations in T are small, so the error in using a corrected standard rather than a real atmosphere is small.

Thus, a complete formula which gives the sky radiance, L_A, at the time of the ERTS overpass from L_{MEAS} made at another solar zenith angle and air mass is:

$$L_A = L_{MEAS}(\phi) \left[\frac{1 - \tau}{1 - \tau^{m_o}}\right] \frac{T_{ERTS}}{T_Z} , \tag{14}$$

in which ϕ, the scattering angle to the observer, equals the scattering angle to ERTS, and T_{ERTS} and T_Z are given by Equation 13 for the zenith angles at the time of the ERTS passage and the time of the L_{MEAS} readings.

The validity of this equation is demonstrated in Figures 4 and 5. Figure 4 shows ground-based sky radiance measurements as a function of the scattering angle for a range of solar air masses. Each of the curves was obtained by pointing the RPMI at the sun and then sweeping it in azimuth and in elevation, taking sky radiance readings at 10 degree intervals. Alongside each curve, the solar air mass at the time of the observations is given. The curve defined by the open squares, which falls steeply, is for a range of solar air masses, and was produced by recording the zenith sky radiance over a period of several hours. Application of Equation 14 to

these data in Figure 4, assuming $T_{ERTS} = 1$, gives the results shown in Figure 5. Except for about ± 5 percent of scatter, all the points now follow the same line. By selecting L_A from the curve at the scattering angle which exists at the time of ERTS overflight, and multiplying this value by T_{ERTS}, the desired value of L_A at the time of the ERTS overflight is determined.

These observations are continuing in order to establish the repeatability and the accuracy of the derived L_A when measurements at only one or two angles are used.

VI. MACHINE PROCESSING OF ERTS AND RPMI DATA

The ERTS CCT's and RPMI measurements are machine-processed in the Bendix Earth Resources Data Center (ERDC) pictured in Figure 6. The nucleus of this center is a Digital Equipment Corporation PDP-11/15 computer with 32 K words of core memory, two 1.5 M-word disc packs, two 9-track 800 bpi tape transports, a line printer, a card reader, and a teletype unit. Other units are an Ampex FR-2000 14-track tape-recorder; a bit synchronizer and tape deskew drawers which can reproduce up to 13 tape channels of multispectral data from high density tape recordings; a high-speed hard-wired special-purpose computer for processing multispectral data; a 70-mm laser film recorder for recording imagery on film; and a color moving-window computer-refreshed display.

Different approaches for computing target reflectance from ERTS data are being investigated in the ERDC. Some of these are summarized in the block diagram of Figure 7. The approach illustrated in the figure that leads to the most accurate transformation of ERTS data to reflectance is the application of Equation 5 and the full set of solar and atmospheric parameters (L_A, H_o, τ, and H_{sky}) as defined in Section V.

Another approach, also illustrated in Figure 7, operates on the assumption that RPMI measurements concurrent with the spacecraft overflight are unavailable. In this case, the objective is to make best use of atmospheric parameters determined from previous RPMI missions (i.e., historic values) which have been stored in the computer data base. The accuracy of computational strategies, such as assuming that some of the atmospheric parameters can be neglected (i.e., $L_A = 0$), assuming that some are the same as those derived from a standard atmosphere, etc. are also being explored.

The accuracy of each approach is being carefully determined by comparing reflectance generated from ERTS tapes to reflectance of ground truth targets whose reflectance is measured directly with the RPMI. This step is also shown in Figure 7.

These approaches to the machine processing of ERTS CCT's are illustrated, using ERTS data acquired on 27 March, 14 April and 21 May over Lake Huron and the four small lakes, Orchard, Lower Long, Forest, and Island, which are located in Oakland County, Michigan. Personnel from Bendix, Cranbrook Institute, and Oakland University deployed (1) RPMI's to measure atmospheric parameters and spot reflectance of the lakes, (2) a Secchi Disk to determine the depth of light penetration into the water, and (3) Forel-Ule instrumentation to determine water color.

One of the first data reduction steps is to transform RPMI measurements into a complete set (H_o, τ, H_{sky}, and Z) of solar and atmospheric parameters. These parameters for the 27 March mission are recorded in Table 1. Two methods of utilizing these parameters to obtain a quick-look view of the ERTS scene is to utilize Equation 5 to transform ERTS data to reflectance units and then to produce a color-coded or gray-scaled computer printout of the ERTS scene, as shown in Figure 8. In this case, the color on the TV monitor and the symbol on the computer print-out is directly related to target reflectance. The scenes shown in Figure 8 are those of Orchard Lake. The lake is approximately three miles on a side and the scene is approximately six miles on a side.

To obtain statistical information (i.e., average counts, average radiance, average reflectance, standard deviations, etc.) on specific target areas, such as the deep water in Orchard Lake, etc., the gray-scale print-out is used as a map to establish the coordinates of the target, using scan-line count and resolution element numbers. These coordinates, input to the computer, define data areas (edits) where the desired statistical computations are performed.

the lakes; Huron, Orchard, Lower Long, and Forest; was obtained. The results of these computations, recorded in Table 2, show that the reflectance of the lakes vary from a high of 4.4 percent (Band 4 in the deep clean area of Lake Huron) to a low of essentially zero in Band 7. Also listed in Table 2 is the spot reflectance of the lakes measured directly with the RPMI. The ERTS MSS Band 4 is shown to be giving a higher reflectance value than the RPMI ground truth value. The reason for this difference has not been established at this time. Also recorded in Table 2 is the ratio of ERTS and RPMI Band 4 to Band 5, the Secchi Disk measurements, and the Forel-Ule measurements. Quick-look analysis of the data in Table 2 shows a strong correlation between the ERTS reflectance ratios (Bands 4 to 5), the distance which light penetrates the water, and the water color, i.e., the higher the ratio, the greater the water transparency and the bluer the water. This finding has great value to water quality applications.

To establish the effect of atmospheric scatter (path radiance), L_A, on the accuracy of computing reflectance of lakes from ERTS data, the same lake edits were processed using RPMI-derived L_A values and using $L_A = 0$. The results of this processing are shown in Table 3 and establish that if L_A is ignored (i.e., assumed zero), then errors of 400 to 500 percent result when attempting to determine the reflectance of water surfaces.

To evaluate the possibility of using historical values of atmospheric parameters to reduce ERTS data, atmospheric parameters determined for March were used to process April and May CCT's. The results of this trial are recorded in Table 4 and show errors that also range up to 400 percent. The error here, however, is not as large as that which results from neglecting path radiance completely; i.e., $L_A = 0$. The error in this reflectance computation is caused primarily by the improper choice of L_A, which can not be assumed to be a constant. This could have been predicted since the scattering angle, ϕ, varies from month to month with the sun angle, i.e., $\phi = 180 - Z$.

VII. SUMMARY

This ERTS experiment is determining the procedures and techniques for obtaining and utilizing solar and atmospheric parameters in the machine processing of spacecraft data. Results of field test show that the RPMI will provide the full range of solar and atmospheric measurements needed by machine processing techniques to transform spacecraft data into absolute target reflectance.

The results of processing ERTS CCT's and RPMI ground truth measurements gathered in Michigan on 27 March 1973 establish that the removal of atmospheric parameters from ERTS data permits the computation of the absolute reflectance of lakes. The reflectance of these lakes, in deep water areas, was determined to range from 5 percent in Band 4 to zero in Band 7. Lake water quality, as indicated by water transparency and color, appears measurable in the reflectance derived from ERTS Bands 4 and 5 and the ratios of the reflectances of these bands.

Neglecting path radiance, L_A, in the computation of lake reflectance results in errors in the order of 400 to 500 percent in Bands 4 and 5. When atmospheric parameters (H_o, τ, H_{sky}, and L_A) derived for the March mission were applied to the ERTS data acquired in April and May again, the major source of error, which ranged from 200 to 400 percent in lake reflectance computations, was found to be contributable to an improper choice of path radiance, L_A. This error was expected since this parameter changes from month to month as the scattering angle ($\phi = 180 - Z$) changes as a function of sun zenith angle. A more accurate technique for predicting path radiance based on previous measurements is under development.

The research reported here is continuing. Field measurements with RPMI's are made on every suitable ERTS overpass of Michigan test sites. The performance achieved by the RPMI calibration technique is being used as a baseline to compare effectiveness of alternative techniques to correct ERTS data for effects of atmosphere that degrade radiometric fidelity of spacecraft data. It is hoped that the results of this research will contribute to the identification of the most cost-effective grouping of instruments and processing techniques to achieve radiometric calibration of ERTS data gathered on a world-wide basis.

VIII. REFERENCES

1. S. Q. Duntley, J. I. Gordon, and J. L. Harris; Applied Optics; June 1973; "Measuring Earth-to-Space Contrast Transmittance from Ground Stations"; pgs 1317-1324.

2. ERTS Data User Handbook; NASA Document 71SD4249; Revised Sept 1972; pg G-14.

3. R. H. Rogers and K. Peacock; "Investigation of Techniques for Correcting ERTS Data for Solar and Atmospheric Effects"; NASA-CR-131258, E73-10458; April 1973.

4. M. P. Thekaekara et al.; NASA Document SP-8005; Revised May 1971.

5. S. L. Valley, Editor; Handbook of Geophysics and Space Environments; AFCRL; 1965; pgs 7-14 to 7-35.

Table 1. Atmospheric Parameters
March 1973

Parameter	Band Number 4	5	6	7
Solar Irradiance outside Atmosphere, H_o (mw/cm^2)	18.62	15.2	12.55	25.58
Beam Transmittance, τ	0.752	0.824	0.852	0.877
Sky Irradiance, H_{sky} (mw/cm^2)	1.9	1.25	0.9	1.46
Path Radiance, L_A (mw/cm^2 - Sr)	0.268	0.127	0.081	0.103
Sun Zenith Angle, Z	48.0°			

Table 2. March Mission

Lake	Lake Reflectance, ρ, Computed from ERTS Data and RPMI Atmospheric Measurements — Band 4	5	6	7	Lake Reflectance, ρ, Measured Directly by RPMI — Band 4	5	6	7	Band 4 to Band 5 Reflectance Ratio ERTS	RPMI	Secchi Disk Readings (Light Penetration in Meters)	Forel-Ule Number (Water Color)
Huron	4.4	0.06	0	0	-	-	-	-	73.3	-	-	-
Orchard	4.0	0.52	0	0	2.4	0.72	0.22	0	7.7	3.3	5.0	X
Lower Long	3.6	1.2	0.27	0.15	1.8	1.0	0.5	0	3.0	1.9	4.0	XIV
Forest	3.3	1.2	0	0	1.55	1.0	0.5	0	2.75	1.55	3.0	XVII

Table 3. Effect of Atmospheric Scatter (Path Radiance) L_A on Lake Reflectance Derived from ERTS Data

Lake	Band 4		Band 5	
	$L_A = 0.268$	$L_A = 0$	$L_A = 0.127$	$L_A = 0$
Huron	4.4	15.6	0.06	5.5
Orchard	4.0	15.1	0.52	6.0
Lower Long	3.6	14.7	1.2	6.6
Forest	3.3	14.6	1.2	6.6
Island	3.97	15.0	1.6	7.1

Table 4. Using March (Historic) Atmospheric Parameters to Compute Lake Reflectance in April and May

MSS Band	Orchard			Lower Long			Forest		
	March	April	May	March	April	May	March	April	May
4	4.0	5.7	8.5	3.6	5.8	7.6	3.3	5.8	7.5
5	0.52	2.1	5.1	1.2	3.0	4.2	1.2	3.2	4.3
6	0	0.98	4.1	0.27	2.5	3.9	0	2.5	4.3
7	0	0.23	3.9	0.15	2.7	3.5	0	1.9	4.0

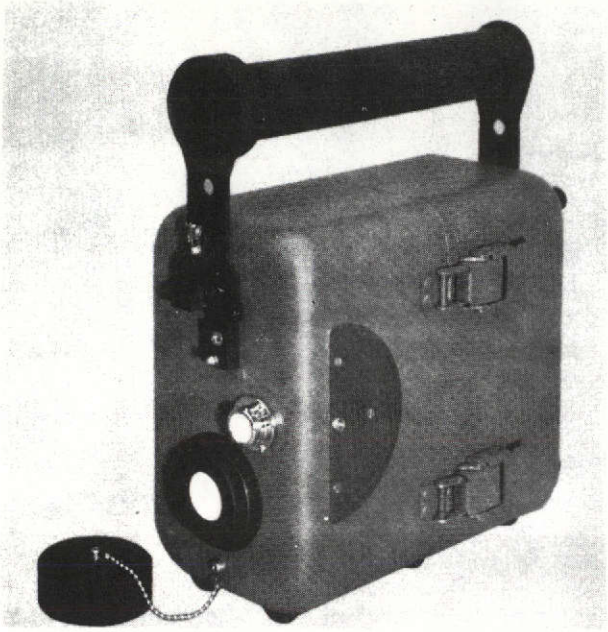

RPMI assembled

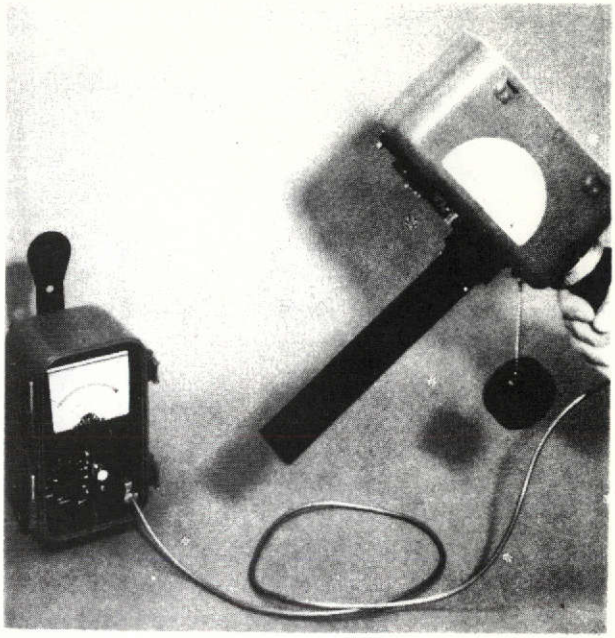

Reflected Radiation — Used with small calibration panels and cards, to obtain direct measurement of truth site reflectance. Reflectance also immediatel derived from ratio of reflected radiance and global irradiance.

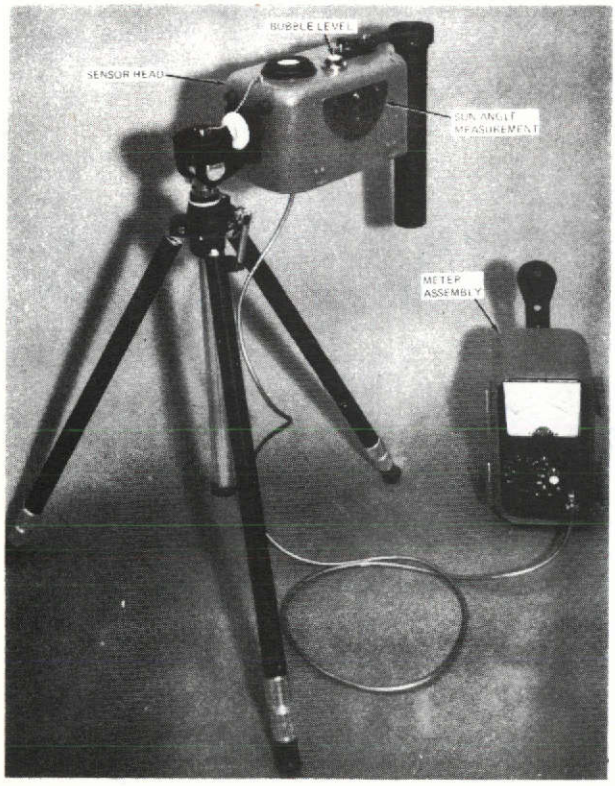

Global Irradiance (H) — 2π steradian field of view for measuring downwelling (incident) radiation ERTS MSS bands. Bubble level aids this measurement.

Sky Irradiance (H_{SKY}) — Block sun to measure global irradiance minus direct sun component, in every ERTS MSS band. Angle from zenith to sun is also measured in this mode by reading sun's shadow cast on sun dial.

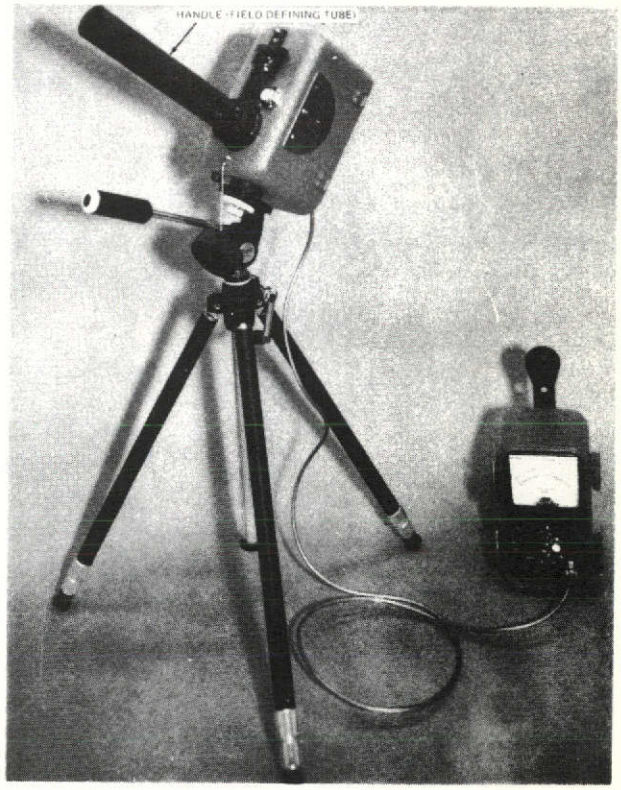

Radiance from Narrow Solid Angles of Sky — Handle serving as field stop permits direct measurements through a 7.0^{o} circular field of view. This mode is also used to measure direct beam irradiance.

Figure 1. Radiant Power Measuring Instrument

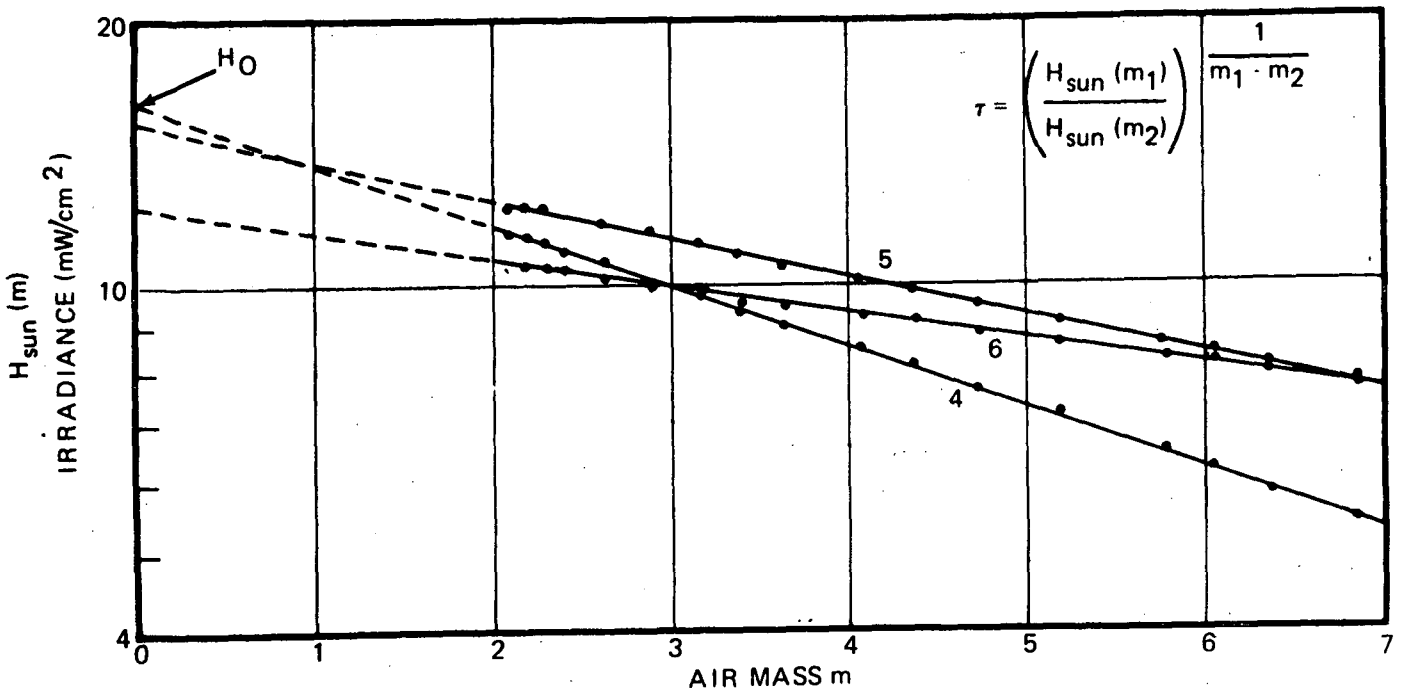

Figure 2. Atmospheric Extinction Curves

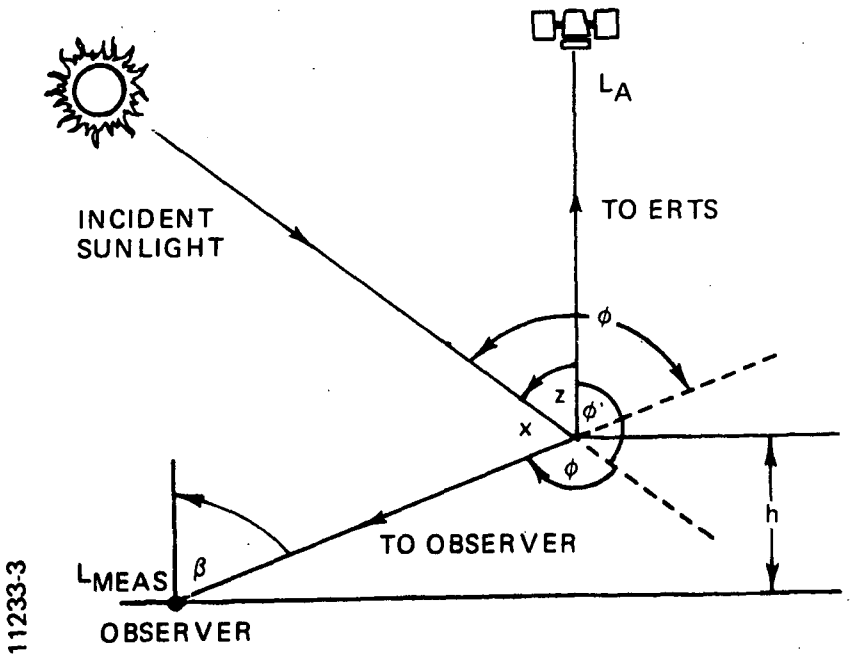

Figure 3. Sky Radiance Measurements

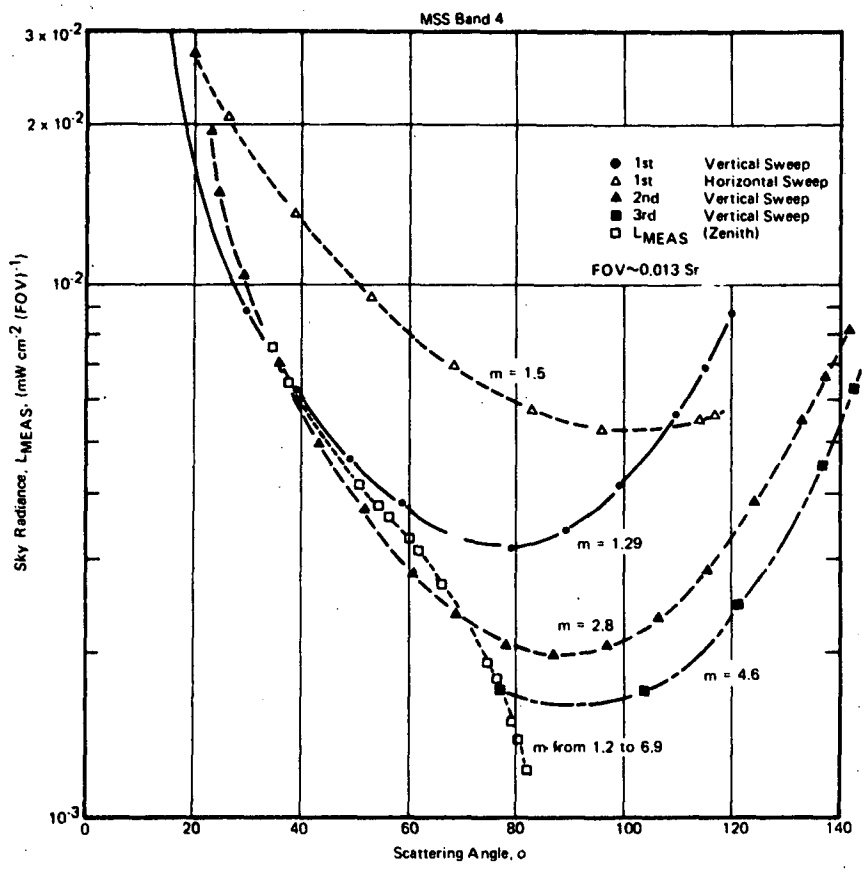

Figure 4. RPMI Sky Radiance Measurements

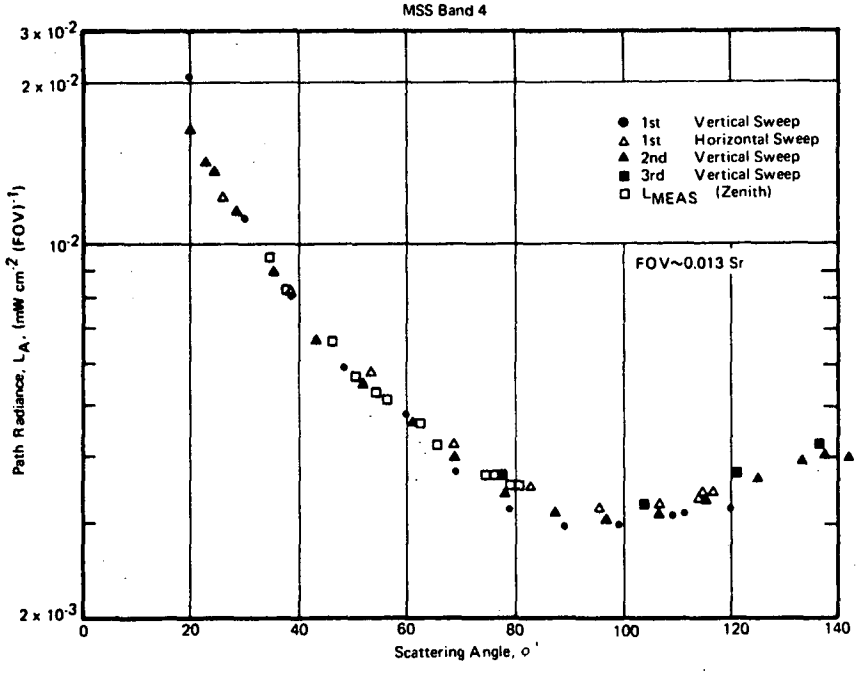

Figure 5. Path Radiance Viewed by ERTS Band 4

Figure 6. Earth Resources Data Center

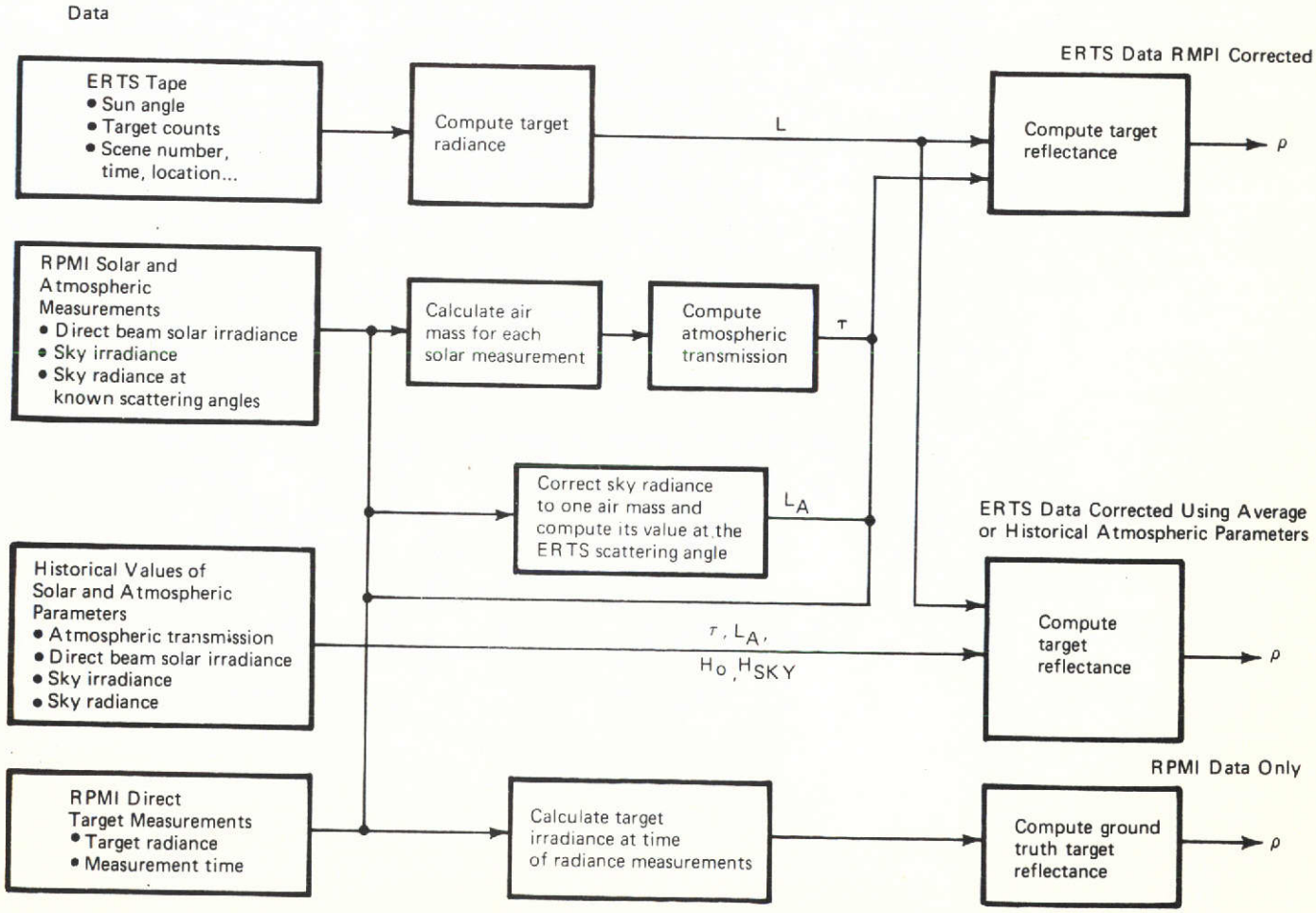

Figure 7. Machine Processing of ERTS and RPMI Data

(END OF APPENDIX A)

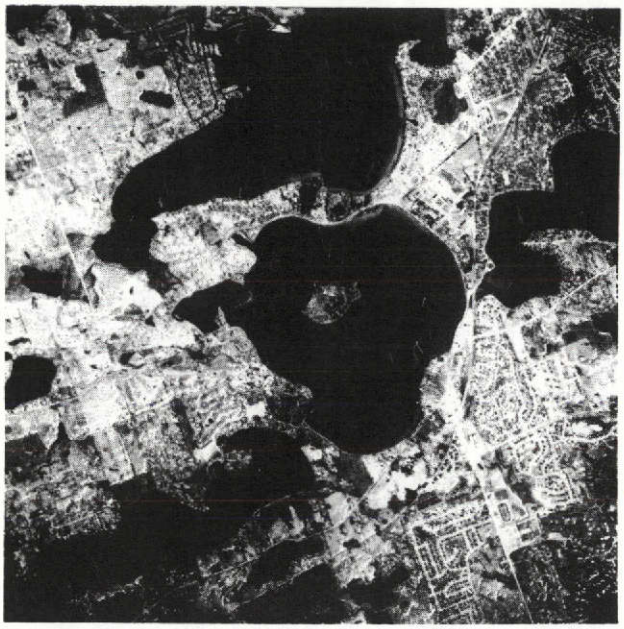

Aerial Photograph

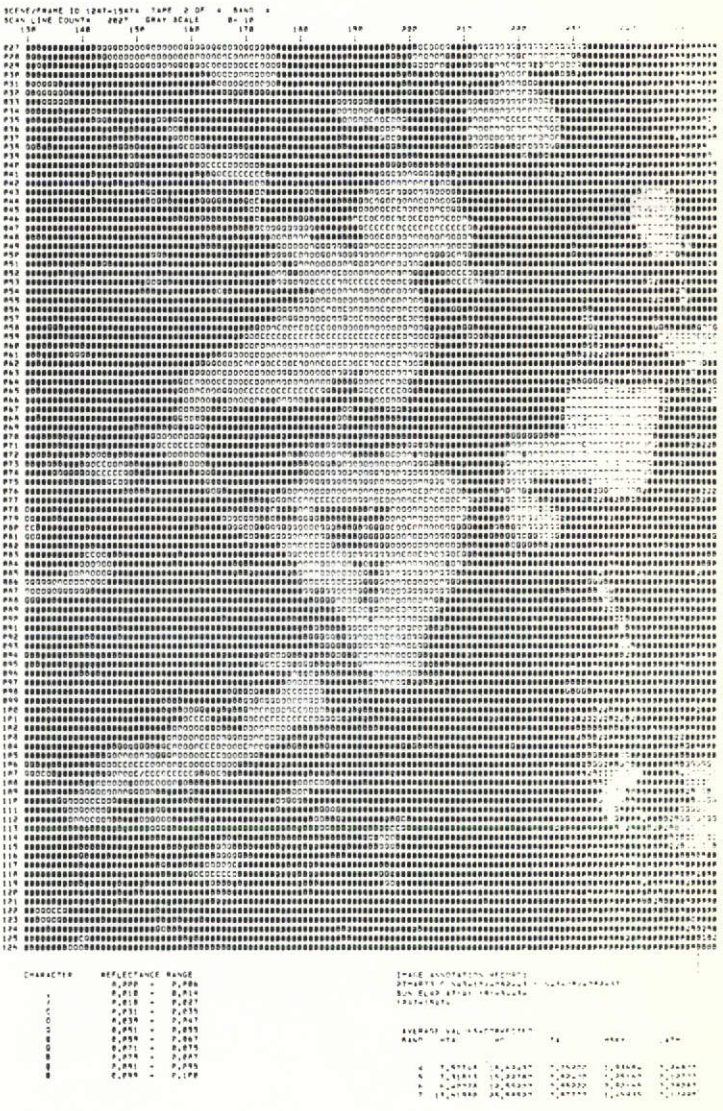

Reflectance Gray Scale Printout

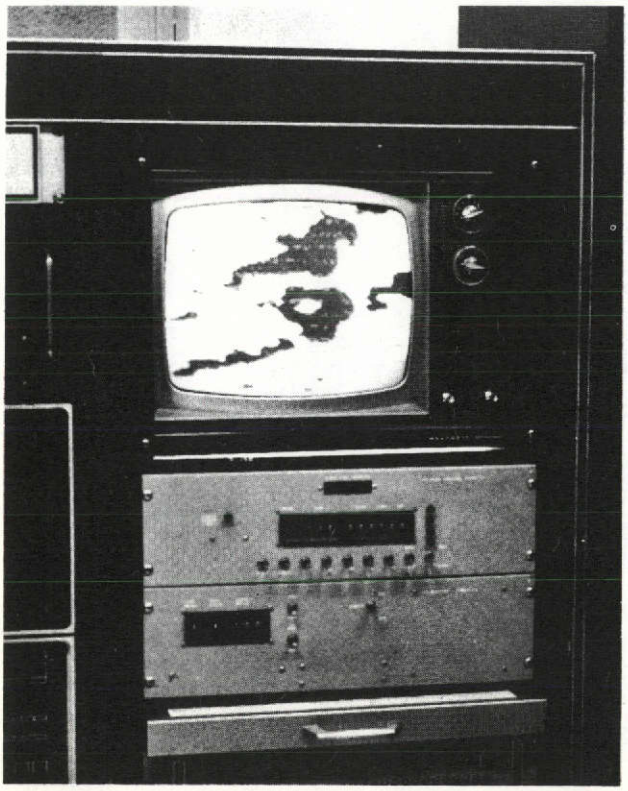

TV Display of ERTS Reflectance

Figure 8. View of Orchard Lake

(END OF APPENDIX A)

APPENDIX B

Figure 20. Forest Lake, Station I.

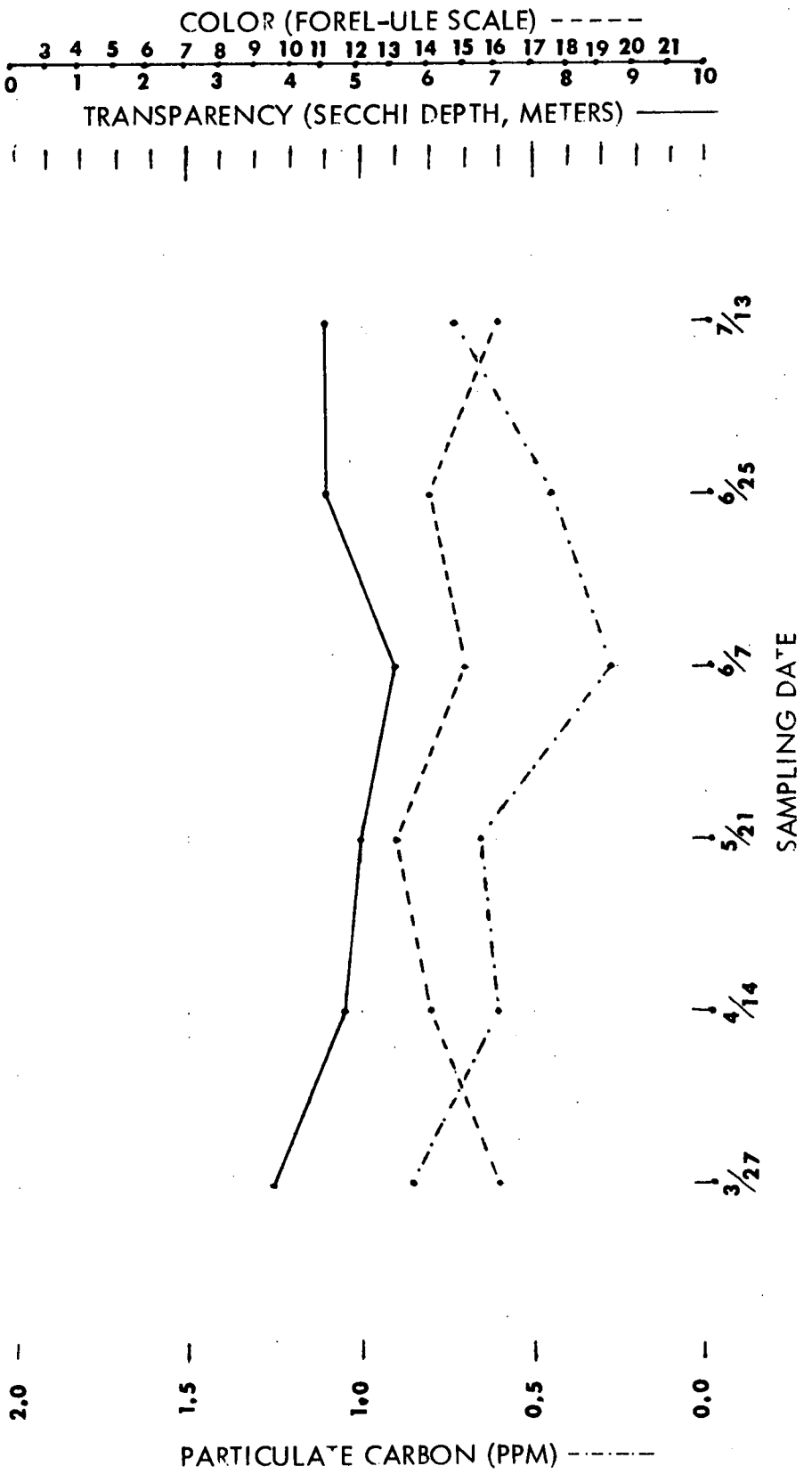

Figure 21. Forest Lake, Station 2.

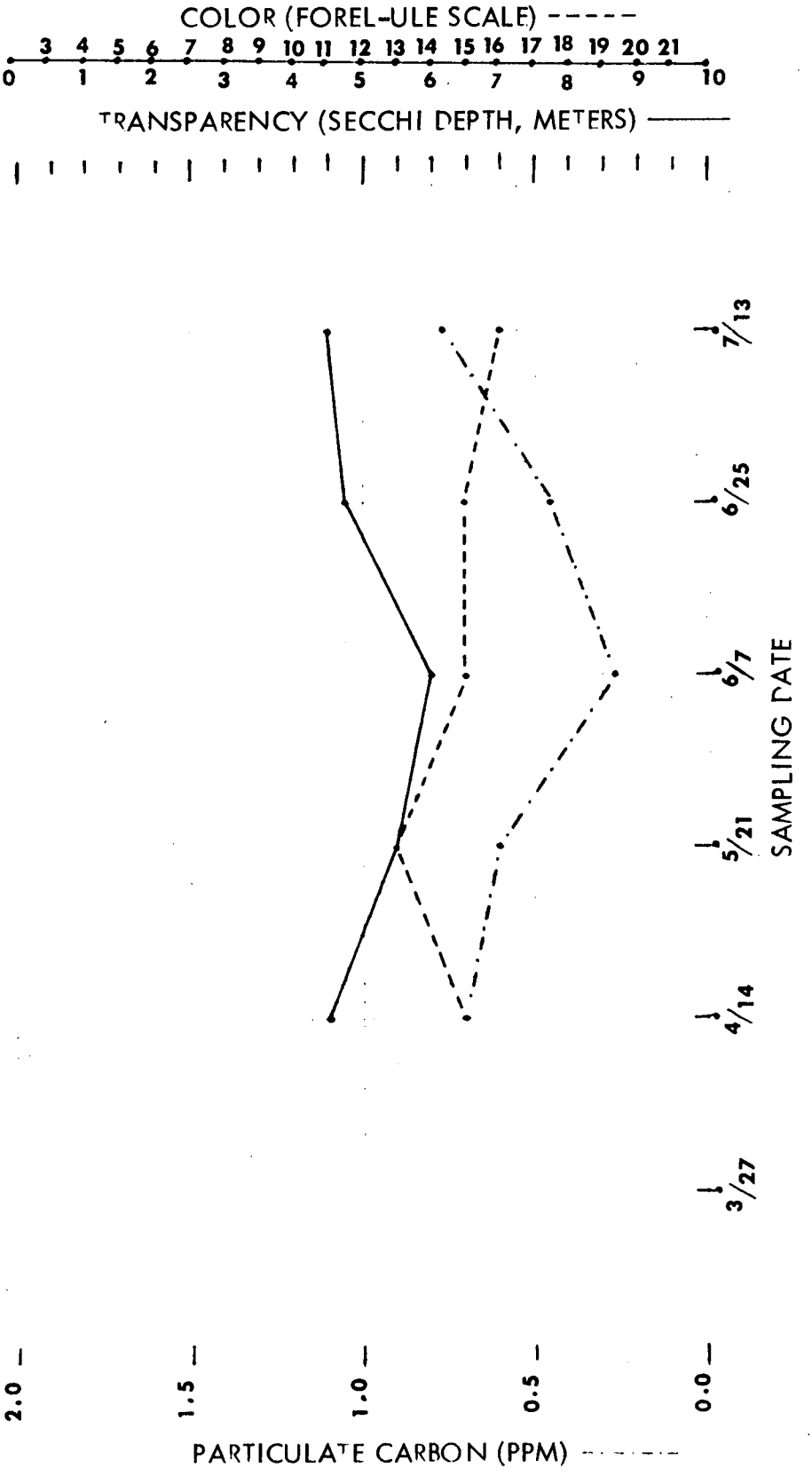

Figure 22. Lower Long Lake, Station 3.

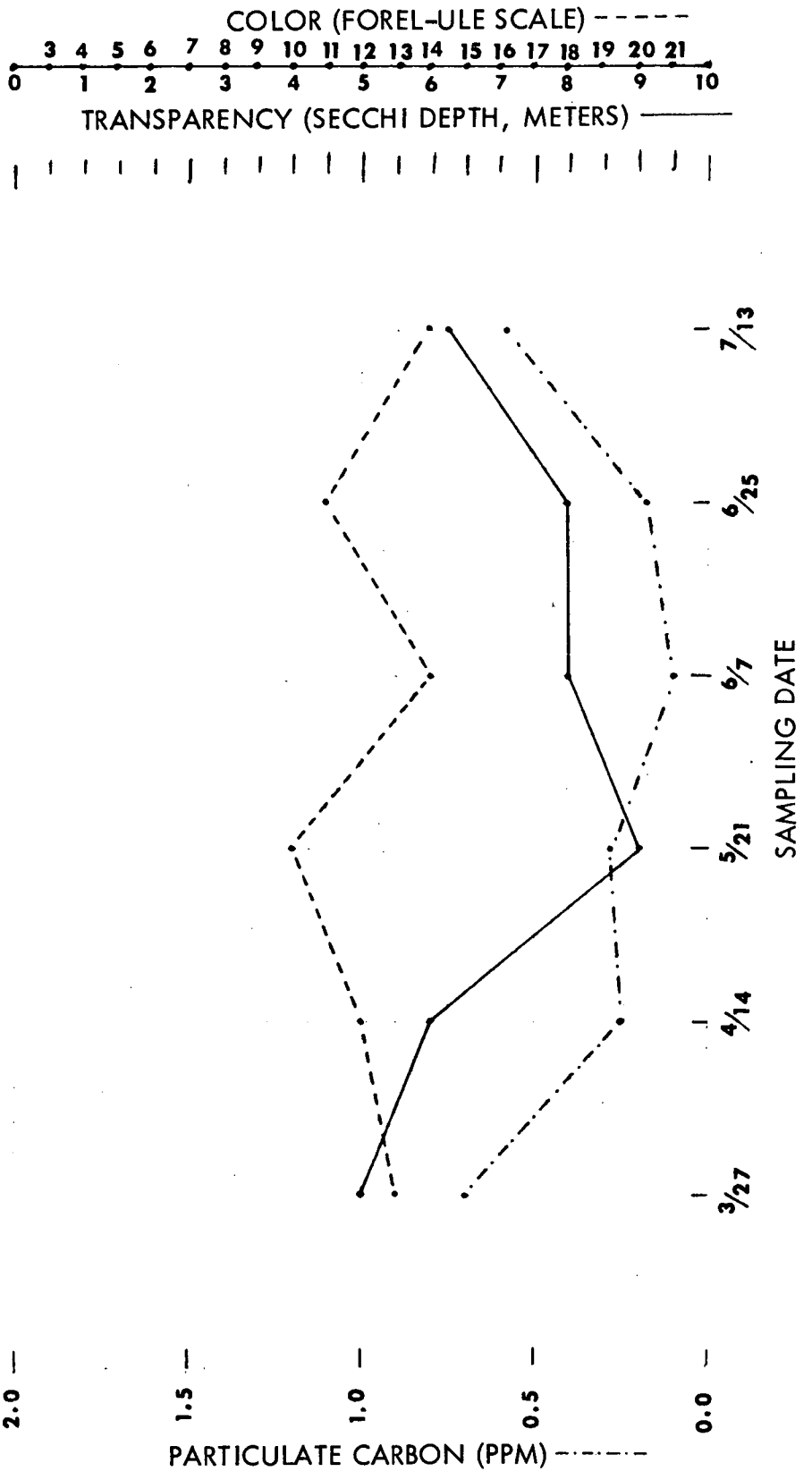

Figure 23. Lower Long Lake, Station 4.

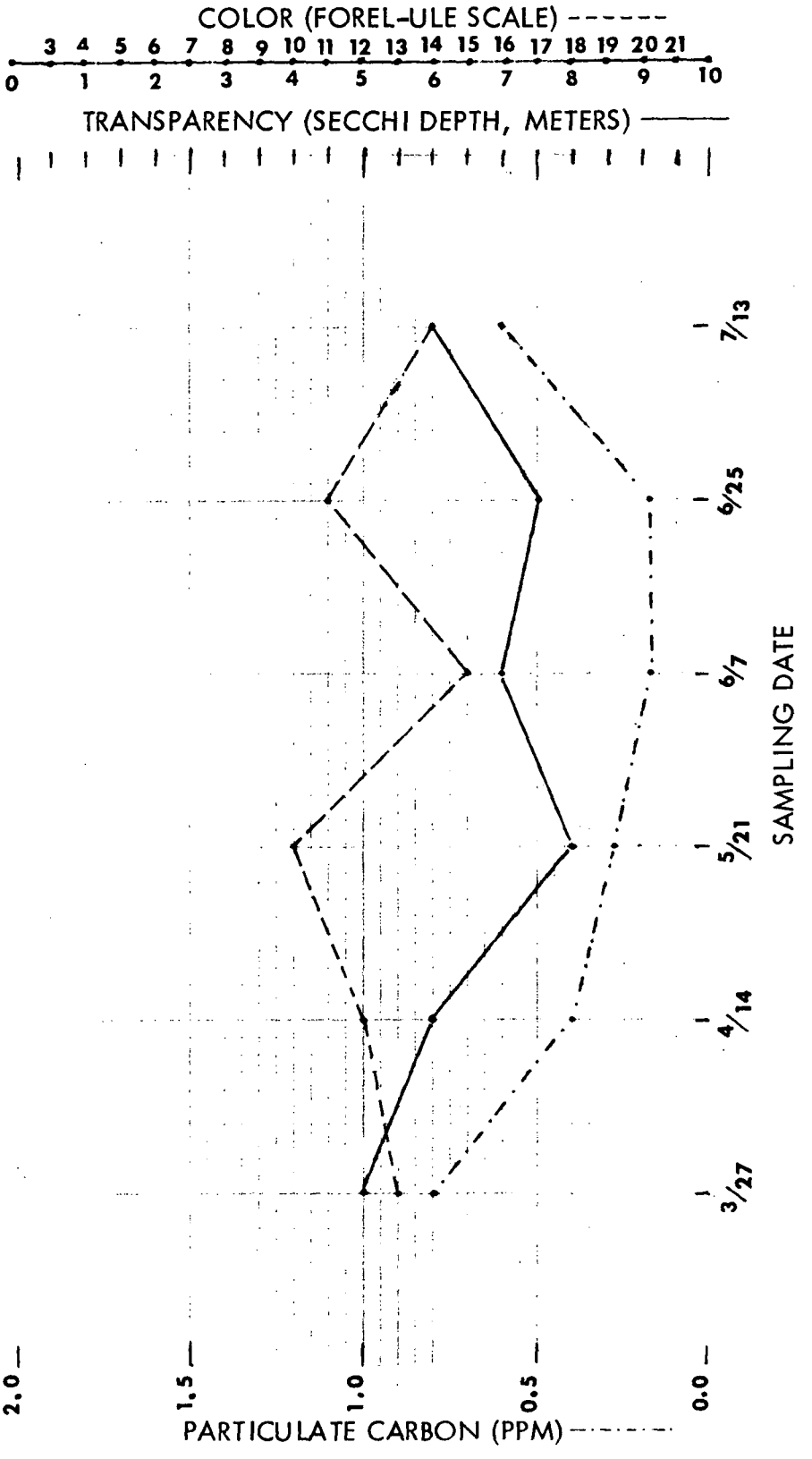

Figure 24. Island Lake, Station 5.

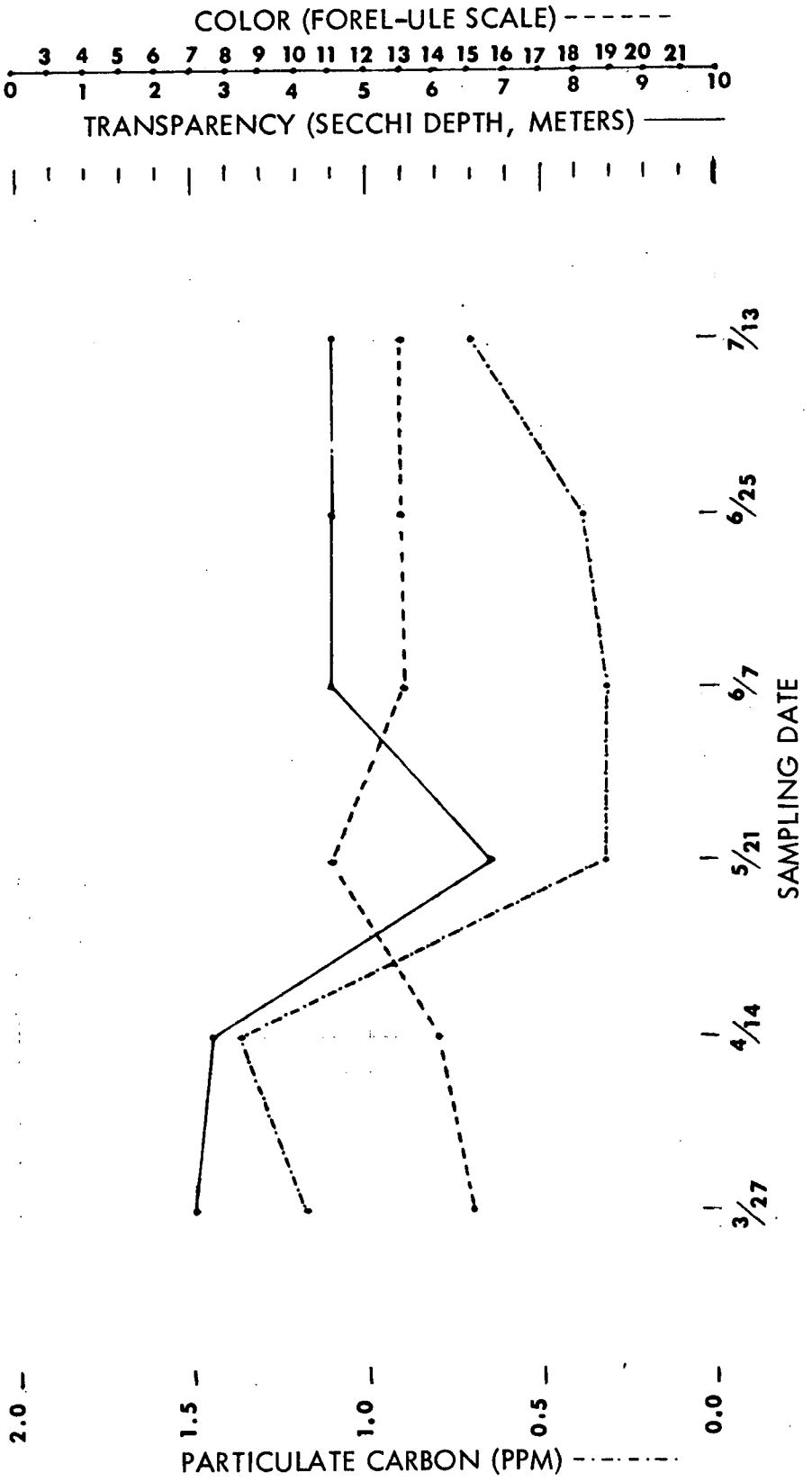

Figure 25. Island Lake, Station 6.

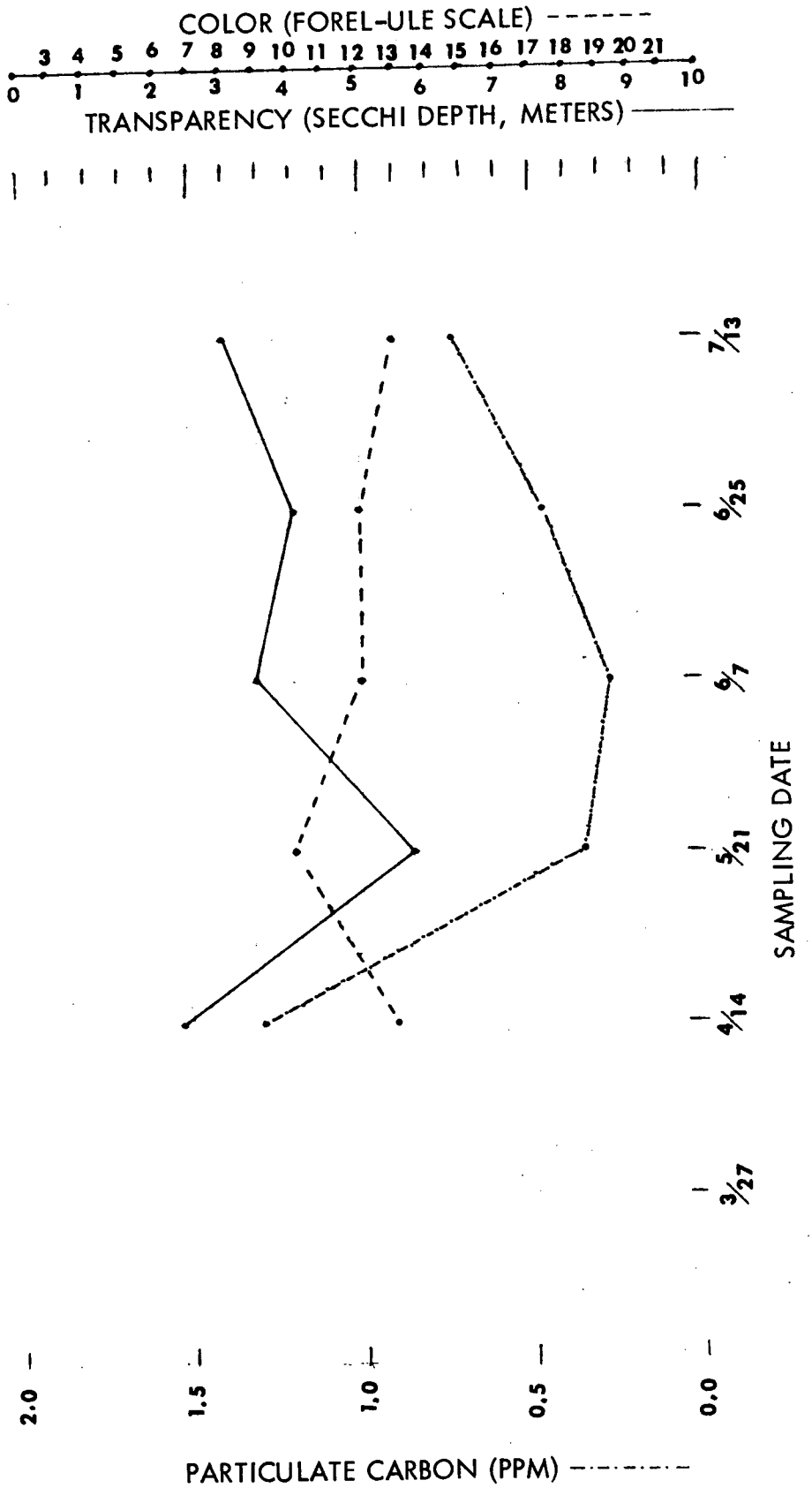

Figure 26. Orchard Lake, Station 7.

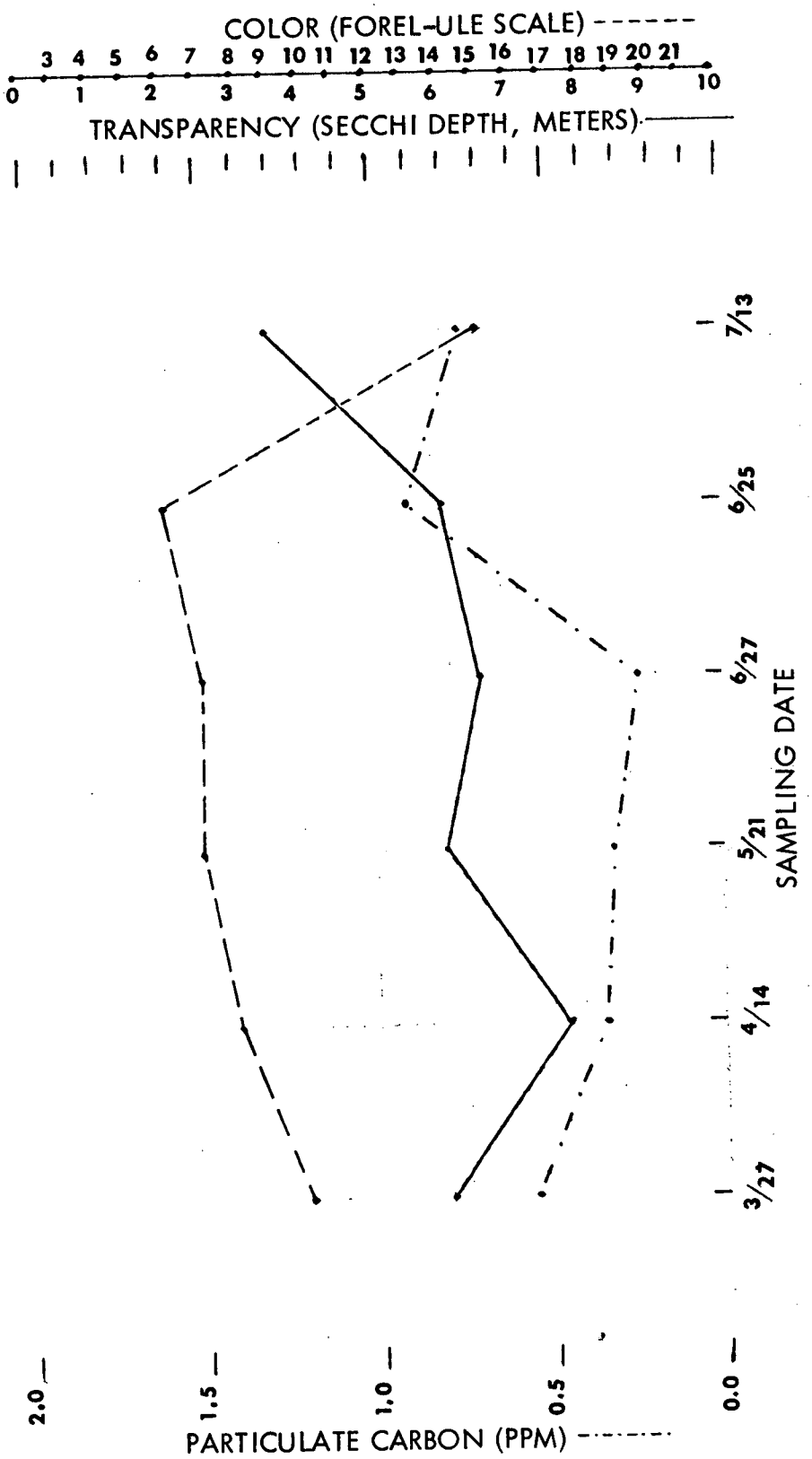

Figure 27. Orchard Lake, Station 8.

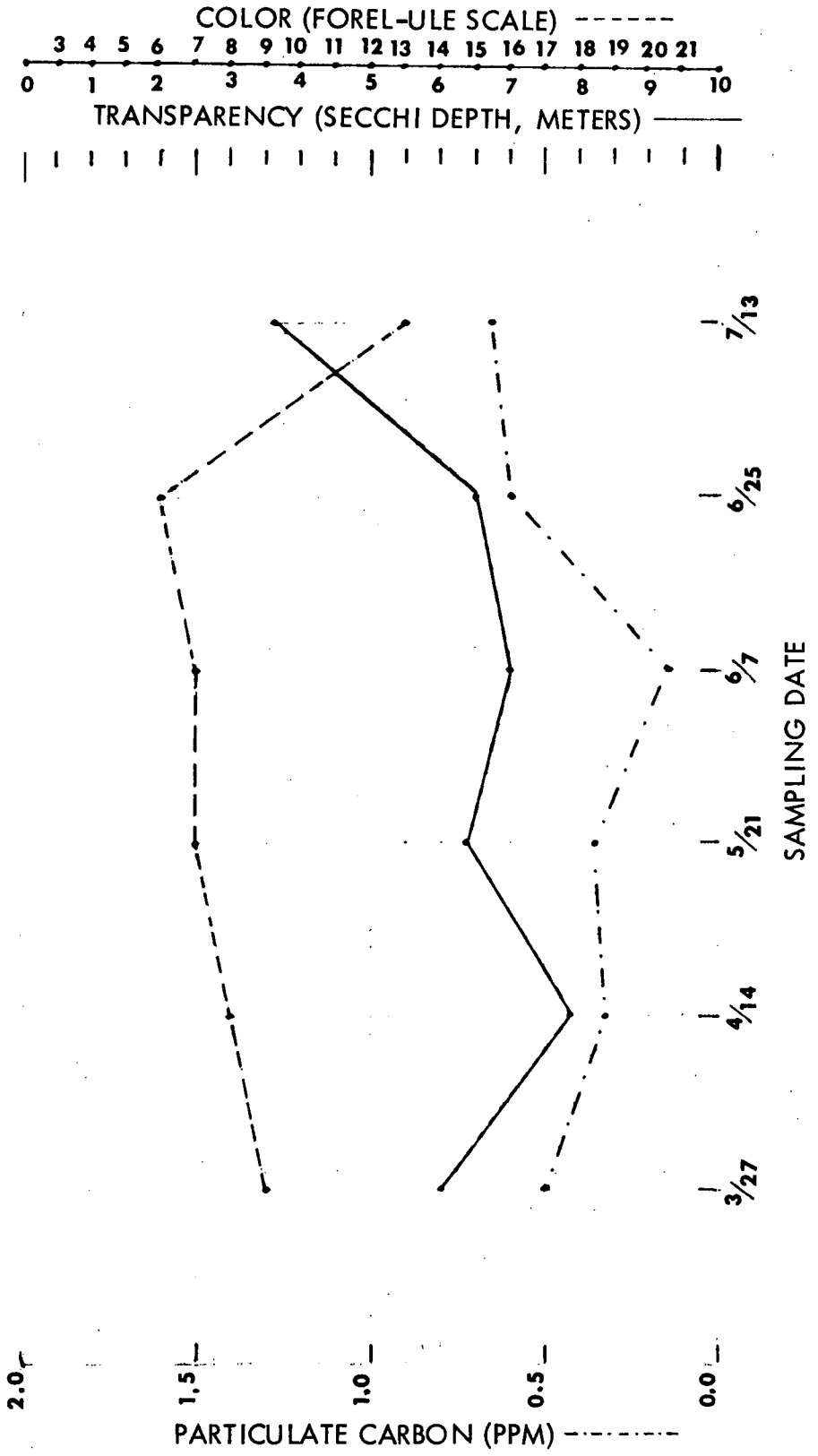

Figure 28. Cass Lake, Station 9.

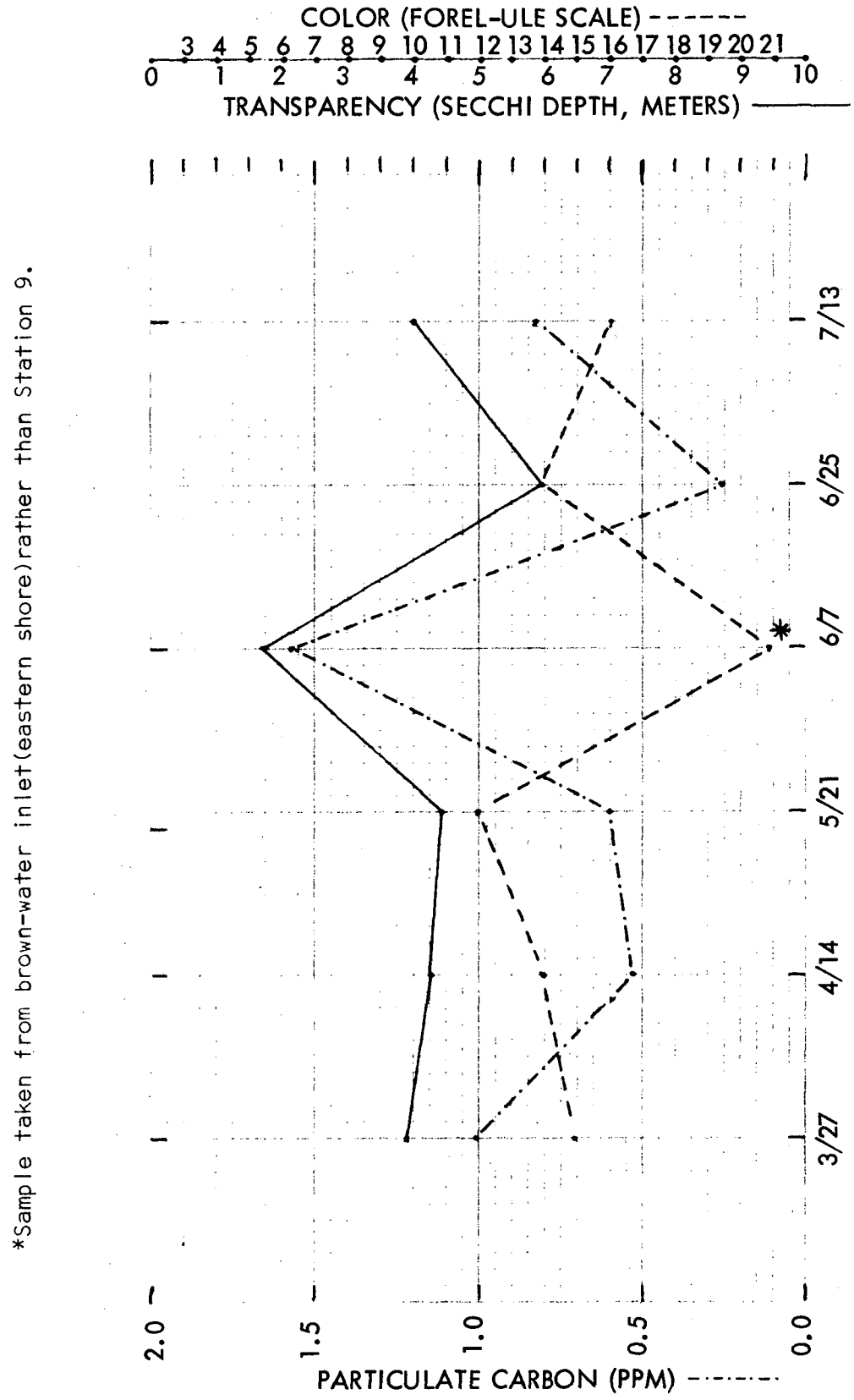

Figure 29. Cass Lake, Station 10.

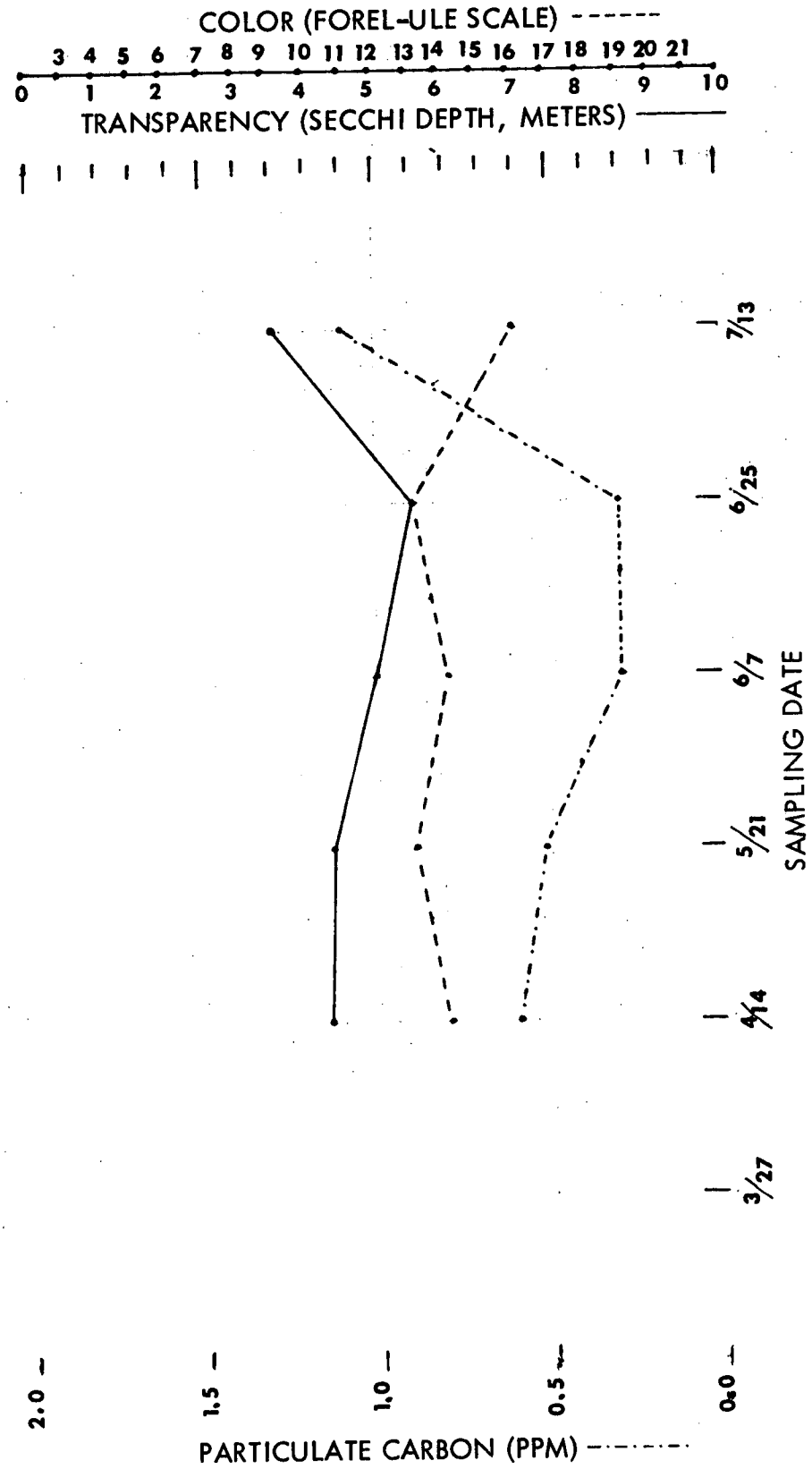

Figure 30. Lake Angelus, Station 11.

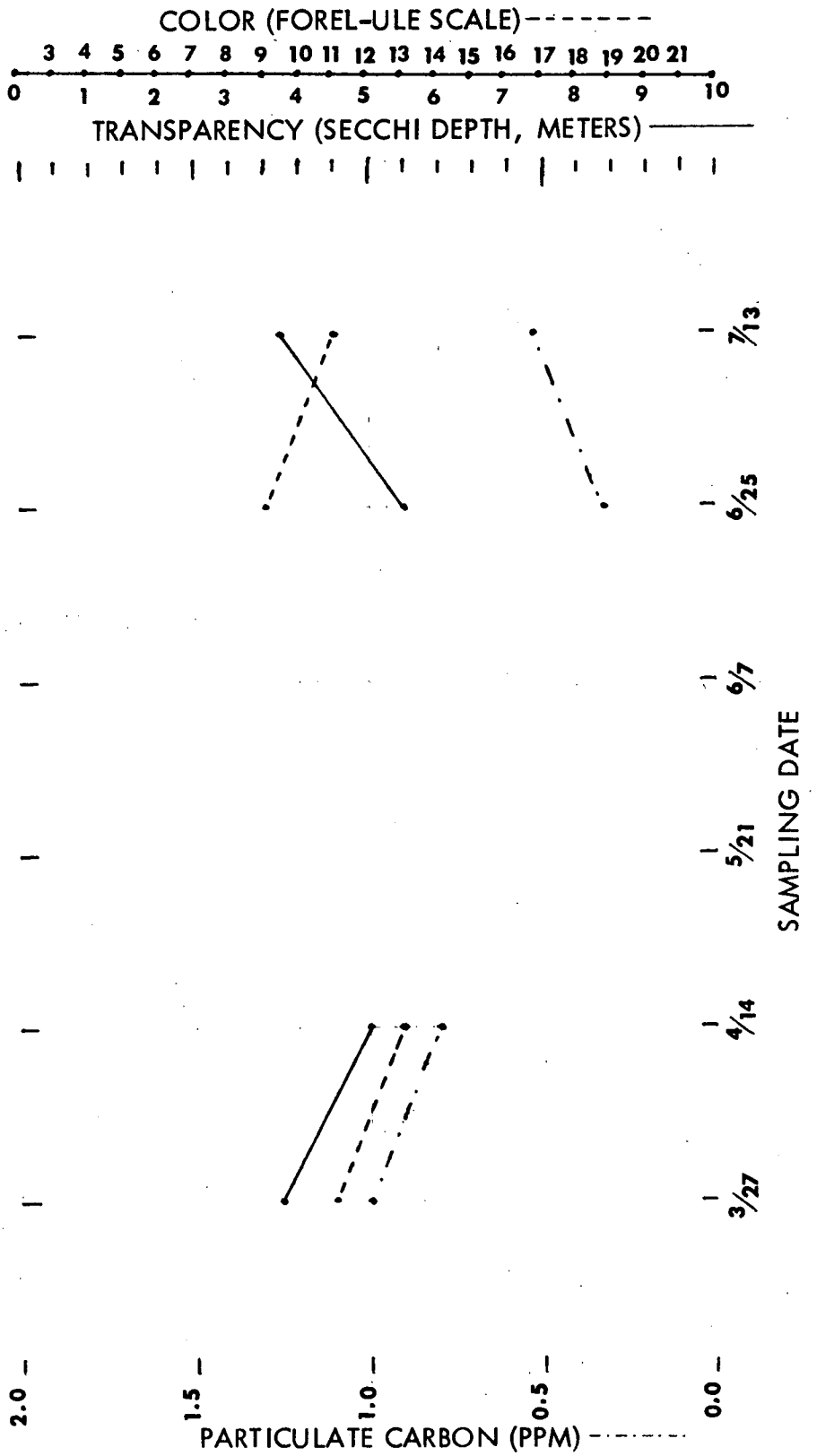

Figure 31. Lake Angelus, Station 12.

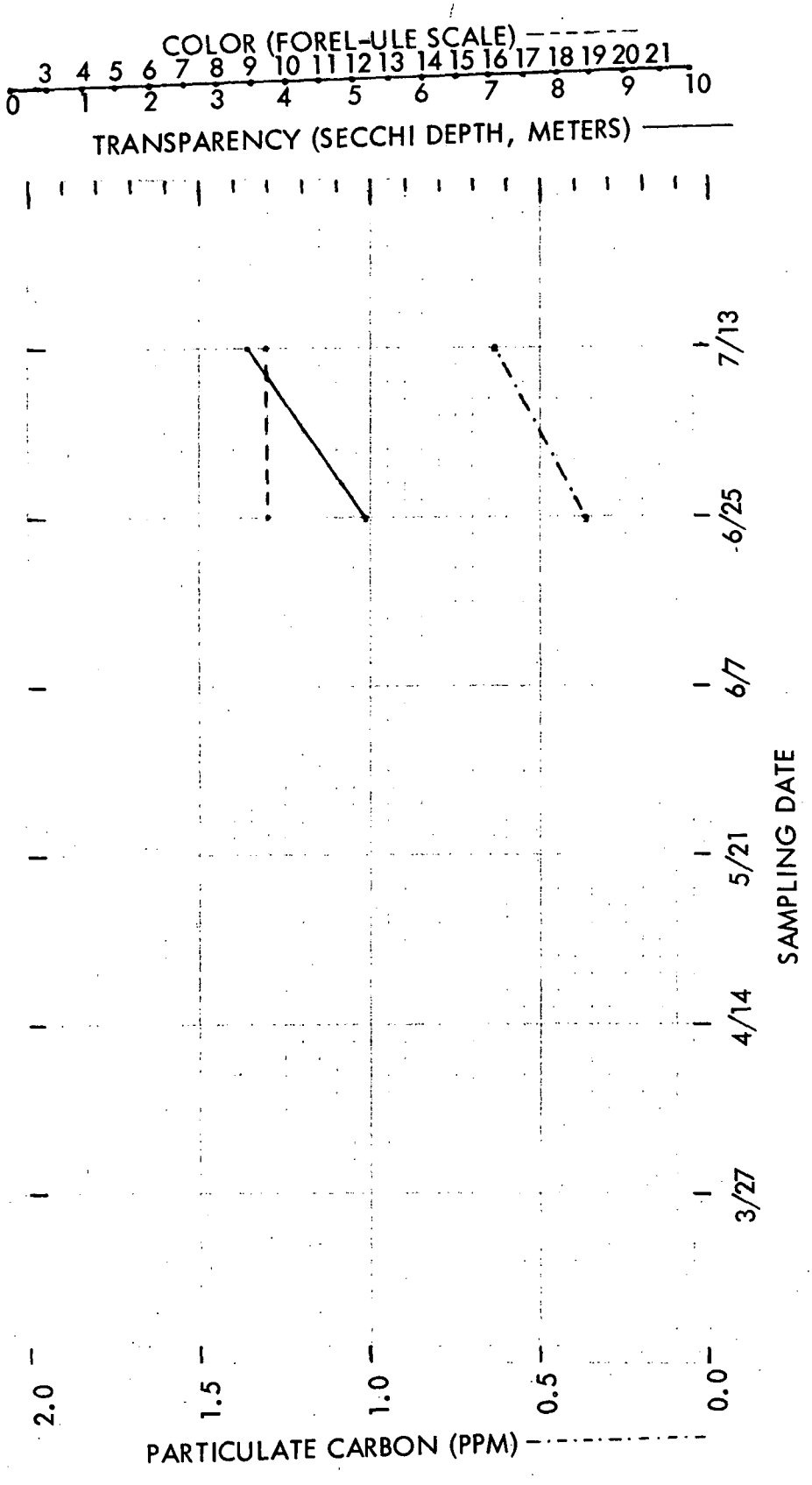

Figure 32. Forest Lake, Station 1. Numbers indicate algal species (see Table 7).

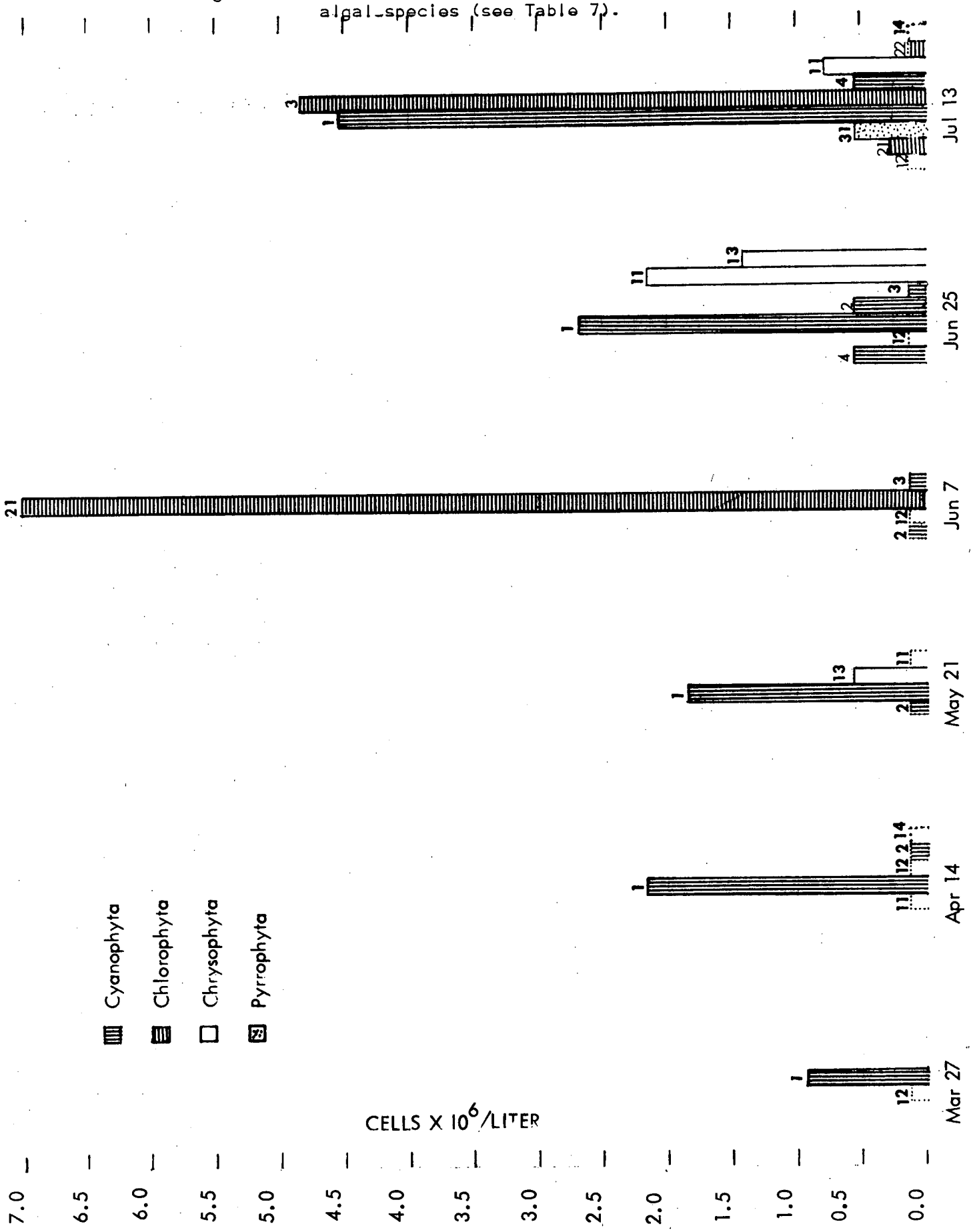

Figure 33. Forest Lake, Station 2. Numbers indicate algal species (see Table 7).

Figure 34. Lower Long, Station 3. Numbers indicate algal species (see Table 7).

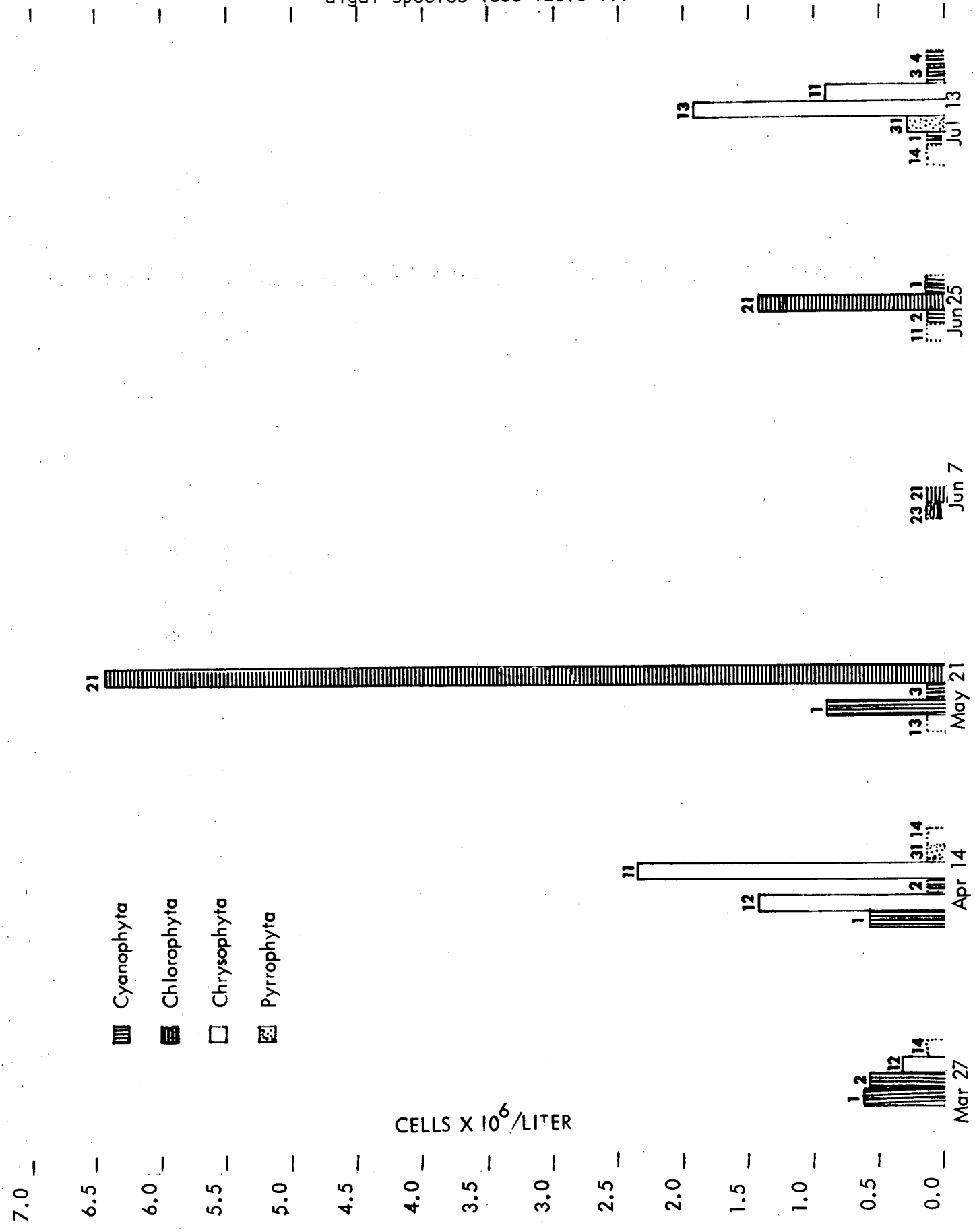

Figure 35. Lower Long Lake, Station 4. Numbers indicate algal species (see Table 7).

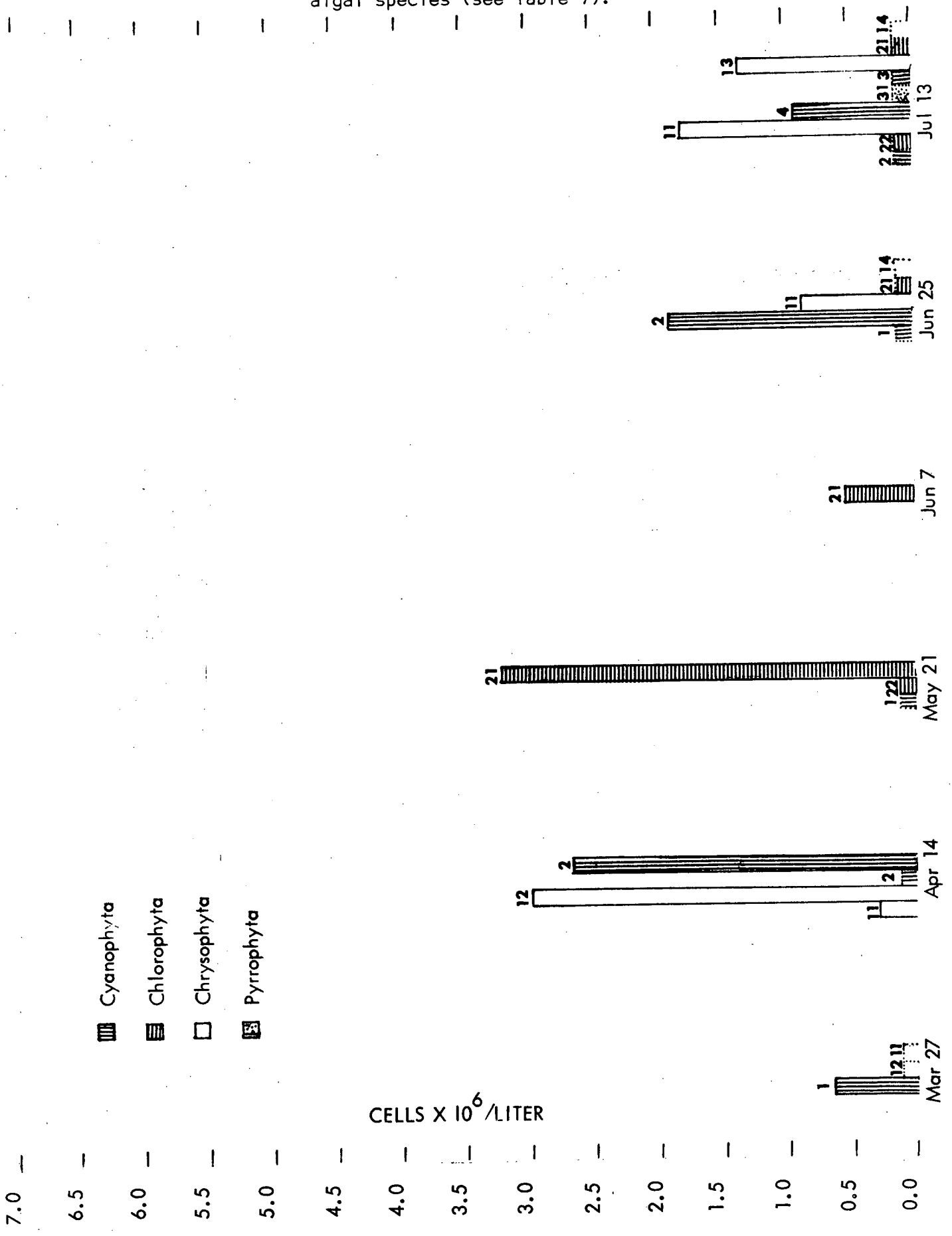

Figure 36. Island Lake, Station 5. Numbers indicate algal species (see Table 7).

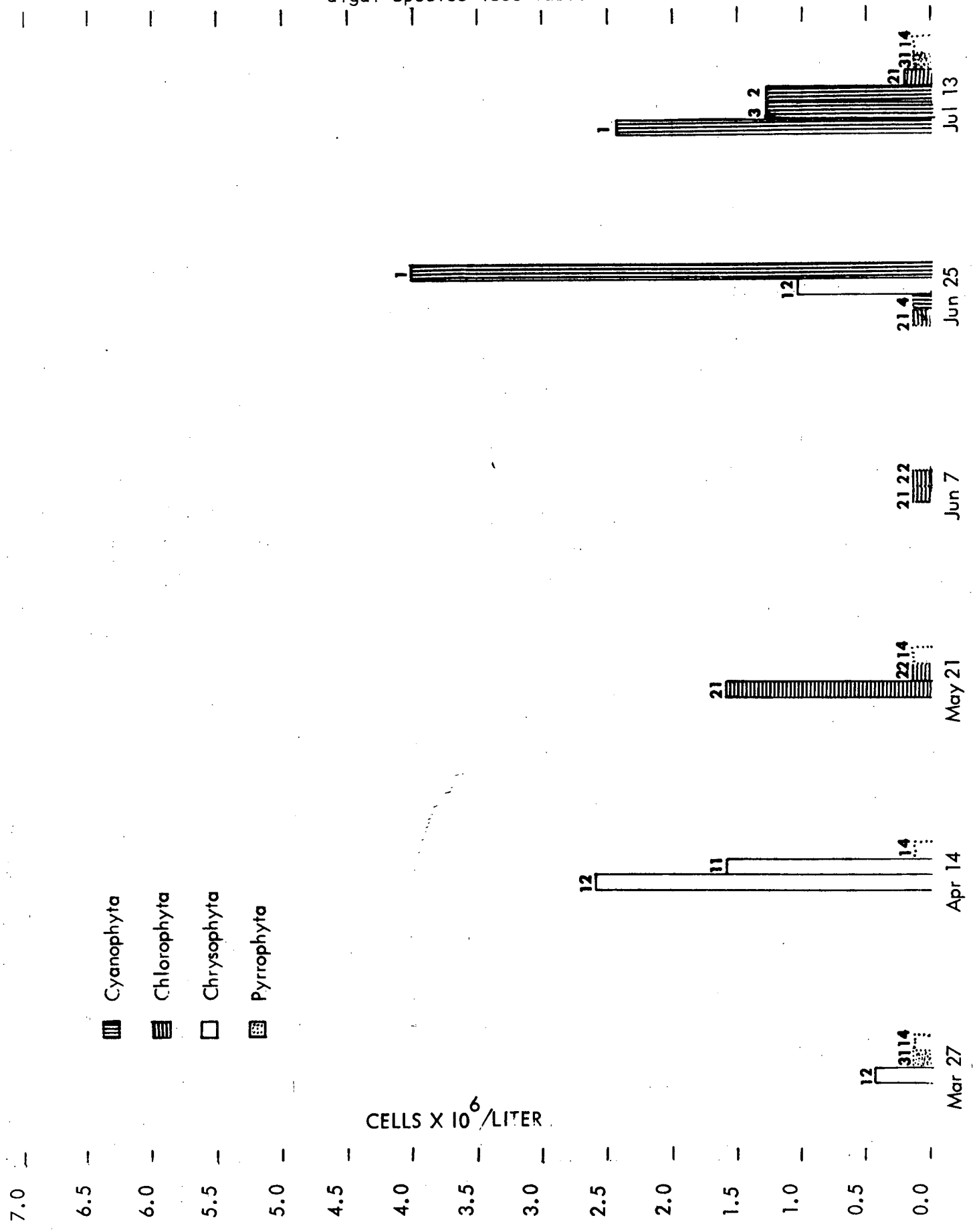

Figure 37. Island Lake, Station 6. Numbers indicate algal species (see Table 7).

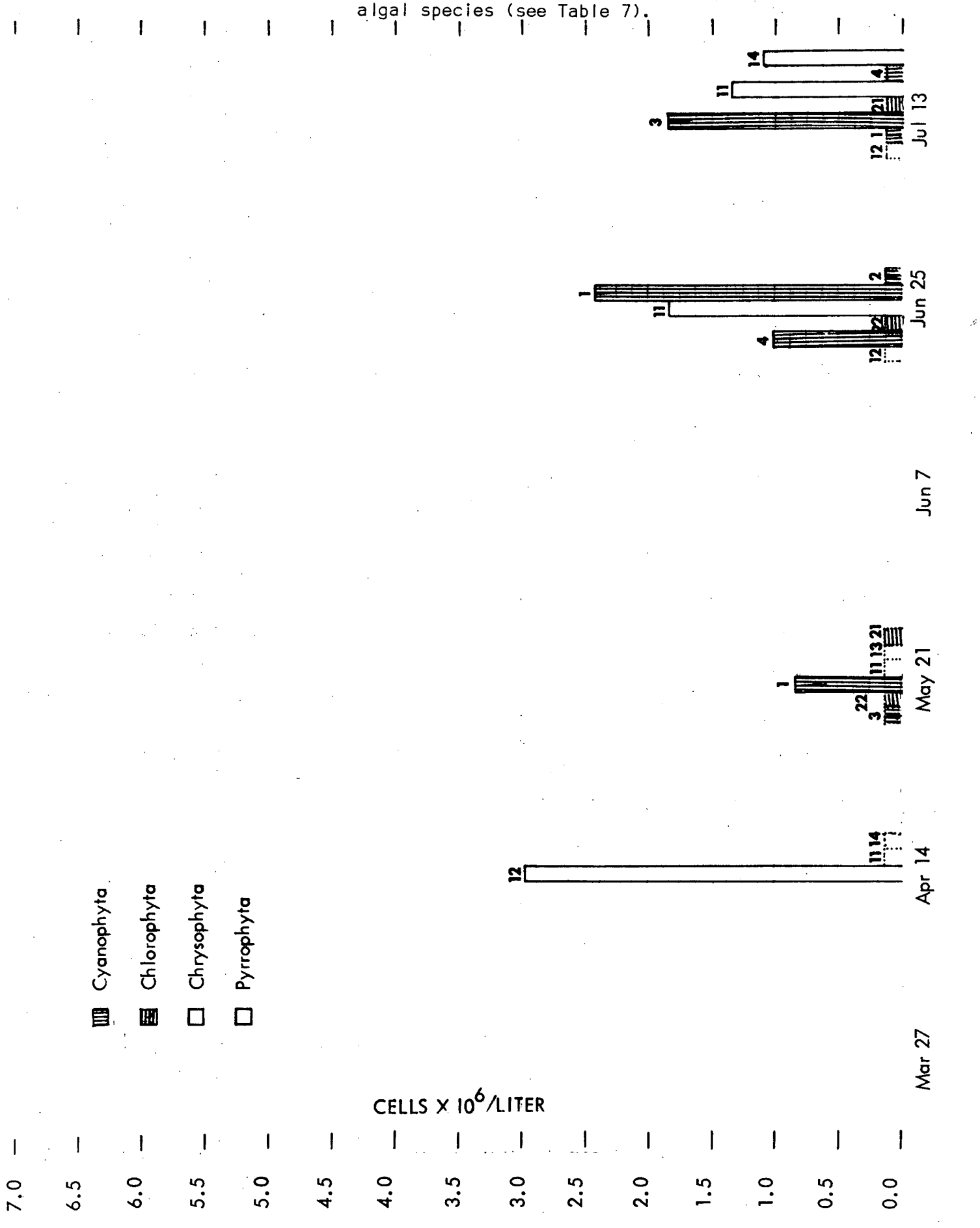

Figure 38. Orchard Lake, Station 7. Numbers indicate algal species (see Table 7).

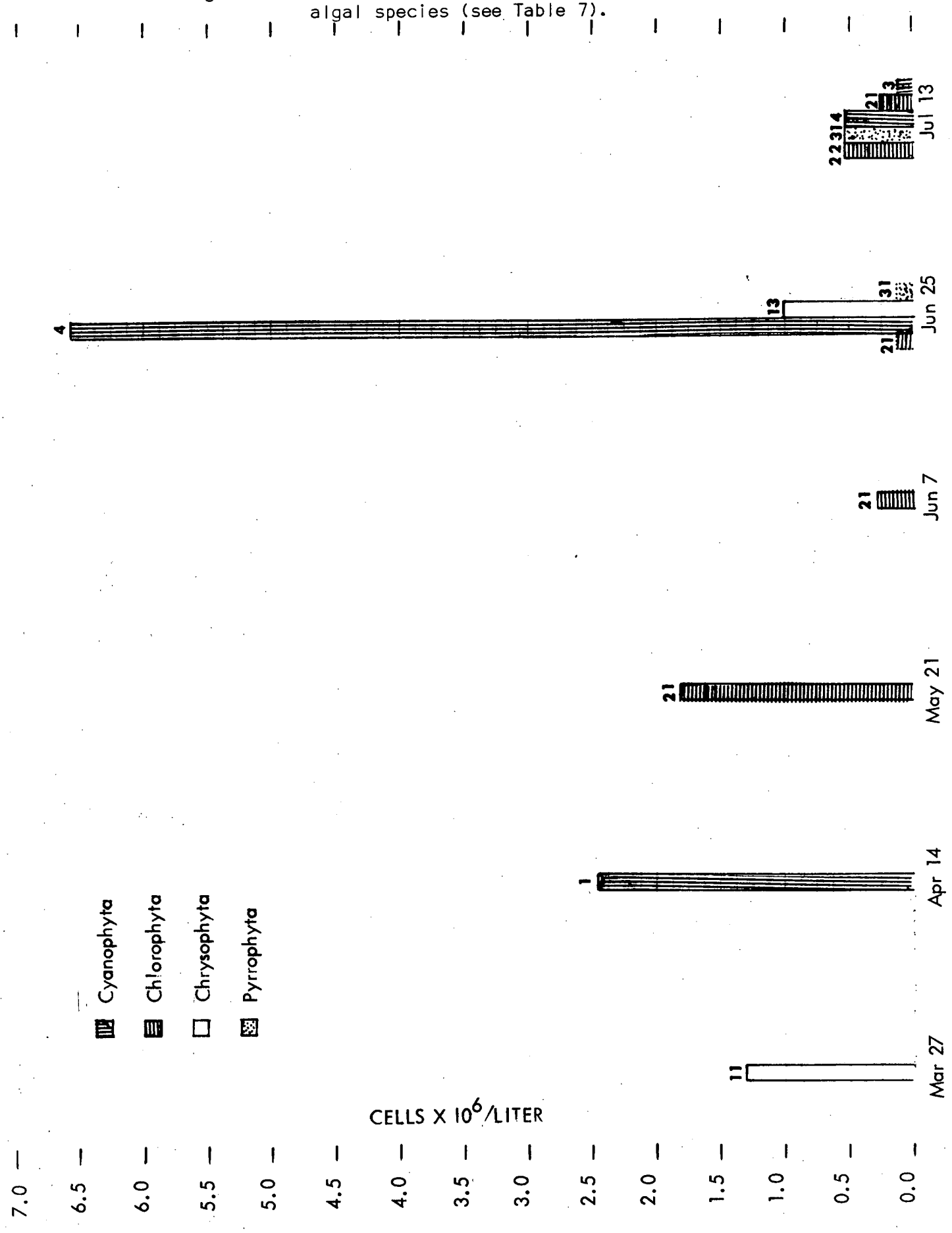

Figure 39. Orchard Lake, Station 8. Numbers indicate algal species (see Table 7).

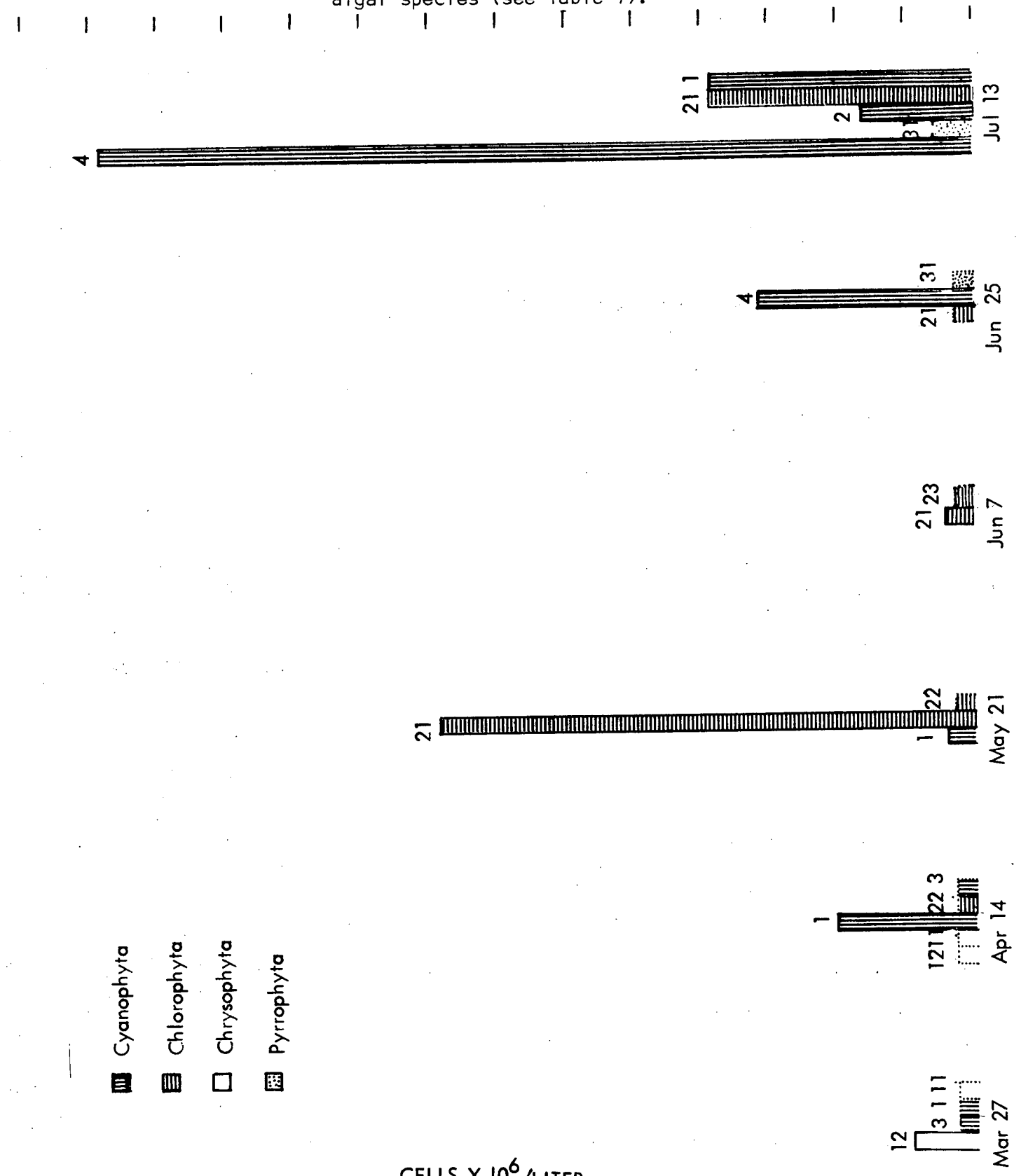

Figure 40. Cass Lake, Station 9. Numbers indicate algal species (see Table 7).

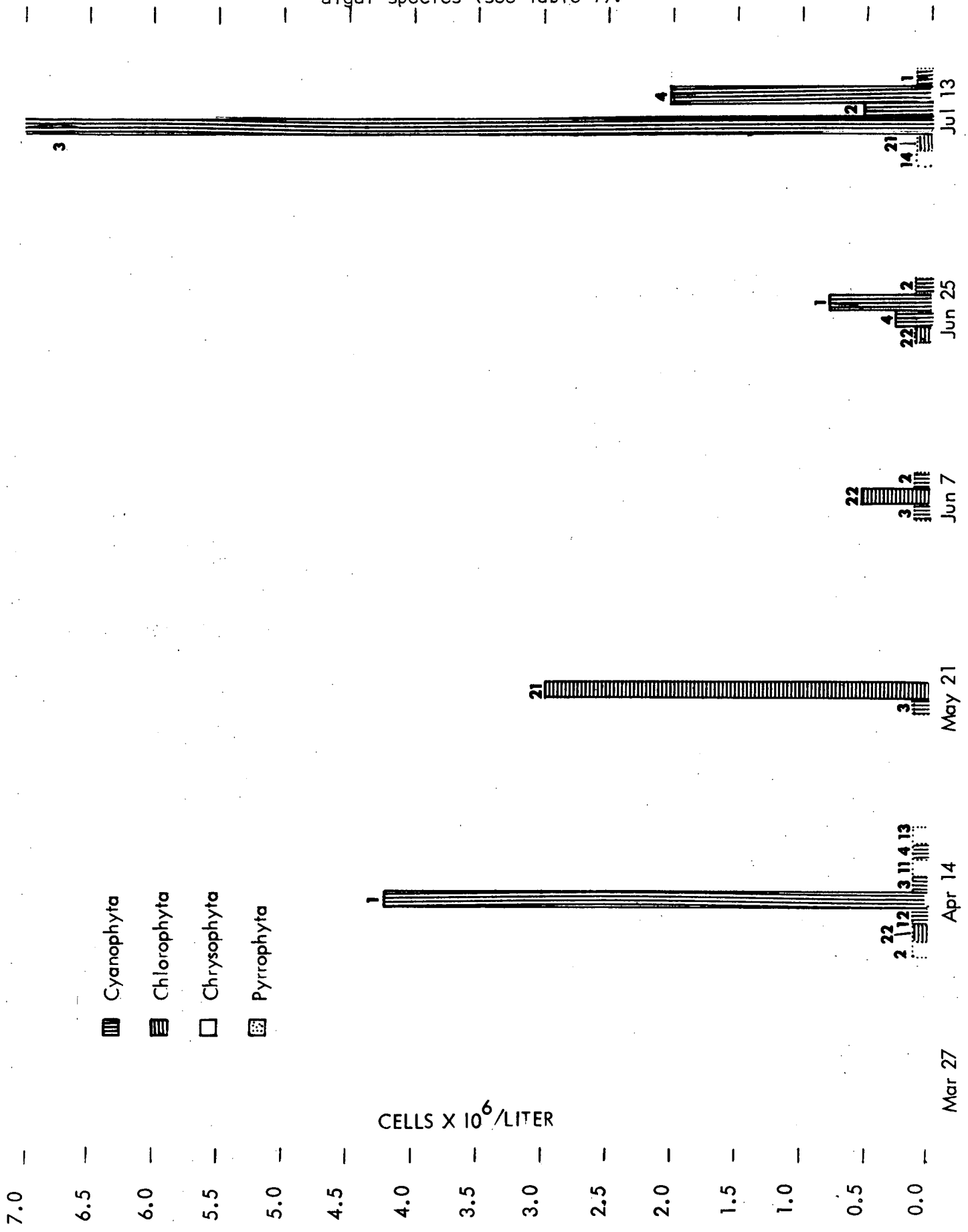

Figure 41. Cass Lake, Station 10. Numbers indicate algal species (see Table 7).

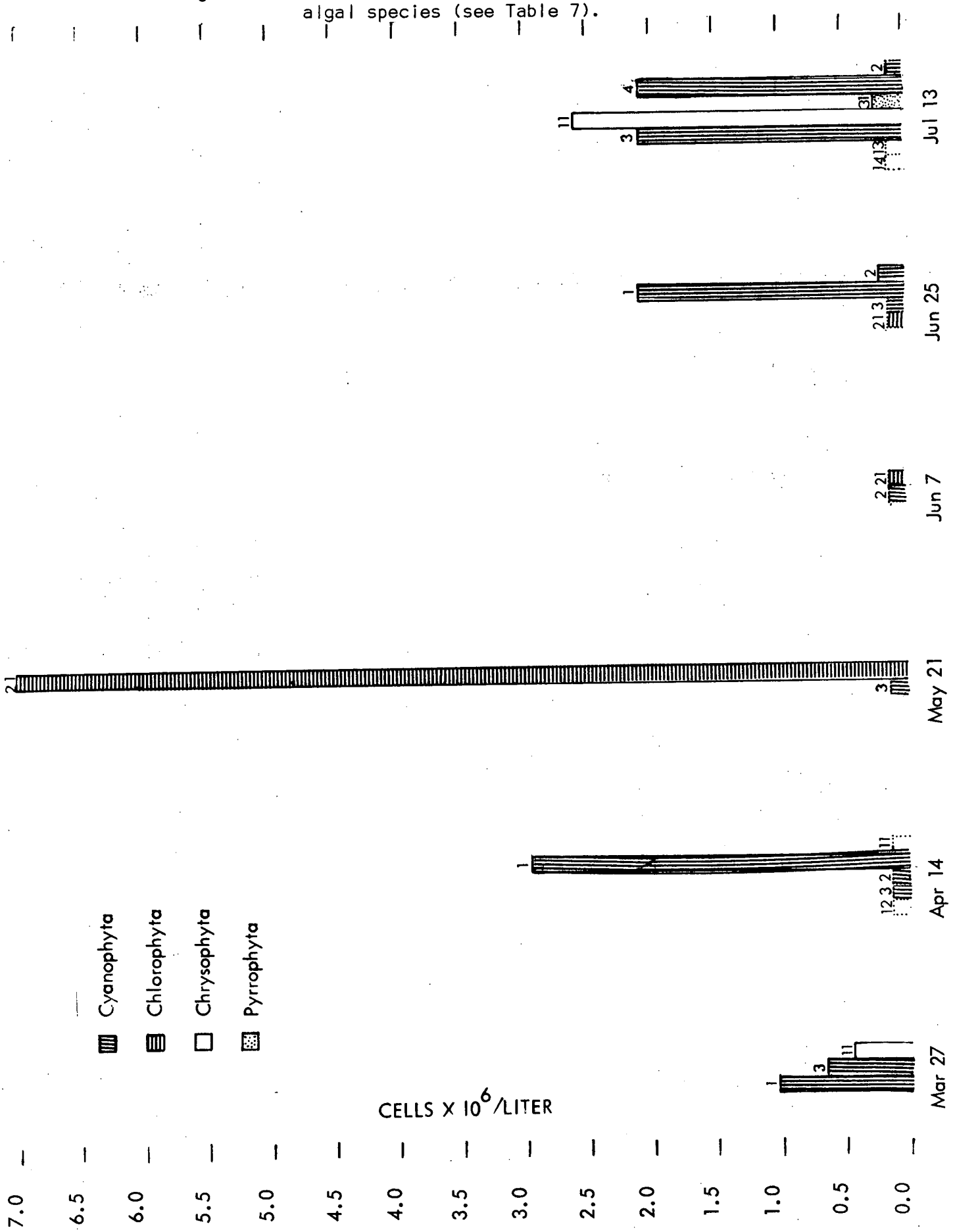

Figure 42. Lake Angelus, Station II. Numbers indicate algal species (see Table 7).

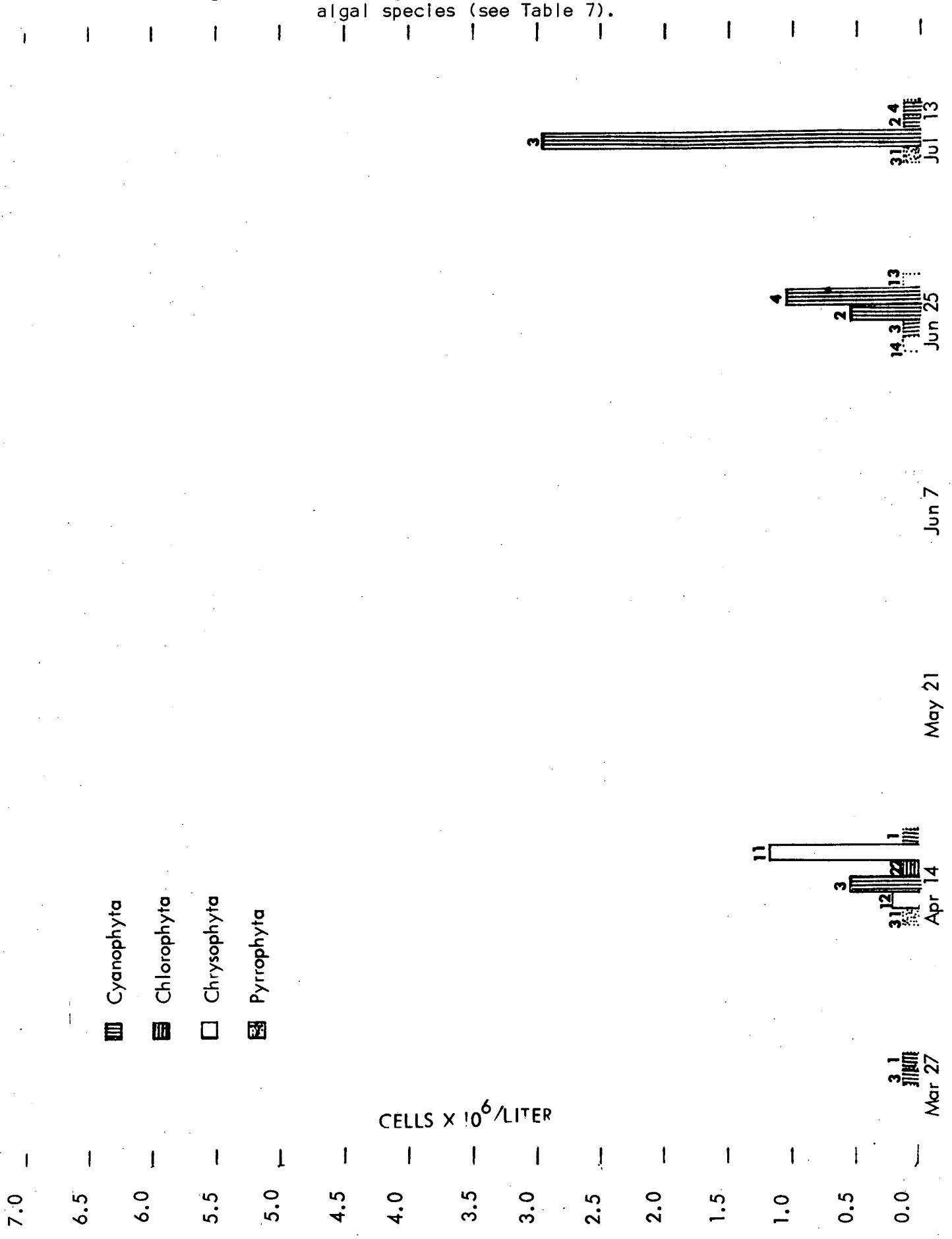

Figure 43. Lake Angelus, Station 12. Numbers indicate algal species (see Table 7).

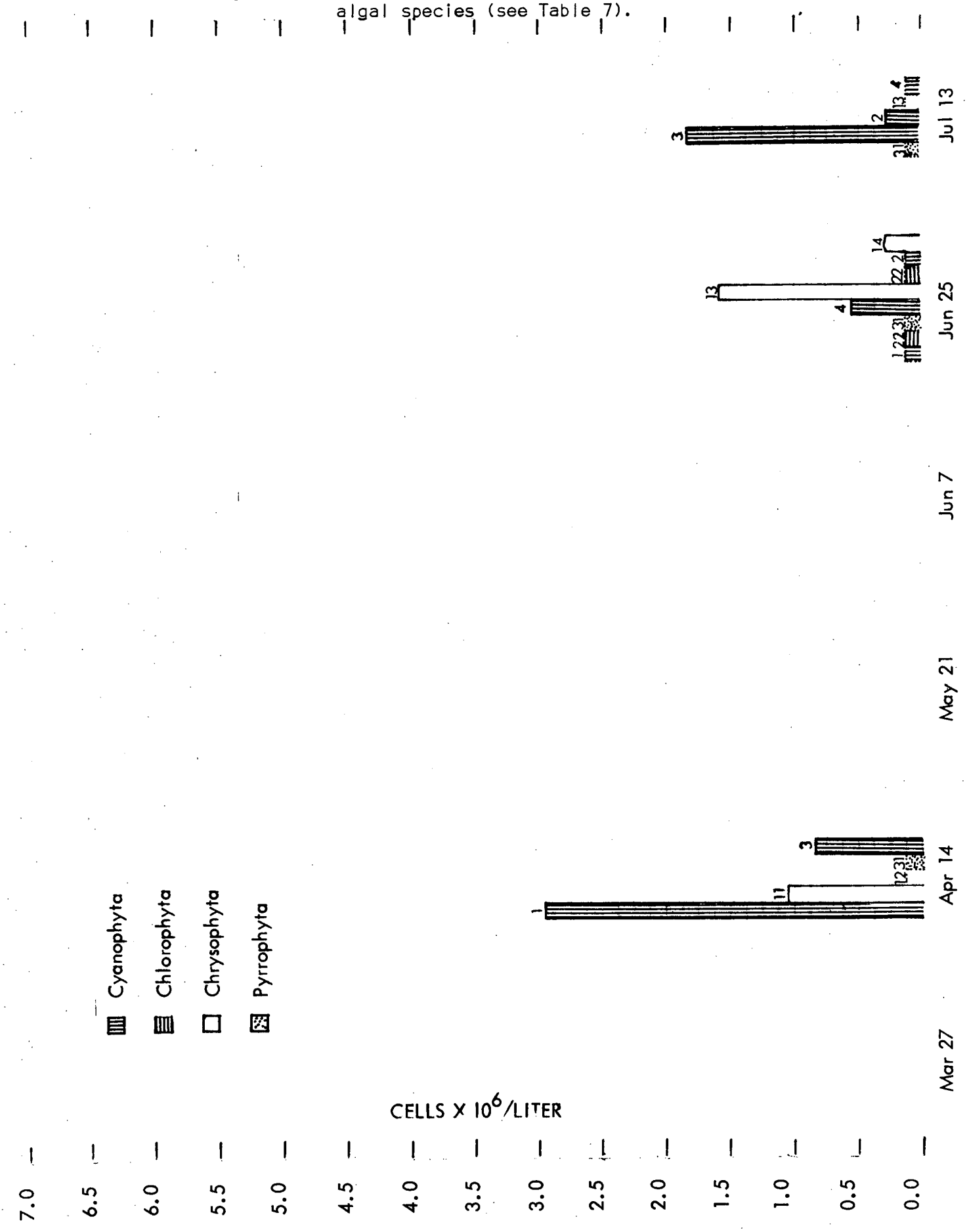

Figure 44. Forest Lake, Station 1.

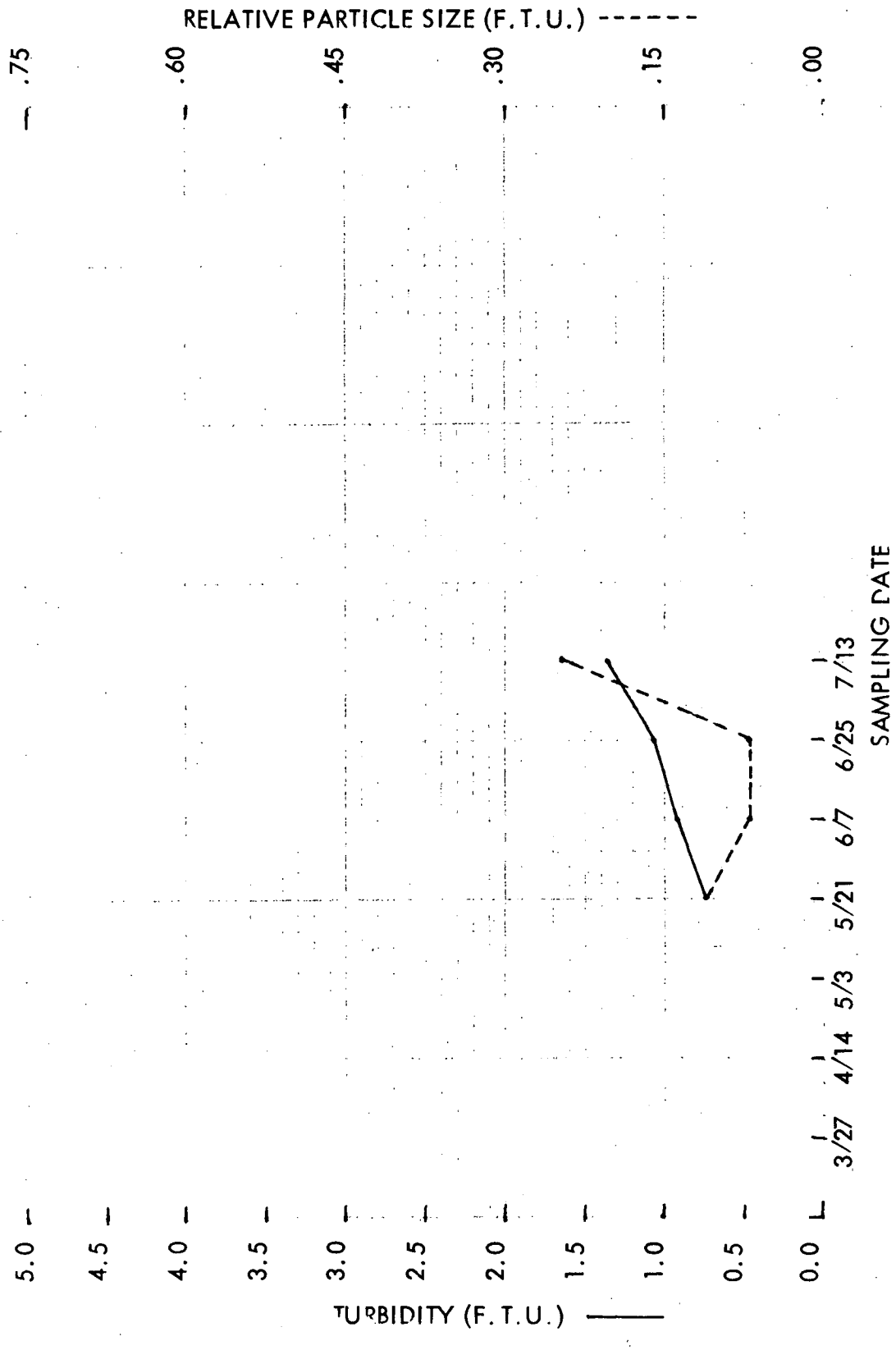

Figure 45. Forest Lake, Station 2.

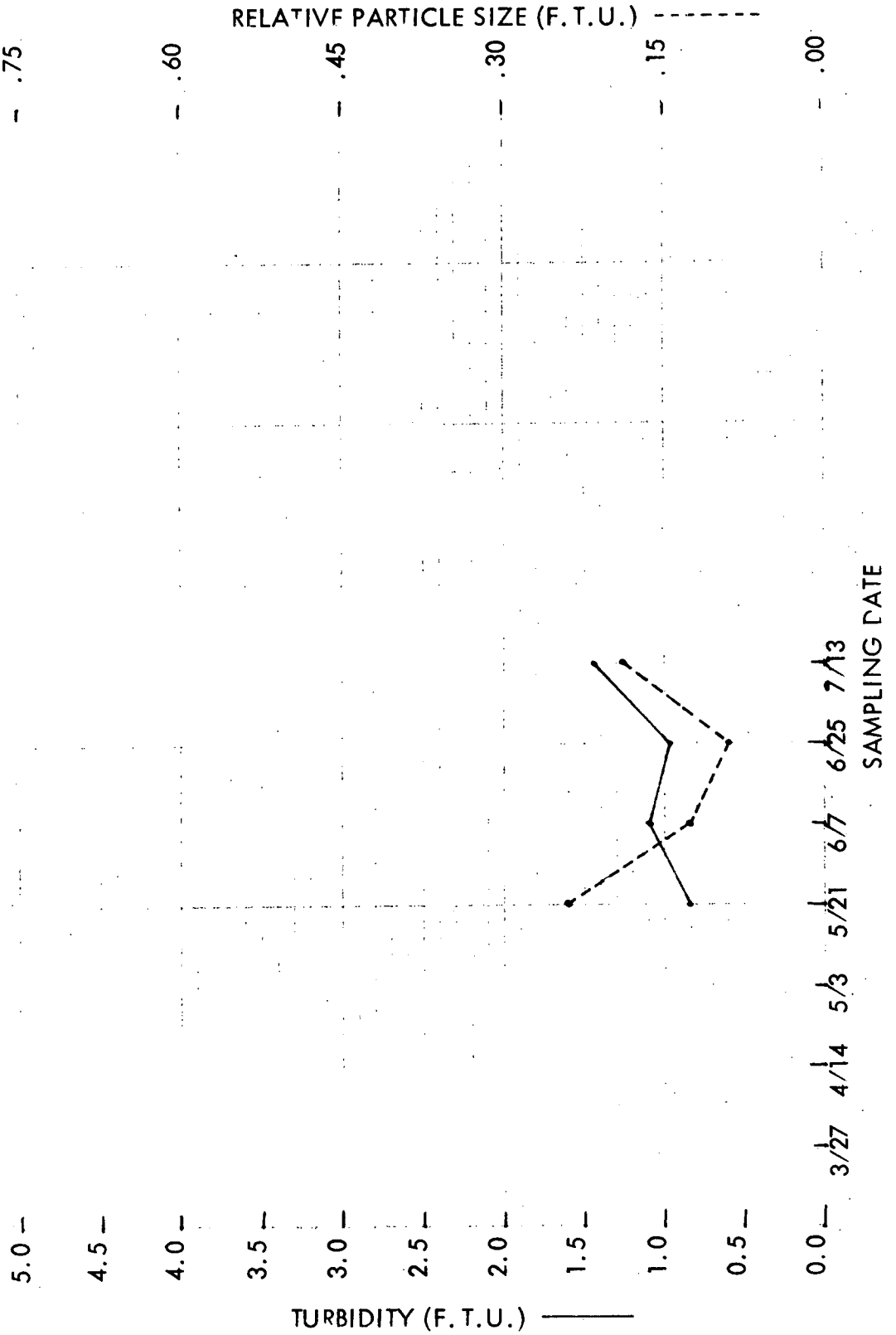

Figure 46. Lower Long Lake, Station 3.

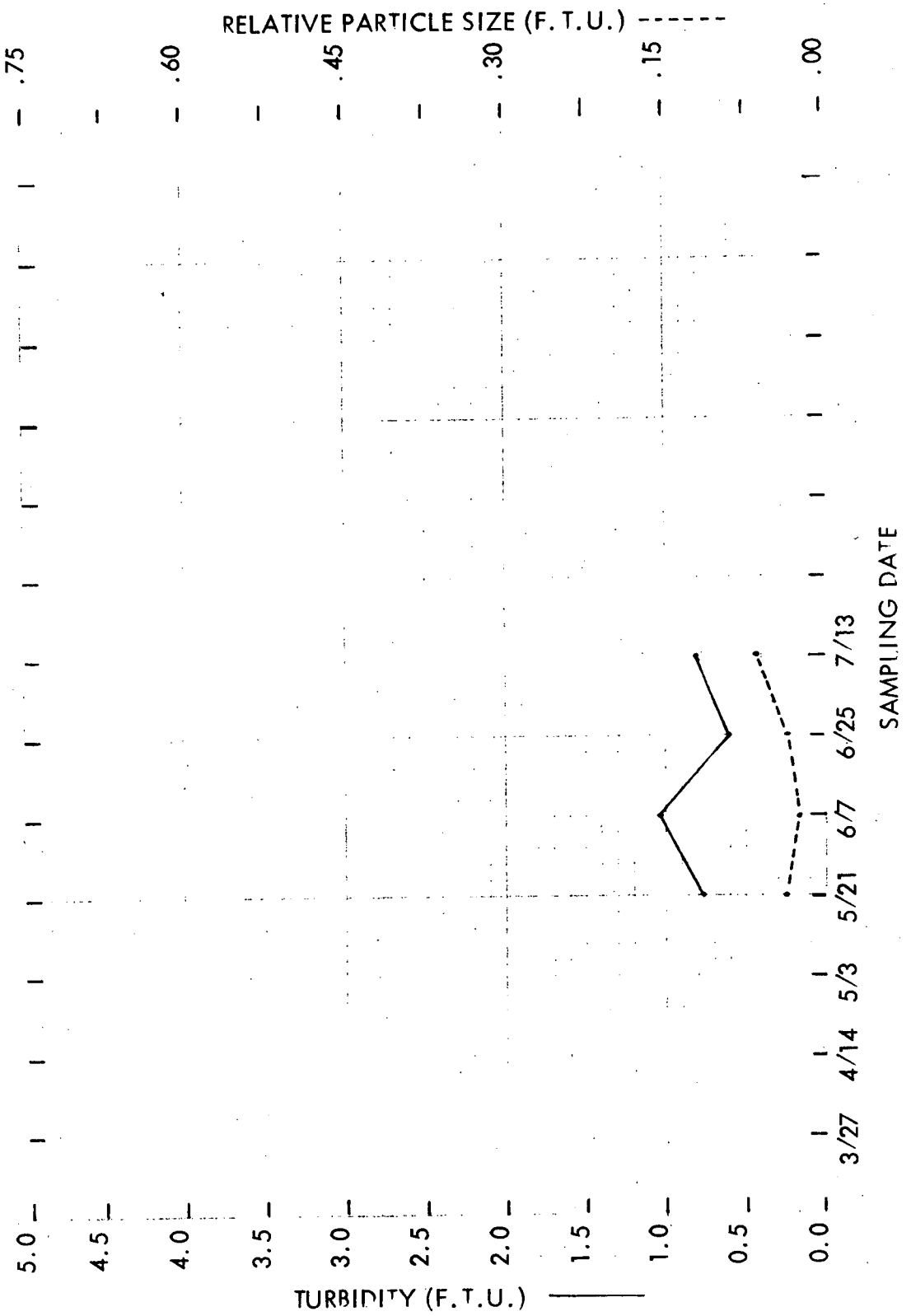

Figure 47. Lower Long Lake, Station 4.

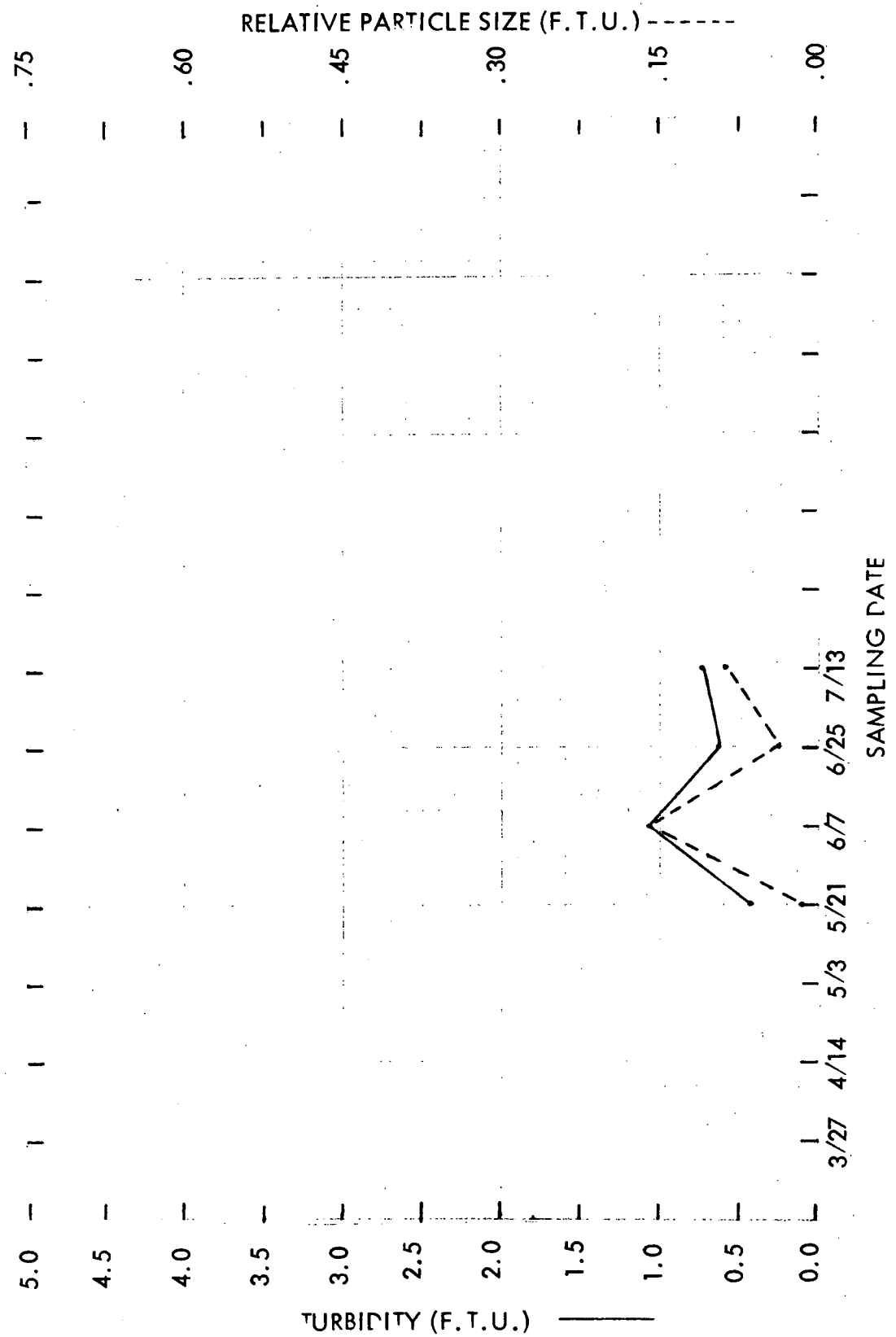

Figure 48. Island Lake, Station 5.

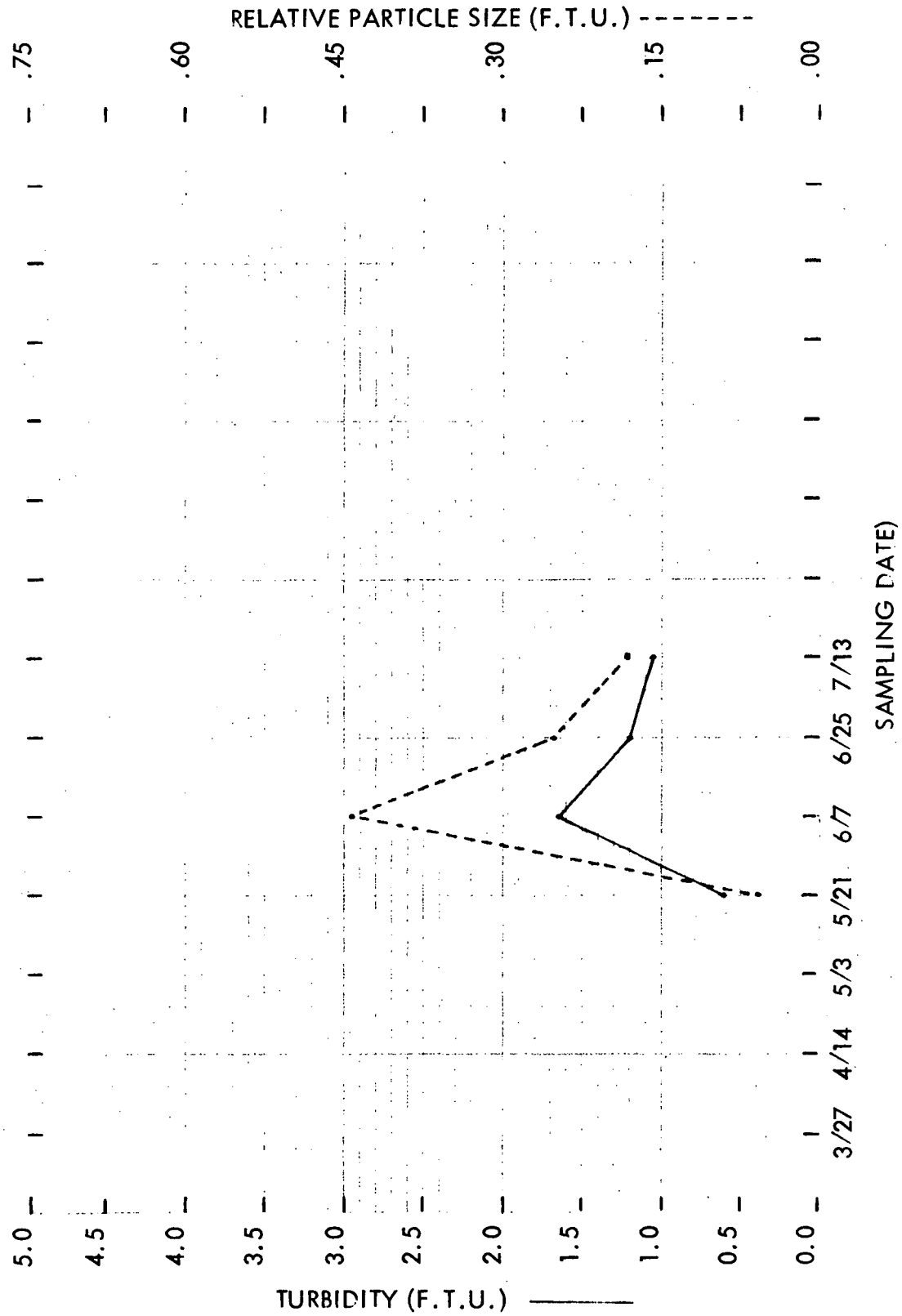

Figure 49. Island Lake, Station 6.

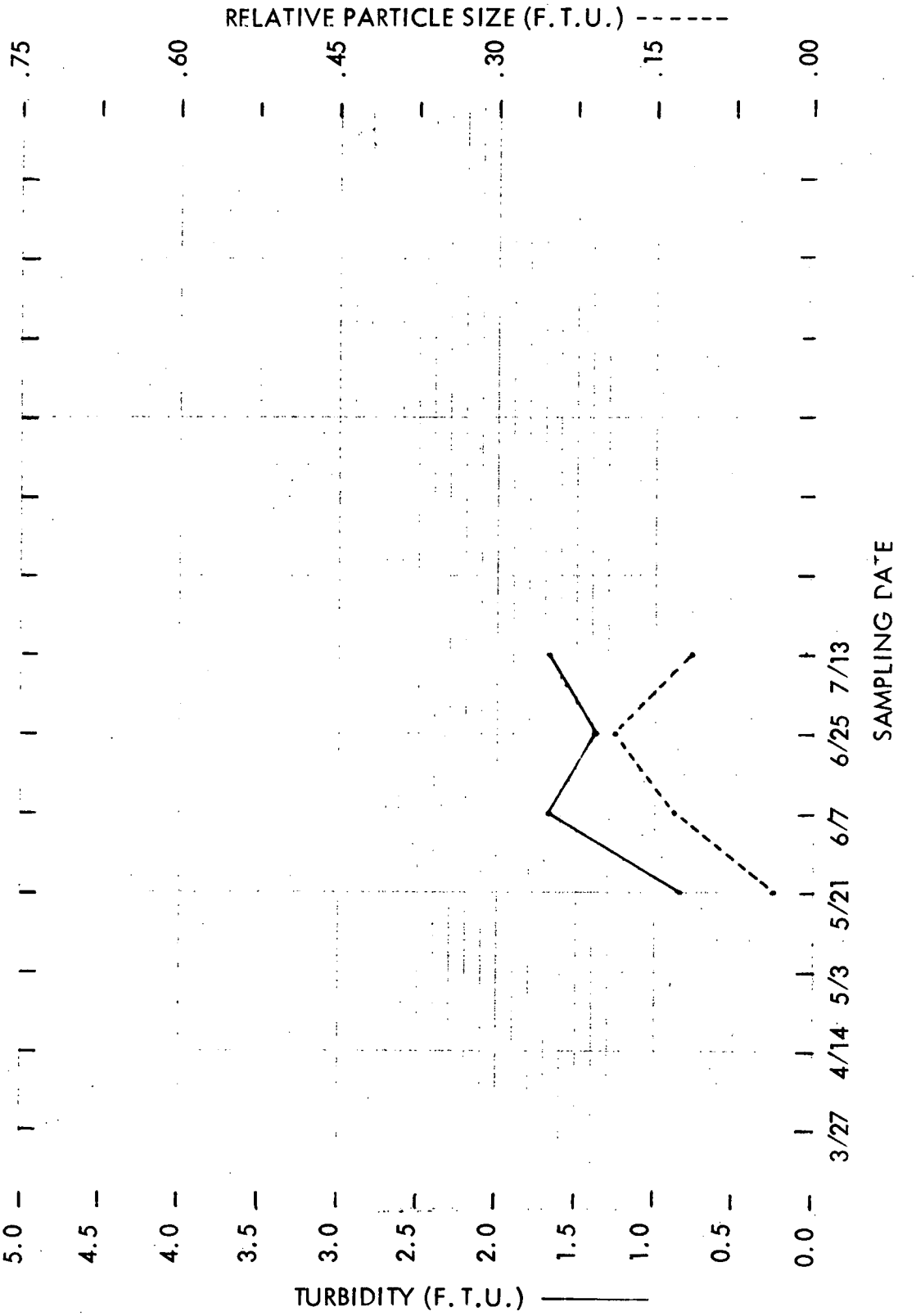

Figure 50. Orchard Lake, Station 7.

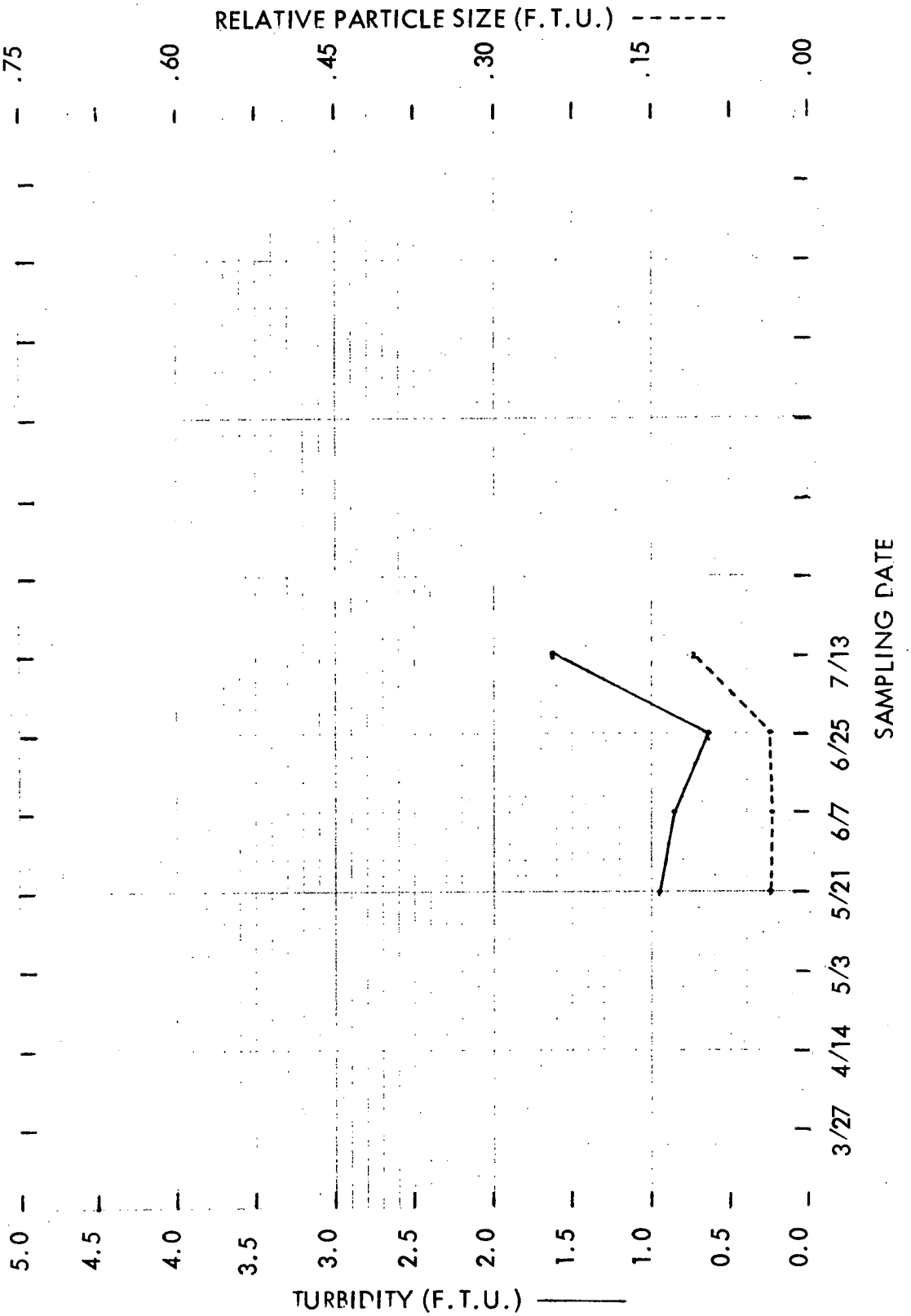

Figure 51. Orchard Lake, Station 8.

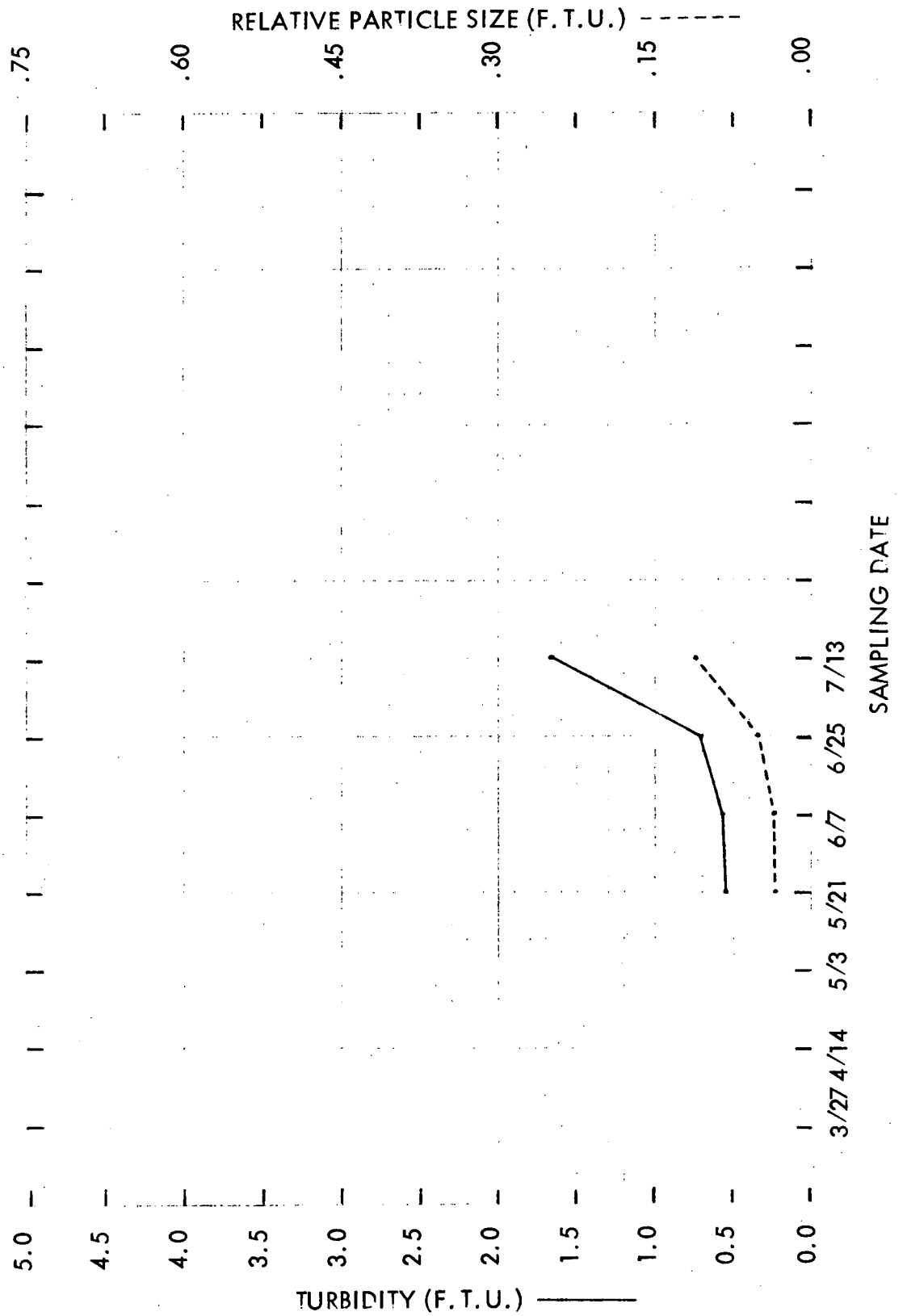

Figure 52. Cass Lake, Station 9.

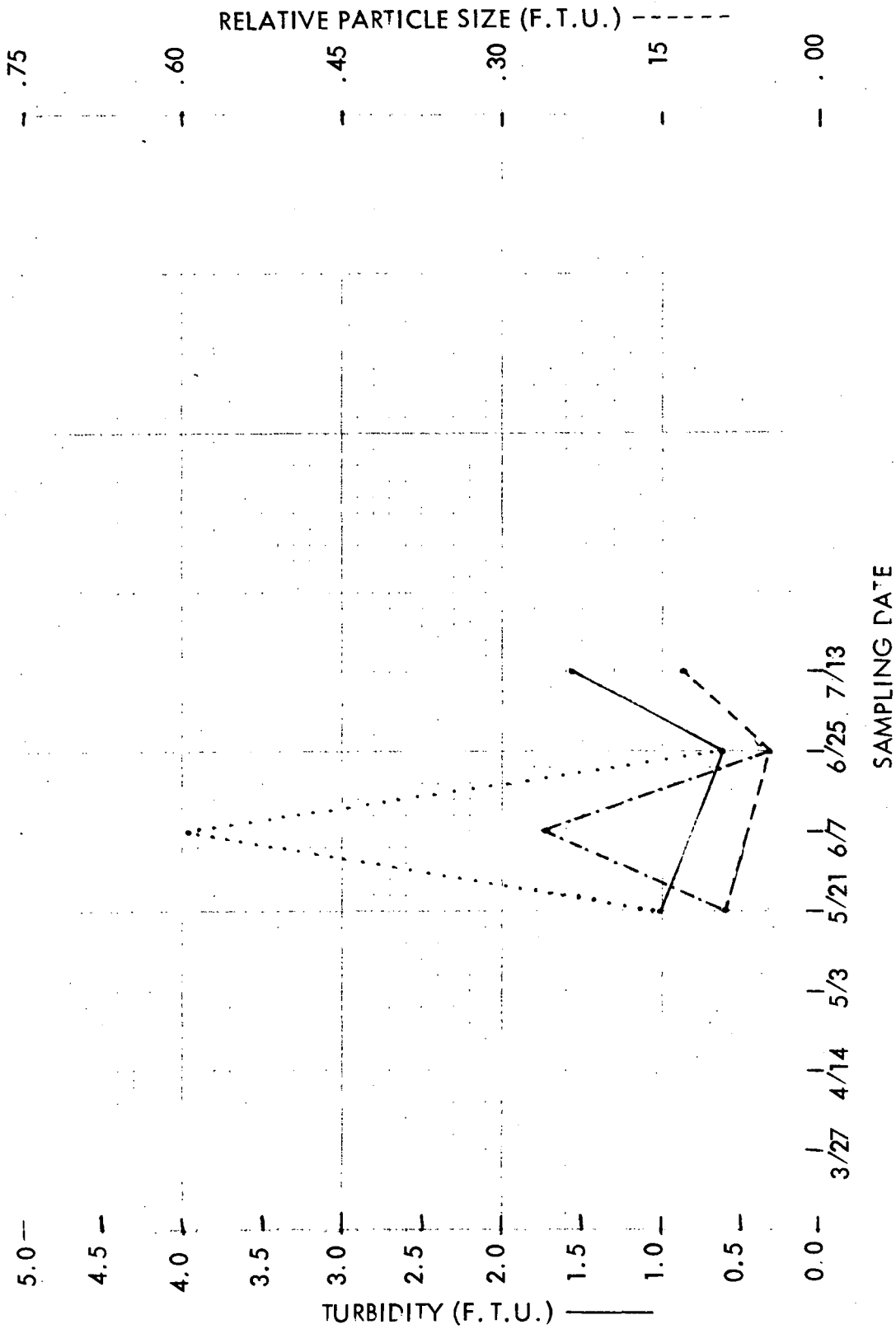

Figure 53. Cass Lake, Station 10.

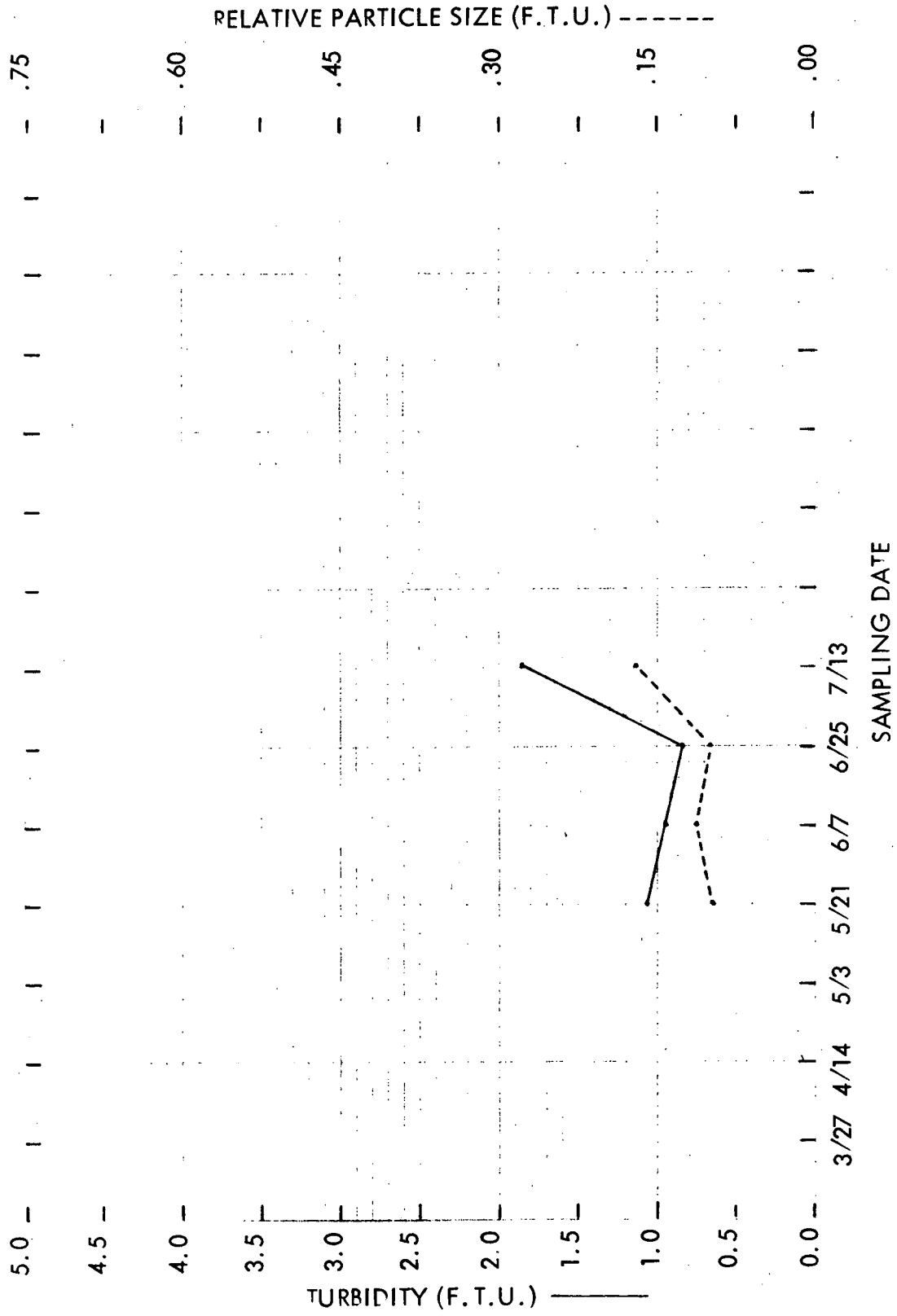

Figure 54. Lake Angelus, Station II.

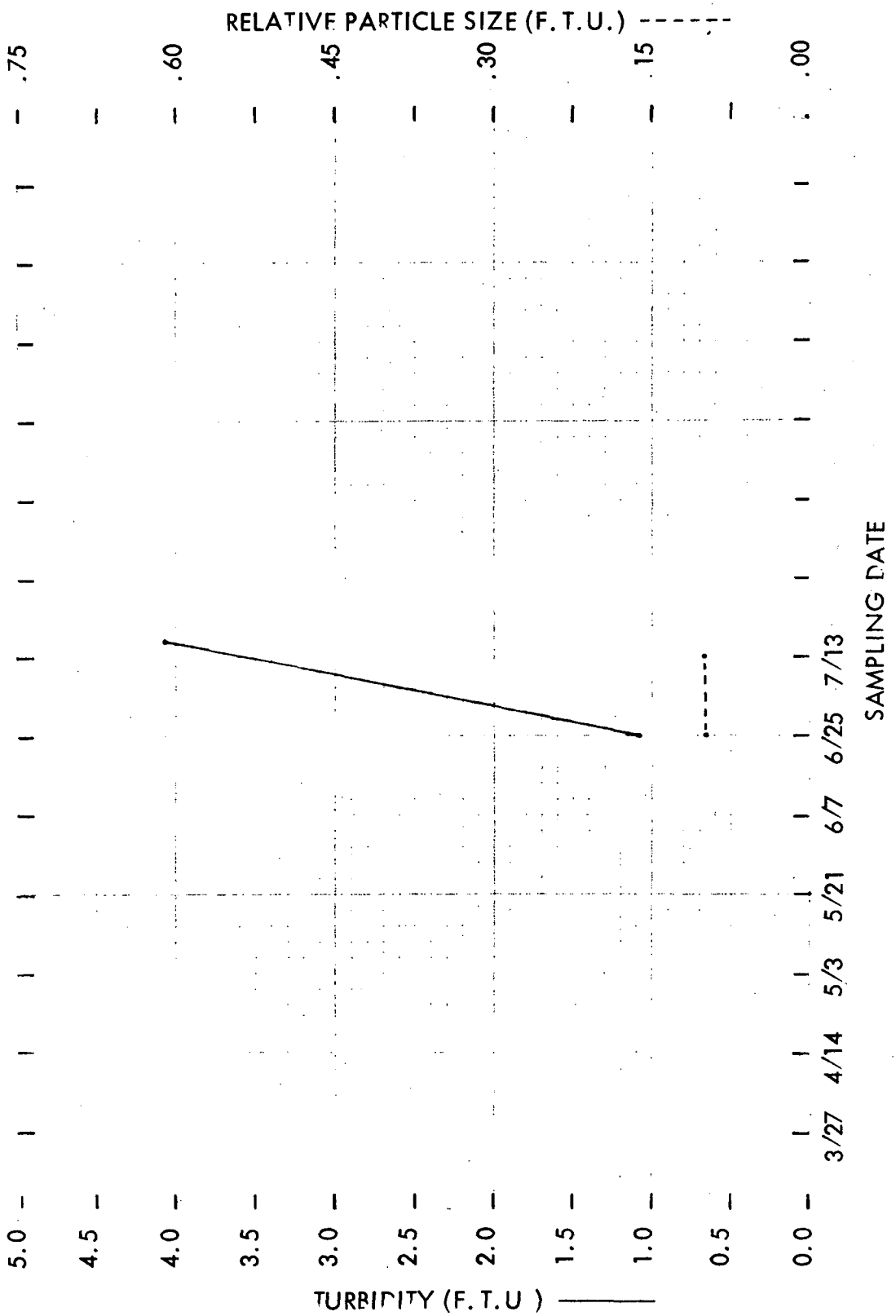

Figure 55. Lake Angelus, Station 12.

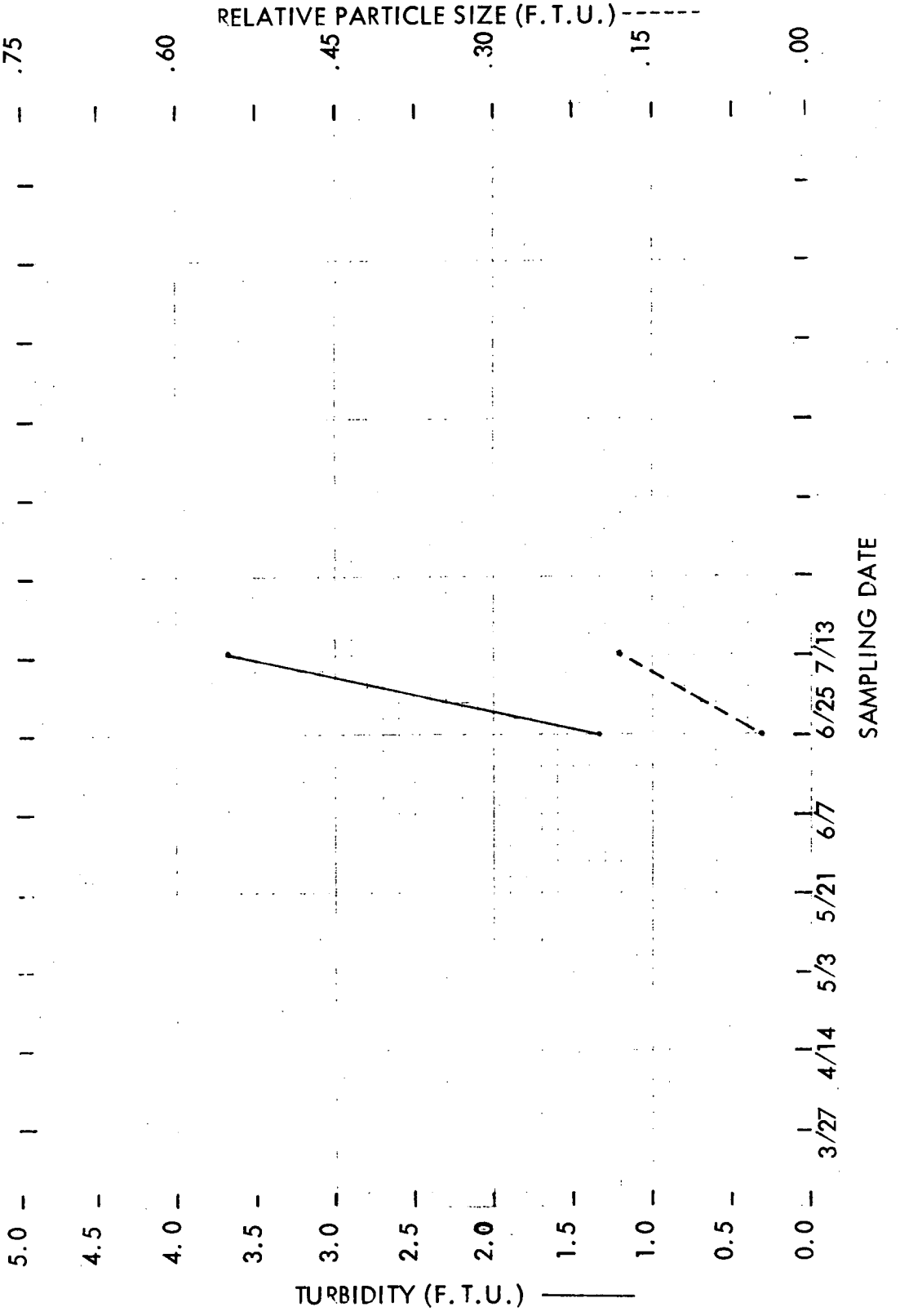

Figure 56. Forest Lake, Station 1.

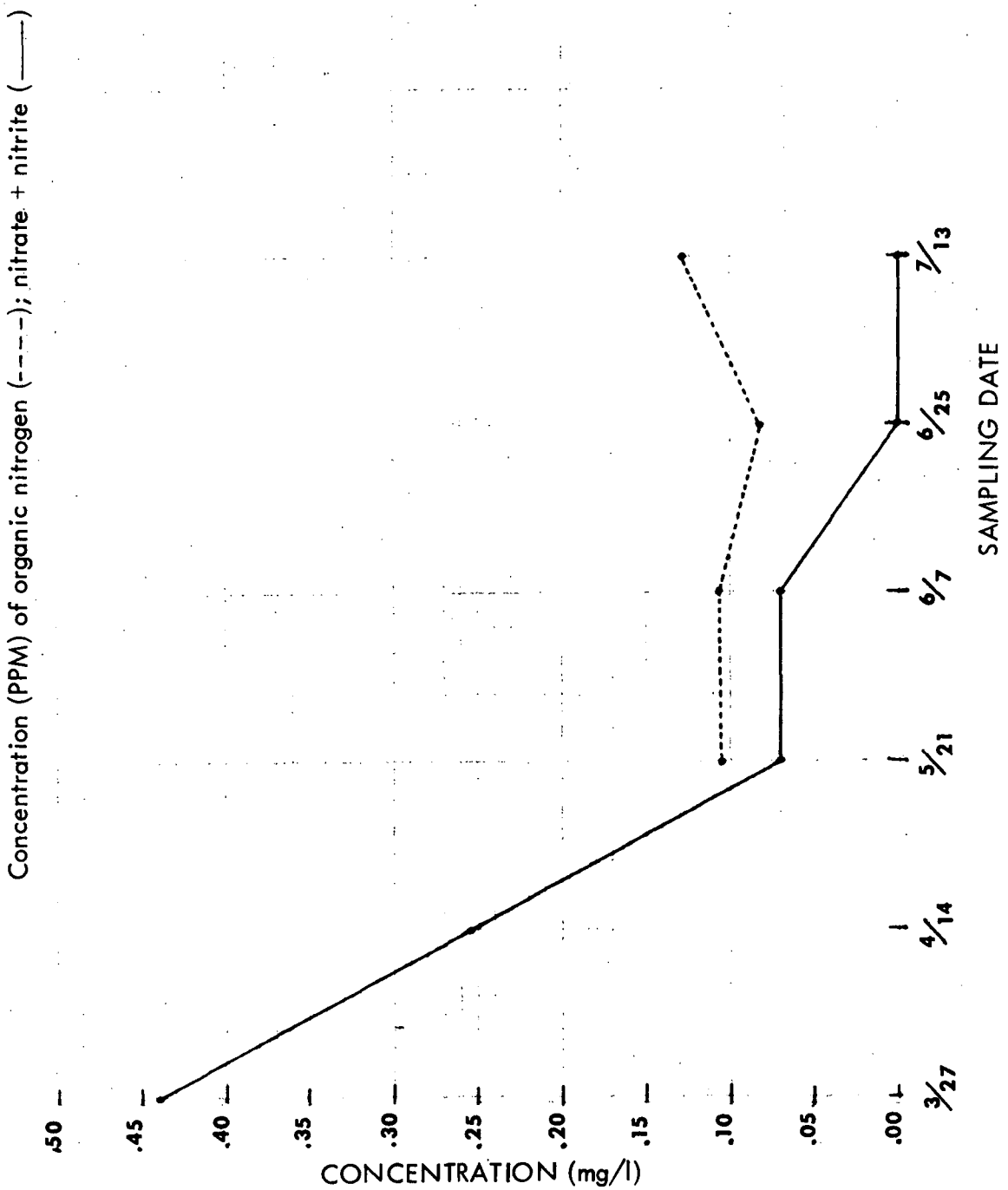

Figure 57. Forest Lake, Station 2.

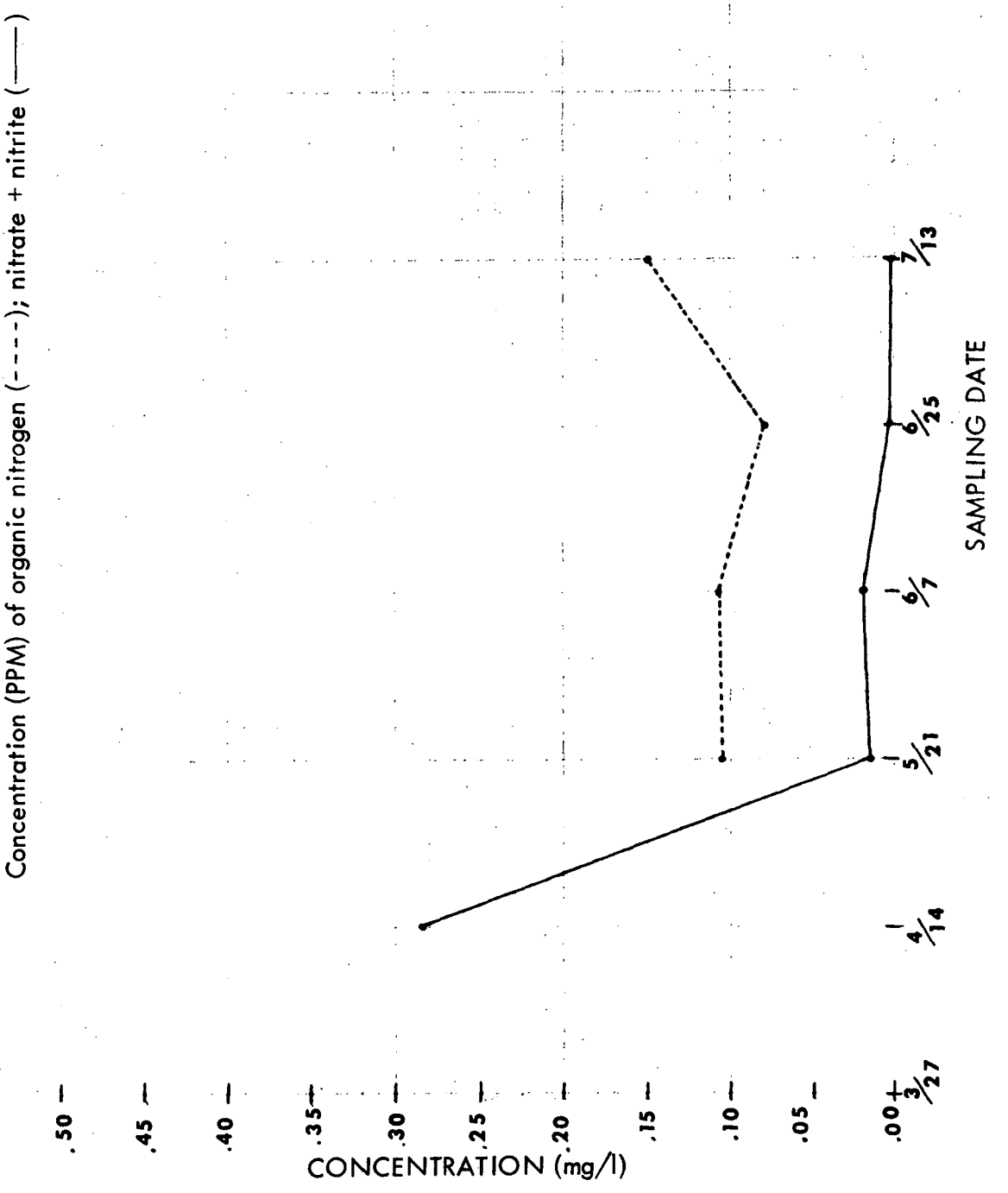

Figure 58. Lower Long Lake, Station 3.

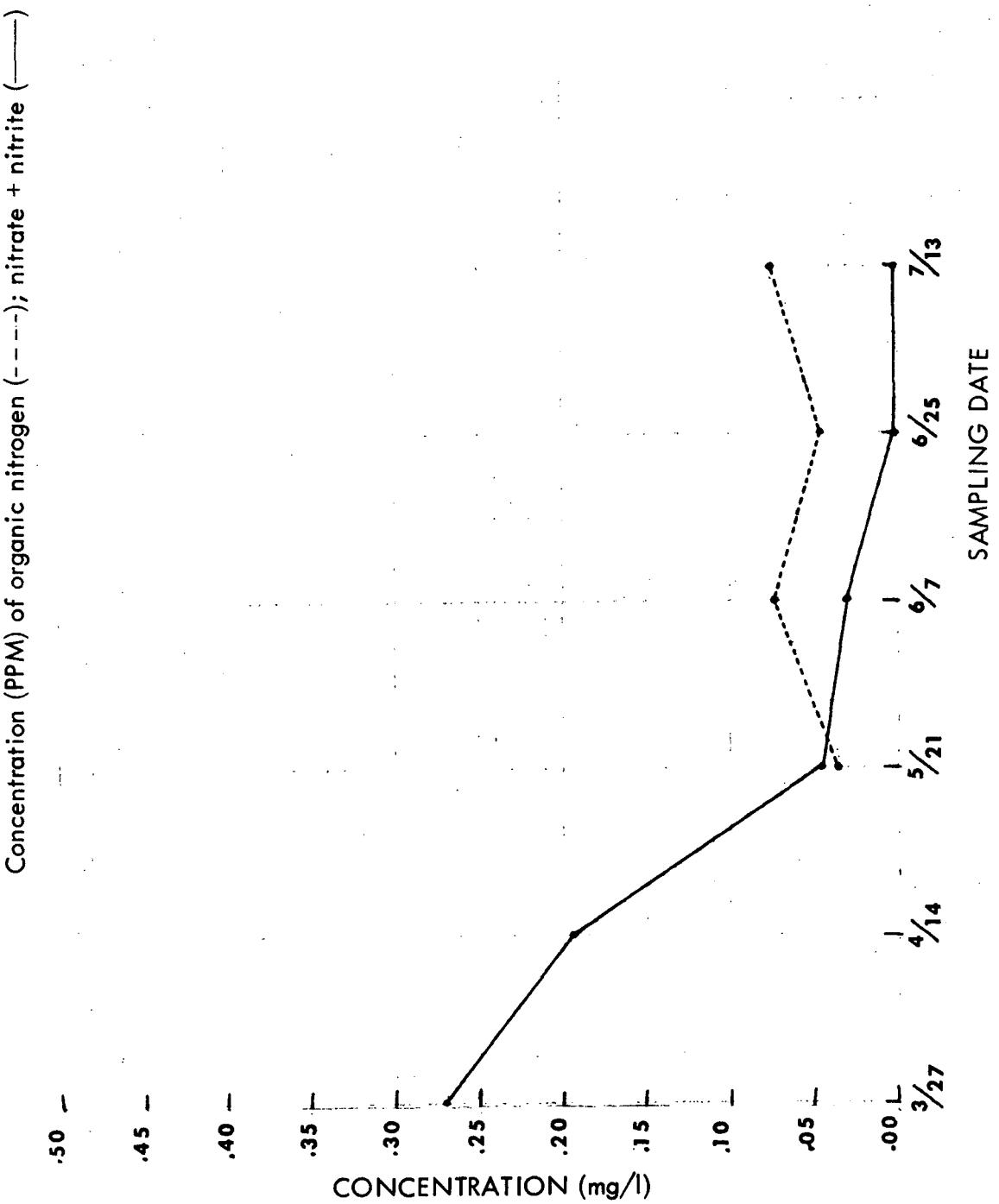

Figure 59. Lower Long Lake, Station 4.

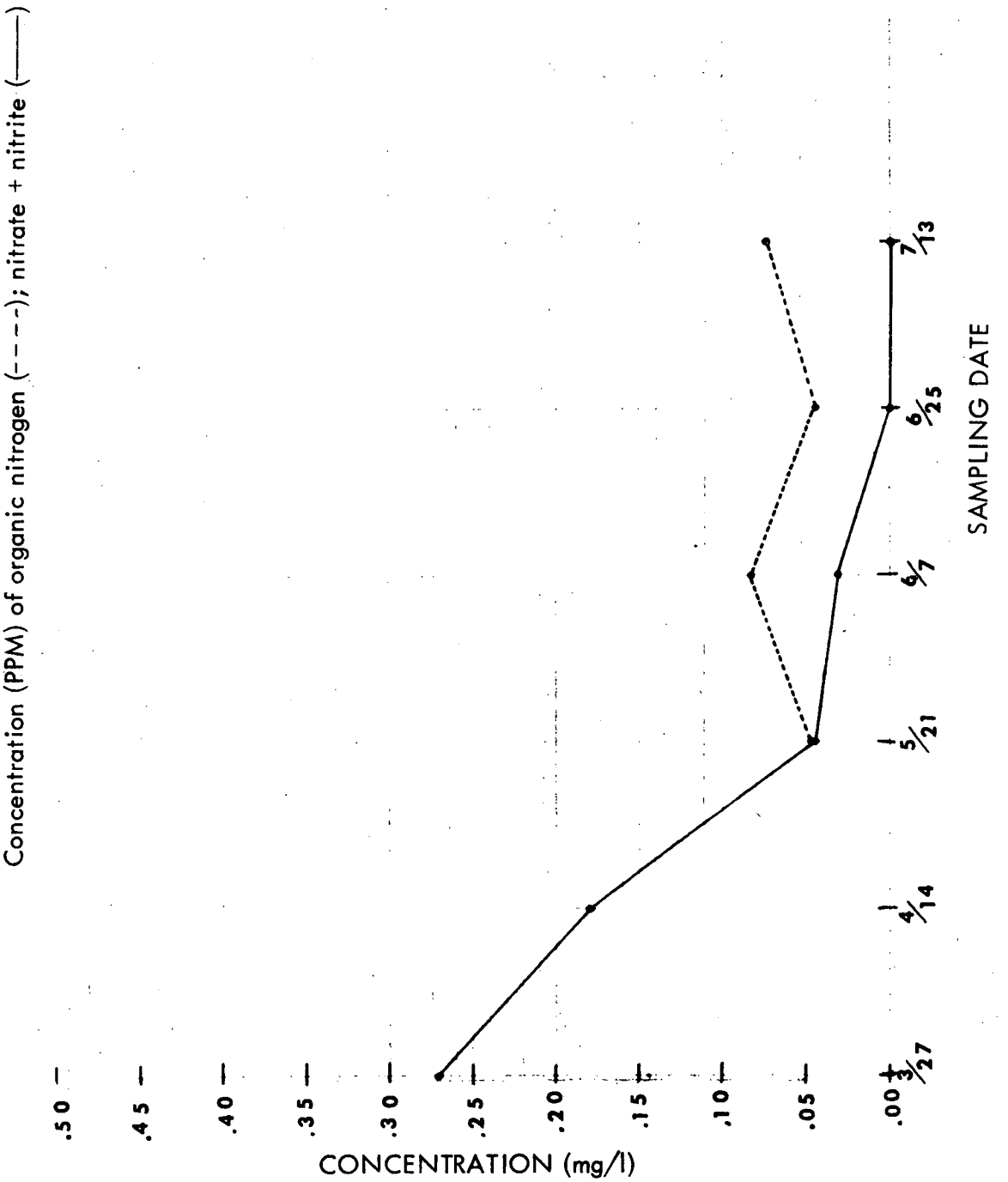

Figure 60. Island Lake, Station 5.

Figure 61. Island Lake, Station 6.

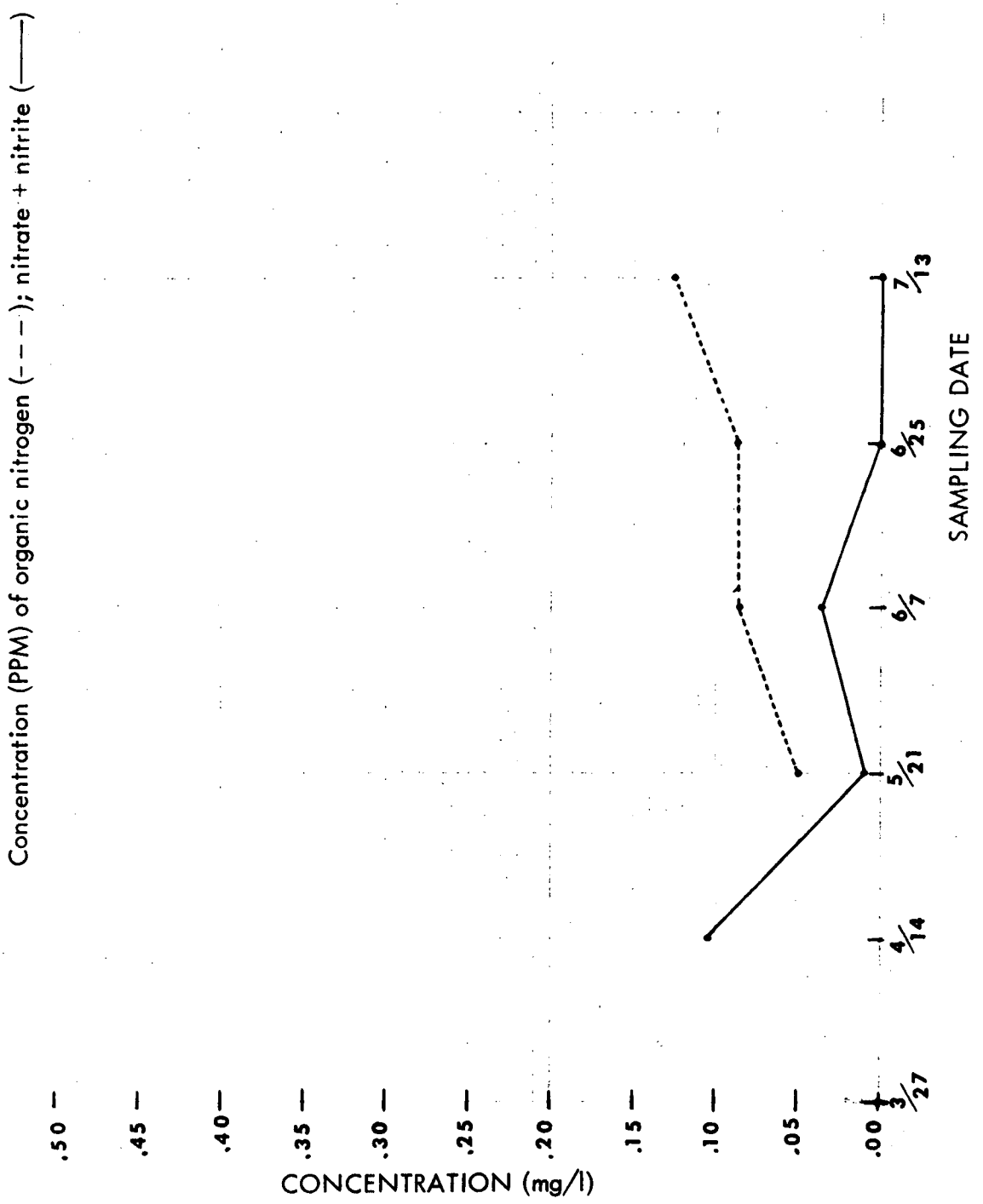

Figure 62. Orchard Lake, Station 7.

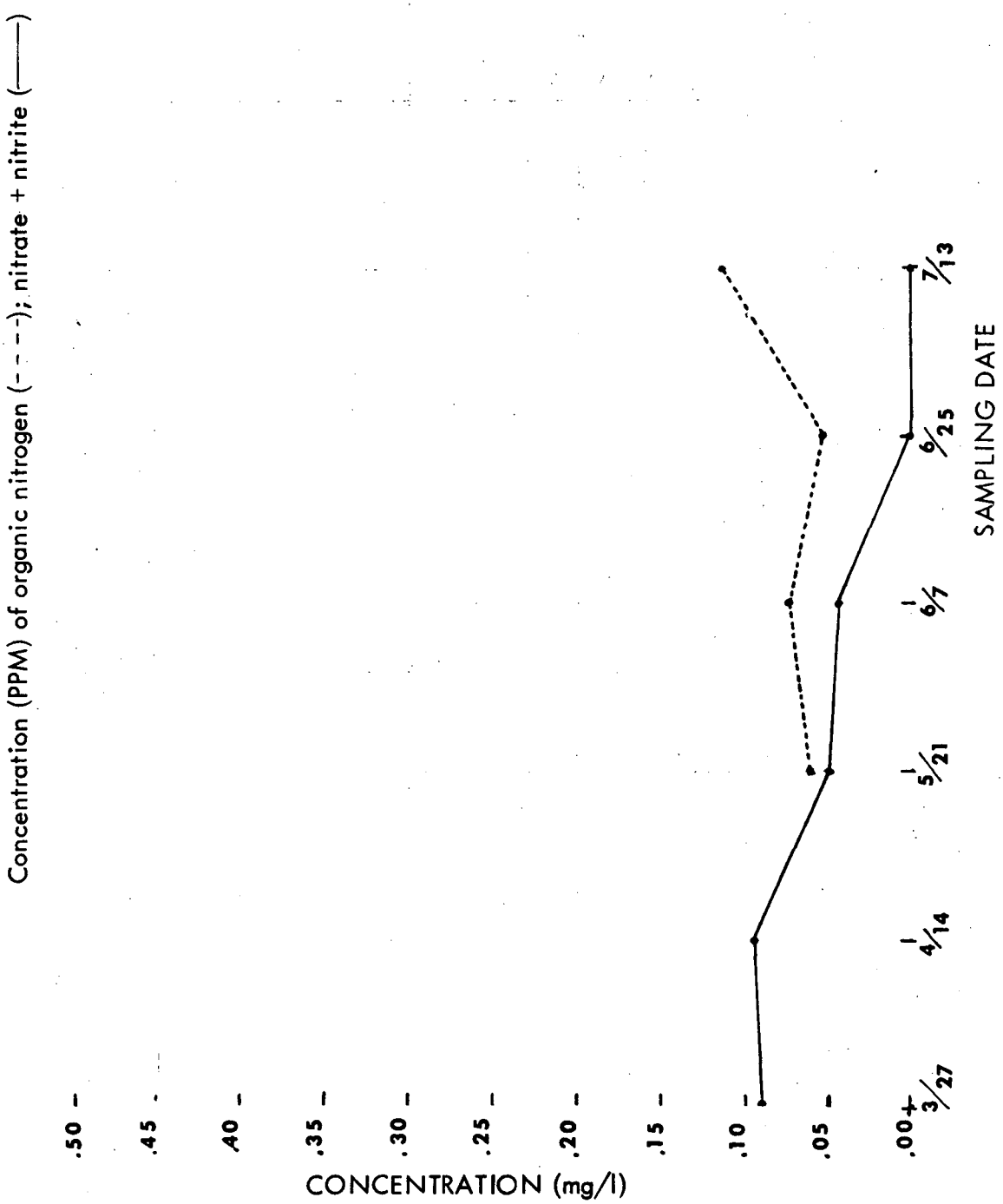

Figure 63. Orchard Lake, Station 8.

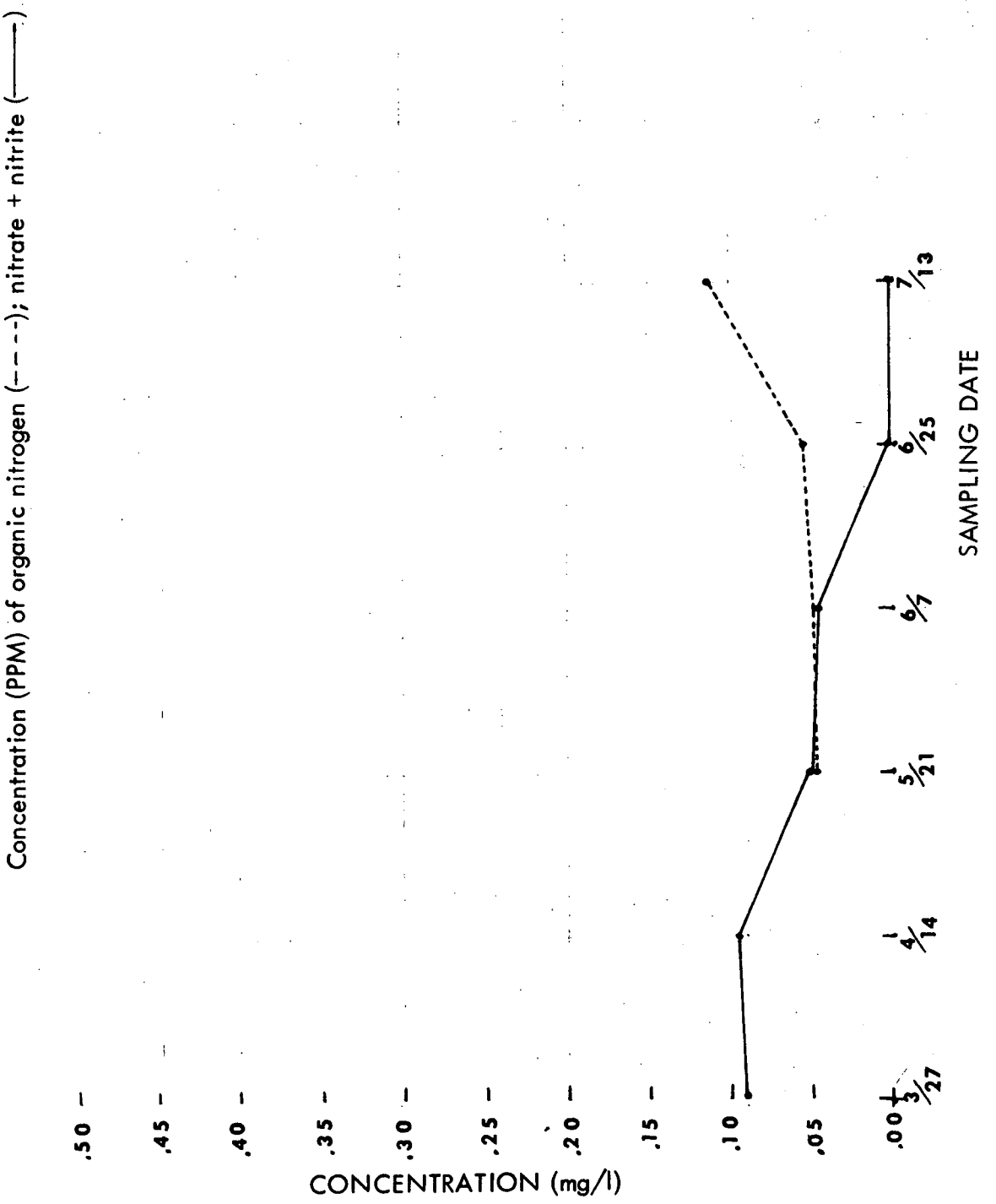

Figure 64. Cass Lake, Station 9.

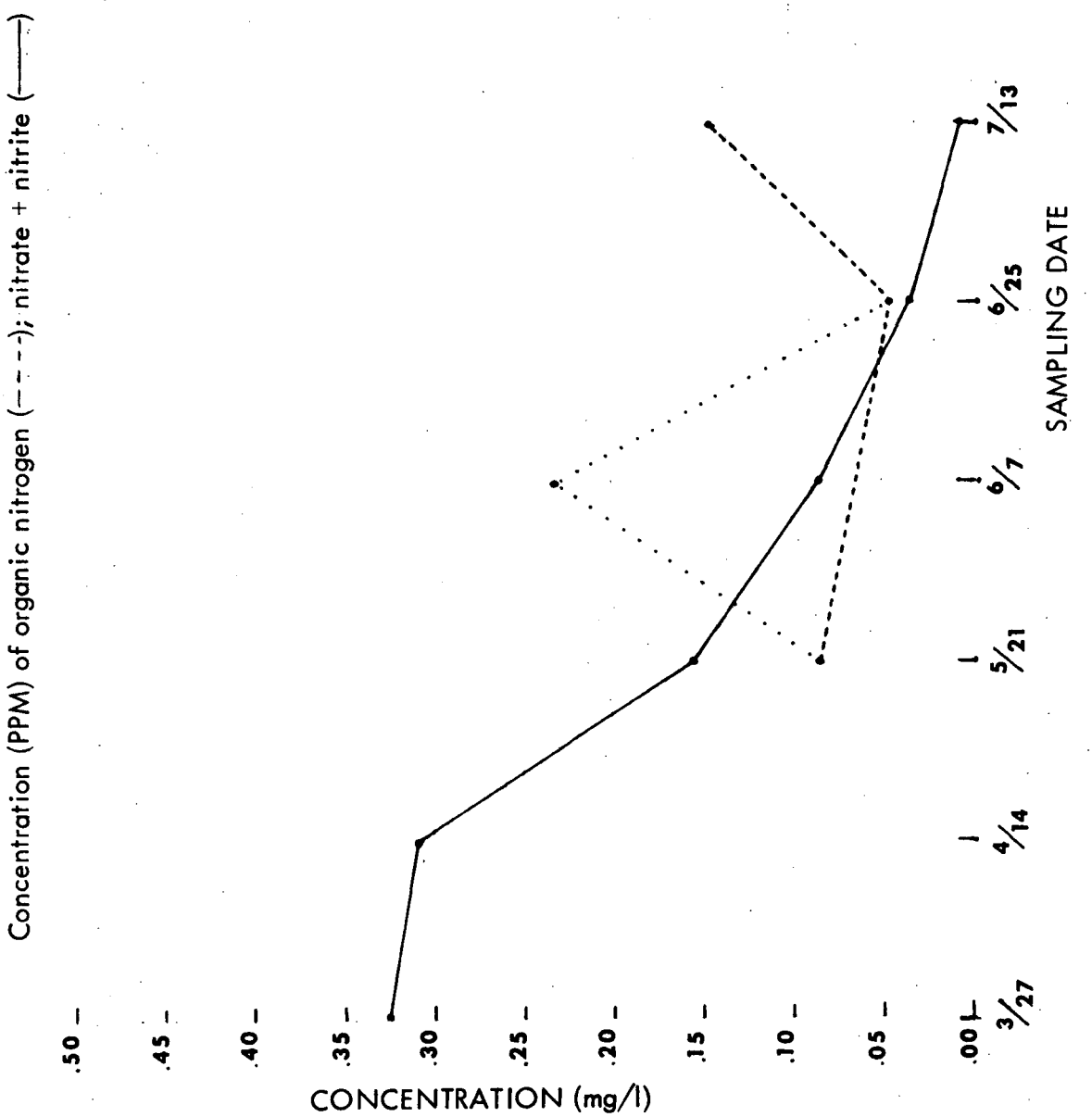

Figure 65. Cass Lake, Station 10.

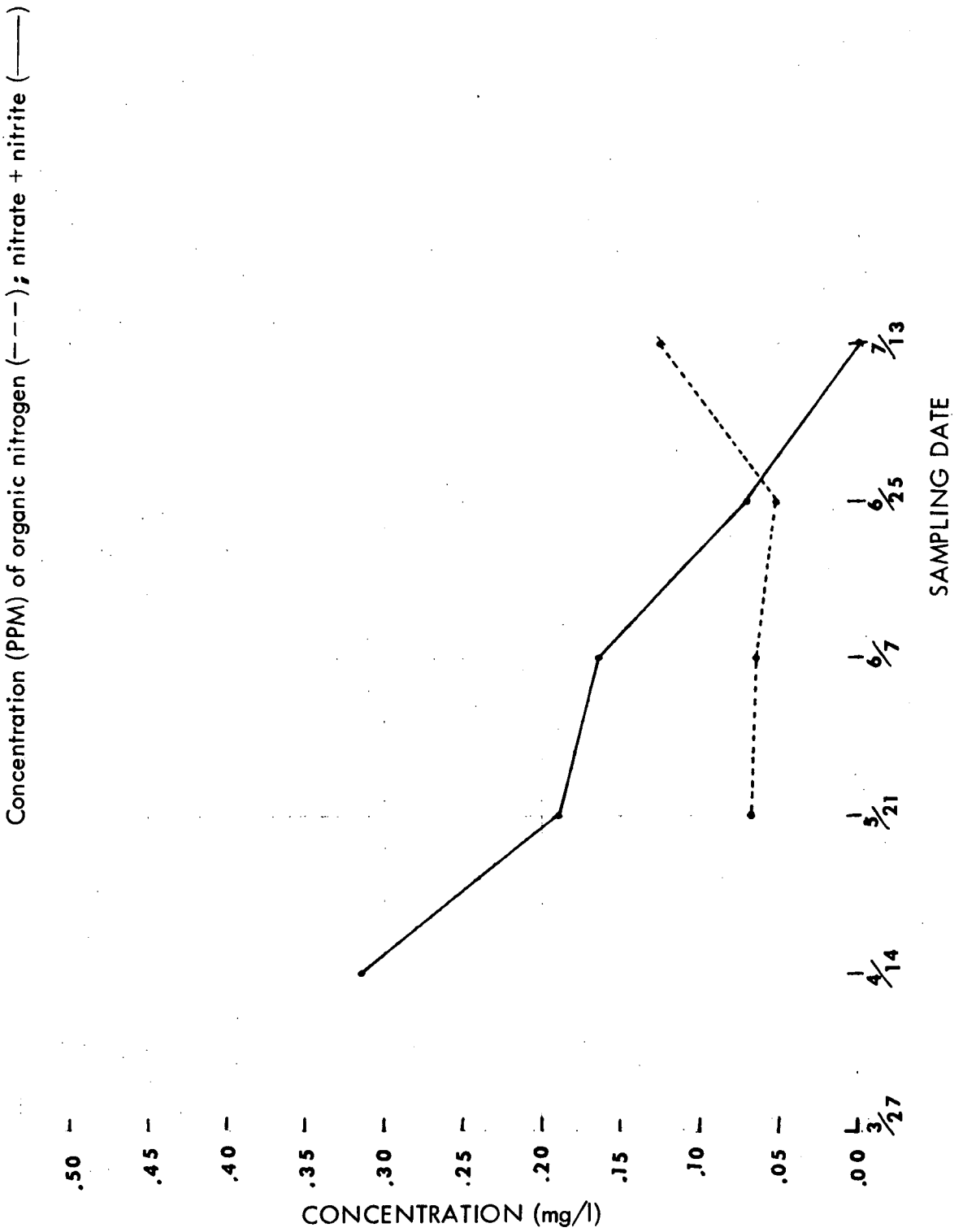

Figure 66. Lake Angelus, Station II.

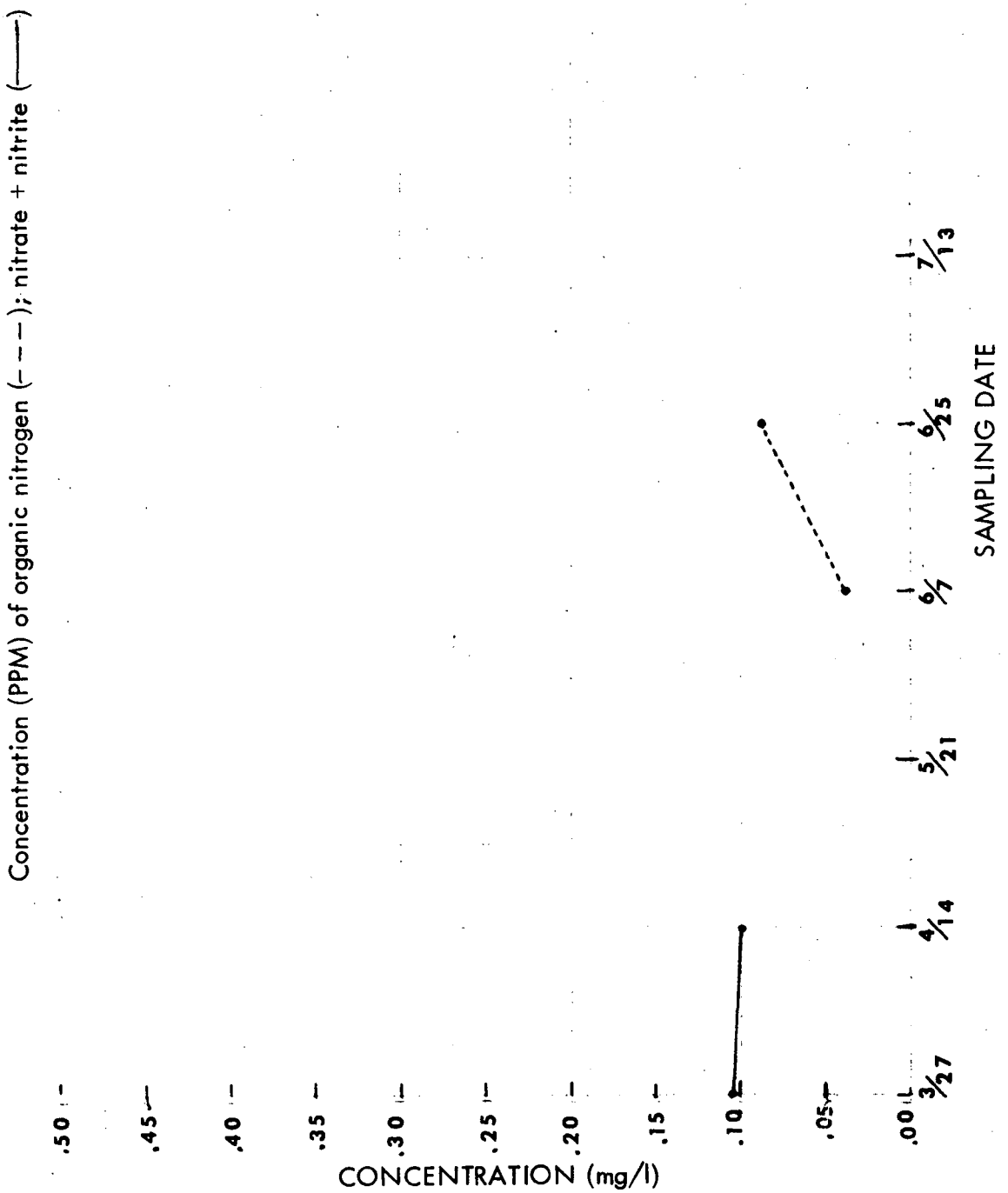

Figure 67. Lake Angelus, Station 12.